UNIVERSITY OF CALIFORNIA
RIVERSIDE

Disparities in Drinking Water Quality Driven by Geogenic Groundwater Contamination

A Dissertation submitted in partial satisfaction
of the requirements for the degree of

Doctor of Philosophy

in

Environmental Toxicology

by

Miranda L. Aiken

June 2022

Dissertation Committee:
Dr. Samantha Ying, Chairperson
Dr. Jay Gan
Dr. Peter Homyak

The Dissertation of Miranda L. Aiken is approved:

_____

_____

_____

Committee Chairperson

University of California, Riverside

Acknowledgements

I would like to thank the following scientists for assistance in the theoretical and technical aspects of this work – Dr. Michael Schaefer, Dr. Macon Abernathy, Dr. Claudia Avila, Benjamin Maki, Dr. Clare Pace, Dr. Maithili Ramachandran, Dr. Hoori Adjami, Dr. Kurt Schwabe, Dr. Bruce Ravel, David Lyons (UCR Environmental Science Research Lab), and each member of my dissertation committee, Dr. Peter Homyak, Dr. Jay Gan, and Dr. Samantha Ying.

Dedication

Whenever I got discouraged, I would always think about this specific section. The work herein is a testament to their love and support.

Thank you to my lab mates and mentors that constantly reminded me that I did deserve to be here and can, in fact, do what I set my mind to. Thank you to Dr. Claudia Avila who led the way. Thank you for providing me invaluable friendship and constant reassurances when needed. Who demonstrated incredible teaching pedagogy and who I am pretty positive shaped the teacher and mentor I hope to one day become. Thank you to Dr. Macon Abernathy who has been a constant support. Thank you for your attention to detail, which I greatly admire, and your patience in demonstrating so many skills. Thank you for always being in the office so I had someone to complain to. Thank you to Danielle Stevenson, Ben Maki, Monica Hope, and Shannel Thorpe for fostering a lab environment that made it so easy to come into work every day. Thank you all for showing me what a lab group can really do for each other. I will forever model future group environments after what we have created here.

Thank you to Sam. You have demonstrated what academia can (and should!) be. A collection of friends who will not compete with you but ask you how they can help. A space where we can critically think about not only really cool science, but about the barriers that is also preventing really cool science. You have directly shaped the scientist I am today and will continue to grow into and for that, I thank you. Your impact continues with us.

Thank you to my friends for reminding me that life exists outside of work. I would have never been on nearly as many adventures if I did know have the joy of being your friend. Thank you to Dr. Aalekhya Reddam, Dr. Tori McGruer, and Dr. Sophia Parks for their friendship from day one and honesty, forever. I cannot imagine grad school without the community we shared. I will forever cherish your love, kindness, and courage you have brought into my life.

Thank you to each and every member of my family that have endlessly supported me and allowed me to be in a position to pursue this degree. You have provided me with a home to return to and kind works when I needed them the most.

Thank you to my partner, Bryan Sevener. You didn't sign up for any of this but have been here to celebrate my successes and console my failures for the past 5+ years. Thank you for your letters in parking tickets, making sure my water bottle was always full, and your endless love.

It takes a village to mentor a scientist and I am testament to this. Thank you to each and every person who I have exchanged thoughts with over the past 5 years. The experience has been invaluable. I will do everything within my power to continue to support other young scientists in the ways in which I have been supported. This is not just my success, but all of ours. Thank you.

ABSTRACT OF THE DISSERTATION

Disparities in Drinking Water Quality Driven by Geogenic Groundwater Contamination

by

Miranda L. Aiken

Doctor of Philosophy, Graduate Program in Environmental Toxicology
University of California, Riverside, June 2022
Dr. Samantha Ying, Chairperson

In California, up to 46% of the state's total water supply is from groundwater and its geogenic contamination may affect a large area, number of wells, and number of people throughout the state. The presence of geogenic contaminants, such as chromium (Cr) and manganese (Mn), in groundwater is due to the interplay between complex processes (i.e., biogeochemical reaction networks) involving mineral dissolution, diffusion, redox transformation, sorption, and precipitation. To effectively evaluate the safety of our drinking water it is critical that we understand the network of biogeochemical reactions that control geogenic metals cycling. The overarching goal of this dissertation work is to explore how fluctuating redox conditions from micron- to field-scale may influence the release of geogenic metals and threaten drinking water sources.

To first address this goal on the micro-scale, we investigated how the co-occurrence of iron (Fe) and Cr minerals in reduced zones of soil aggregates may alter the redox potential of Mn oxides within oxidized zones at diffusion-controlled soil interfaces. Altering the oxidation state and structure of Mn oxides can impact the oxidation of

Cr(III), a non-toxic mineral, to Cr(VI), a mobile and highly toxic groundwater contaminant. Simultaneously, the oxidation of Cr minerals by Mn oxides will also release soluble Mn, a secondary contaminant, through reductive dissolution.

On a state-wide scale, we then investigated the groundwater contamination by redox controlled groundwater contaminants, such as Mn, within public water systems relying on groundwater resources. Larger systems that treated for primary contaminants often saw associated benefits of less Mn, however, this was not observed within small systems or systems without treated groundwater.

Further, we investigated differences in Mn contaminant exposure between private, shallow well users and deeper, public well users in California's Central Valley. We found that, despite predicted differences in redox status groundwater based on well-depth, this led to no differences in Mn concentration in groundwater. However, lack of monitoring or treatment of private wells and the high associated costs may lead to exposure to concentrations of Mn exceeding regulatory standards.

Table of Contents

Chapter 1: Introduction to geogenic contamination of groundwater 1

1. Global water quality 1
2. Water quality in California 1
3. Subsurface biogeochemistry and water quality 2
4. Impact of micron-scale redox conditions 4
5. Impact of field-scale redox conditions 8
6. Barriers to addressing diminished groundwater quality 10
7. Importance of interdisciplinary approach 11
8. References 12

Chapter 2: Inhibition of chromium (III) oxidation through manganese (IV) oxide passivation and Fe(II) abiotic reduction 17

1. Abstract 17
2. Introduction 18
3. Materials and Methods 21
   - 3.1. Mineral Synthesis 21
   - 3.2. Multi-chamber Reactor 22
   - 3.3. Aqueous Phase Analysis 23
   - 3.4. Solid Phase Analysis 23
   - 3.5. Bulk X-Ray Absorption Spectroscopy 24
   - 3.6. μ-XRF Imaging and Sample Preparation 25
   - 3.7. X-Ray Photoelectron Spectroscopy Oxidation States 26
   - 3.8. Diffusion Modeling 27
4. Results 28
   - 4.1. Aqueous Fe and Mn dynamics 28
   - 4.2. Aqueous Cr dynamics 30
   - 4.3. Cr and Fe Sorption onto Mn oxides 31
   - 4.4. Effect of Mn oxide crystallinity on Cr and Fe dynamics 35
5. Discussion 38
   - 5.1. Competing Redox Processes that Limit Cr(VI) Production 38
   - 5.2. Impact of Mn Oxide Crystallinity 42
   - 5.3. Diffusion Controls on Redox Reactions 43
6. Conclusions 44
7. References 46

Chapter 3: Assessment of manganese in California's community water systems and geochemical controls of release into groundwater 52

1. Abstract 52
2. Introduction 53
3. Materials and Methods 56
   - 3.1. Data Sources 57
     - 3.1.1. Water Quality Data 57

3.1.2. Community Water System Boundaries 57
3.2. Data Handling 58
3.2.1. Estimating Contaminant Exposure in Community Water Systems 58
3.2.2. Potentially Exposed Population 59
3.2.3. Impact of Treatment Status on Contaminant Exposure 60
3.2.4. Geochemical Controls of Mn Release 61
3.3. Statistical Analysis 61
4. Results 62
4.1. Occurrence of Mn in Community Water Systems within California 62
4.2. Impact of treatment on Mn at point-of-use 65
4.3. Co-occurrence of Mn with other contaminants 66
4.4. Co-occurrence with other redox sensitive groundwater constituents 67
5. Discussion 68
5.1. Mn distribution and reporting in CWS 68
5.2. Mn and impact of treatment 70
5.2.1. Co-treatment of primary contaminants 71
5.2.2. Treatment options and feasibility 72
5.3. Mn Geochemistry of Release 75
6. Data Limitations 77
6.1. Other water type users 77
6.2. Modification of Mn concentration from point-of-use to tap 78
7. Future Implications 79
8. References 81

Chapter 4: Predicting manganese in drinking water accessed by domestic well communities and community water systems in Central Valley, California 89

1. Abstract 89
2. Introduction 90
3. Materials and Methods 93
3.1. Community Water Systems 93
3.2. Domestic Well Communities 94
3.3. Groundwater Mn Concentration Prediction Model 94
3.4. Water quality estimation in Community Water Systems 95
3.5. Population estimates and sociodemographics 96
3.6. Statistical Analysis 98
4. Results 98
4.1. Measured water quality in community water systems 98
4.2. Predicted water quality in domestic wells 101
4.3. Poverty in DWCs 103
4.4. Possible Mn mitigation strategies 105
4.4.1. Changing Well Depth in DWCs 105
4.4.2. Point-of-use treatment 107
4.4.3. Consolidation of DWCs 109
4.5. Limitations of Available Data 110

4.5.1. Spatial and Temporal Limitations of Mn Groundwater Model 110
4.5.2. Data Availability Limitations 111
4.5.2.1 US EPA and USGS 111
4.5.2.2 State Regulatory Agencies 112
4.5.3. Underrepresented Communities 113
5. Future Implications 114
6. References 115

Chapter 5. Conclusions 121

1. Overview 121
2. Multi-scale approach to understanding redox sensitive contaminants 121
3. Use of this work to improve water quality 122

Appendix 1. Appendix to Inhibition of chromium (III) oxidation through manganese (IV) oxide passivation and Fe(II) abiotic reduction 124

1. Reactor Schematic 124
2. Additional Data 124
2.6. Controlled experiments 124
2.7. X-Ray Absorption Spectroscopy 127
2.8. XPS Spectra 128
3. Rates and Coefficients 130
3.9. Diffusion Coefficient 130
3.10. Thiele Modulus 131
3.11. Reaction Rates 131

Appendix 2. Appendix to Assessment of manganese in California's community water systems and geochemical controls of release into groundwater 132

1. Summary of available data 132
2. Statistical Results 133

Appendix 3: Appendix to Predicting manganese in drinking water accessed by domestic well communities and community water systems in Central Valley, California 137

1. Summary of data used 137
2. Distribution of predicted Mn exceedances in DWC and CWS 139
3. Reported Mn Water Quality in Domestic Wells 140
4. Summary of Statistical Results 141
5. Probability of Mn Exceedance for DWC users within CWS boundary 144
6. Probability of Mn Exceedance at various depths 145
7. Summary of DWCs within or outside disadvantaged communities 146
8. Possible point of use treatments for Mn in drinking water 147
9. Appendix References 148

List of Figures

Chapter 1

Figure 1. Diffusion limitations in soil aggregates ……...……5
Figure 2. Overview of biogeochemical reaction networks leading to Cr(III) oxidation…...7
Figure 3. Redox, sorption, and precipitation processes controlling Mn mobility ……...…9

Chapter 2

Figure 1. Aqueous concentration of iron and manganese in pyrolusite reactors …...…..…30
Figure 2. Aqueous concentration of Cr(VI) in pyrolusite reactors ……...…….31
Figure 3. Solid concentration of chromium and iron on pyrolusite minerals ...……..…….32
Figure 4. μ-XRF imaging and Cr K-edge μ-XANES spectra of birnessite ……..……..34
Figure 5. μ-XRF imaging and Cr K-edge μ-XANES spectra of pyrolusite ..……..……35
Figure 6. Aqueous concentration of iron and manganese in birnessite reactors ……...…37
Figure 7. Aqueous concentration of Cr(VI) in birnessite reactors ……..……38

Chapter 3

Figure 1. Mean Mn concentration measured at point of entry ……..……..63
Figure 2. Map of Mean Mn concentration in CWS ……..……. 64
Figure 3. Impact of treatment on Mn concentration within CWS ……...……65
Figure 4. Raw groundwater Mn concentration and primary groundwater contaminants 67
Figure 5. Raw groundwater Mn concentration and redox sensitive constituents …...…….68

Chapter 4

Figure 1. Distribution of mean Mn concentrations at point-of-entry ……...…..…101
Figure 2. Probability map of groundwater Mn in domestic well communities …....…… 102
Figure 3. Poverty in domestic well communities in the Central Valley……...……..104

Appendix 1

Figure S1. Schematic of diffusion limited reactor setup. ……..…….....…..…124
Figure S2. Iron and pyrolusite control reactors run without the addition of $Cr(OH)_3$ …...125
Figure S3. Iron diffusion control reactors run without $Cr(OH)_3$ or Mn oxides. 125
Figure S4. $Cr(OH)_3$ dissolution and diffusion control reactors ……..…….126
Figure S5. Solid concentration of chromium and iron on pyrolusite minerals ……..…126
Figure S6. K^3-weighted EXAFS of pyrolusite solids……..……..……127
Figure S7. XPS Survey spectra of pyrolusite…….……..……128
Figure S8. Fe 2p nd Mn 2p spectra of pyrolusite ……..……...…128
Figure S9. Spectra of O 1s, C 1s (middle), and Cr 2p of pyrolusite ……...…….……129

Appendix 3

Figure S1. Distribution of Mn exceedances in domestic well communities…....…… 139
Figure S2. Map of Mn exceedances for domestic well users within CWS boundaries.....144
Figure S3. Map of Mn exceedances for domestic well users at multiple depths 145
Figure S4. Map of community water systems within disadvantaged communities …..…146

List of Tables

Chapter 2

Table 1. Average oxidation state of pyrolusite ……..……33

Chapter 3

Table 1. Population potentially exposed to Mn above threshold values…..…….…..……63

Chapter 4

Table 1. Summary of spatial integration of available data…….……..… 97
Table 2. Data summary of available Mn concentration data at CWS point-of-entry…....100

Appendix 1

Table S1 Linear combination analysis of Fe EXAFS ……..……..…...……127
Table S2 Thiele Modulus calculations at different aggregate radiuses ……..……..…131
Table S3. Initial rates of Cr(III) oxidation and Mn(II) dissolution ……..……...…131

Appendix 2

Table S1. Open data sources used……..……..…….……132
Table S2. Count of available Mn data from SDWIS……..……..……132
Table S3 Count of water quality data……...…….……...……133
Table S4 Statistical results comparing Mn concentration between CWS sizes ….....…133
Table S5 Statistical results comparing pre- and post-treated Mn concertation …...……134
Table S6 Statistical results comparing co-occurring groundwater quality parameters.….134
Table S7 Correlation results comparing co-occurring groundwater quality parameters in raw groundwater.…….……..…135
Table S8 Correlation results comparing co-occurring groundwater quality parameters in treated groundwater ……135
Table S9. Statistical results comparing Mn and As concentrations by system size ….....136

Appendix 3

Table S1. Publicly available data sources ……..……..……137
Table S2. Count of available Mn data from SDWIS ……..…..……138
Table S3. Summary of mean Mn concentrations by system size……..……..... 138
Table S4. Reported Mn concentrations in domestic wells between 2001-2019..…....…140
Table S5. Summary of statistics comparing predicted Mn at drought depth.....….....…141
Table S6. Summary of statistics comparing predicted Mn at public well depth…..….....142
Table S7. Summary of statistics comparing occurrence of poverty ……...……..142
Table S8. Summary of statistics comparing the probability of the Mn concentration exceeding threshold values within and outside of disadvantaged communities....143
Table S9. DWC population within DAC and outside of DAC……....…… 146
Table S10. Summary of possible point-of-use treatments ……147

Summary of Equations

Chapter 2
Equation 1. Thiele Modulus 27

Chapter 3
Equation 1. Potentially exposed population 60

Appendix 1
Equation 1. Diffusion coefficient 130
Equation 2. Slope of diffusion line 130

Chapter 1: Introduction to geogenic contamination of groundwater

1. Global water quality

The *United Nations Right to Water Initiative* outlines the human right to water sources that are sufficient, physically accessible, affordable, and safe. The UN designates "safe" as free of chemical substances that may threaten a person's health or contain concentrations of toxic substances below standards defined by the local or national governing body (United Nations, 2010). Despite global recognition of the importance of safe drinking water, many anthropogenic and geogenic sources of contamination threaten its safety throughout the world and contribute to continued global health inequalities. Globally, three out of ten people still do not have access to safe drinking water (UNESCO World Water Assessment Programme, 2020). Further changes in seasonal and regional environments due to global climate change and increasing populations requiring access to clean water may continue to exacerbate current drinking water problems.

2. Water quality in California

In 2012, California was the first state in the nation to enact legislation recognizing the Human Right to Water (AB685) and clearly delineating that every individual has the right to safe, clean, affordable, and accessible water adequate for human consumption, cooking, and sanitary purposes. Following this legislation, the California State Water Resources Control Board resolved to "preserve, enhance, and restore the quality of California's water resources and drinking water for the protection of the environment, public health, and all beneficial uses […] for the benefit of present and future

generations" (State Water Resource Control Board, 2021). This legislation and resolution clearly prioritizes California's commitment to ensuring equitable access to safe drinking water. Despite this commitment, contamination of water sources accessed for domestic consumption within California is estimated to contribute to >15,000 premature cancer deaths over the next 70 years, largely due to exposure to the naturally occurring metals such as arsenic (Stoiber et al., 2019). Further sublethal impacts were not examined and may also represent an important consideration when assessing health-based impacts of contaminant exposure.

An important source of freshwater in California is groundwater. This resource supplies over 46% of the state's water supply and if contaminated, it may affect many users statewide (California Department of Water Resources, 2015). Mitigation measures, including monitoring and treatment of groundwater contaminants, will resolve many water quality issues. However, barriers to infrastructure access, whether natural, built, or managerial, may further drinking water driven health disparities within communities dependent upon public water systems or domestic wells (Balazs and Ray, 2014). Insufficient water infrastructure has led to over 3 million Californians served by community water systems to have had at least one contaminant violation between 2005-2015 (Bangia et al., 2020).

3. Subsurface biogeochemistry and water quality

A complex network of biogeochemical mechanisms, including reduction-oxidation (redox) reactions, is responsible for the mobilization of geogenic metal contaminants from aquifer materials into groundwater (Borch et al., 2010). The presence of geogenic

contaminants, such as Cr, As, and Mn, in groundwater is due to sequences of complex processes (i.e. biogeochemical reaction network), including mineral dissolution, diffusion, redox transformation, sorption, and precipitation. Areas in close proximity to soils with high concentrations of As or Cr, such as soils containing arsenopyrite or serpentine minerals, that undergo redox fluctuations through drying and wetting or faster rates of groundwater withdrawal, may be at higher risk of groundwater contamination (Parsons et al., 2013; Fakhreddine et al., 2015; McClain et al., 2019).

Metal speciation directly impacts its mobility, toxicity, and bioavailability within drinking water sources (Borch et al., 2010). For example, Cr(III) is considered a micronutrient, while Cr(VI) is a carcinogen (Costa and Klein, 2006; Zhitkovich, 2011). Within the subsurface, Cr(III) is a hydroxide precipitate that forms strong mineral complexes that further limits its mobility (Rai et al., 1987; Sass and Rai, 1987), whereas Cr(VI) is found as a highly-mobile chromate oxyanion that can migrate into drinking water sources (Cranston and Murray, 1980; Manceau and Charlet, 1992; Oze et al., 2007). Therefore, the pathways through which Cr(III) weathered from Cr(III)-bearing minerals (ultramafic rocks and serpentines enriched with chromite) is oxidized to Cr(VI) is of great interest since Cr(VI) is both more toxic and more mobile (Oze et al., 2007; Hausladen and Fendorf, 2017).

Redox conditions also greatly impact the mobilization of Mn(II) into freshwater resources. Increasing evidence of Mn neurotoxicity has brought more attention to the extent of Mn(II) solubilization and migration into drinking water sources (Spangler and Spangler, 2009; Bouchard et al., 2011; Khan et al., 2012; Coetzee et al., 2016). Oxic

conditions can promote the oxidation of Mn(II) with subsequent precipitation to Mn (III/IV) oxides; however, under anoxic and reducing conditions Mn(III/IV) oxides can be reductively dissolved to Mn(II) (Jurinak, 1957; Puckett and Cowdery, 2002; McMahon and Chapelle, 2008). Seasonal redox fluctuations can lead to the accumulation of secondary Mn(III/IV) minerals within aquifer materials , which can be remobilized if water levels increase to re-saturate the redox fluctuating zone (Gillispie et al., 2016; Ying et al., 2017).

In sum, a diversity of geochemical conditions contribute to contaminate release. Therefore, a systems approach, or the interrogation of the system as a whole, is needed to identify key dynamics that lead to the release and migration of geogenic contaminants into water resources which requires a systems approach to identify key drivers (McMahon and Chapelle, 2008). Unraveling subsurface redox reaction networks from the micron to field scale are important factors to assess risks and possible mitigation options.

4. Impact of micron-scale redox conditions

Our ability to interrogate flow and transport through the heterogeneous, structurally complex soil matrices is vital to our understanding of biogeochemical reactions in soil systems. Large pores within the soil matrix allow solutes to flow with the bulk solution via advection, whereas small pores have a higher tortuosity leading to diffusion dominated transport (i.e. species distribution is controlled by concentration gradients) (Gerke, 2006). Upland soils are often characterized as well-drained, where oxygen diffusion is assumed to proceed rapidly through the soil matrix which promotes aerobic microbial respiration of available soil carbon (Parton et al., 1988). However, due

to aggregation and soil structure, oxygen diffusion into microsites is often outpaced by microbial consumption of oxygen resulting in persistent anaerobic zones (Sexstone et al., 1985; Zausig et al., 1993). The presence of both (1) well-aerated zones where aerobic respiration dominates and (2) anoxic microsites where anaerobic respiration is favorable, controls the rates of carbon mineralization and nutrient cycling (e.g. denitrification and reductive dissolution of iron or manganese) (Pallud et al., 2010; Hall et al., 2013; Keiluweit et al., 2016; Figure 1)

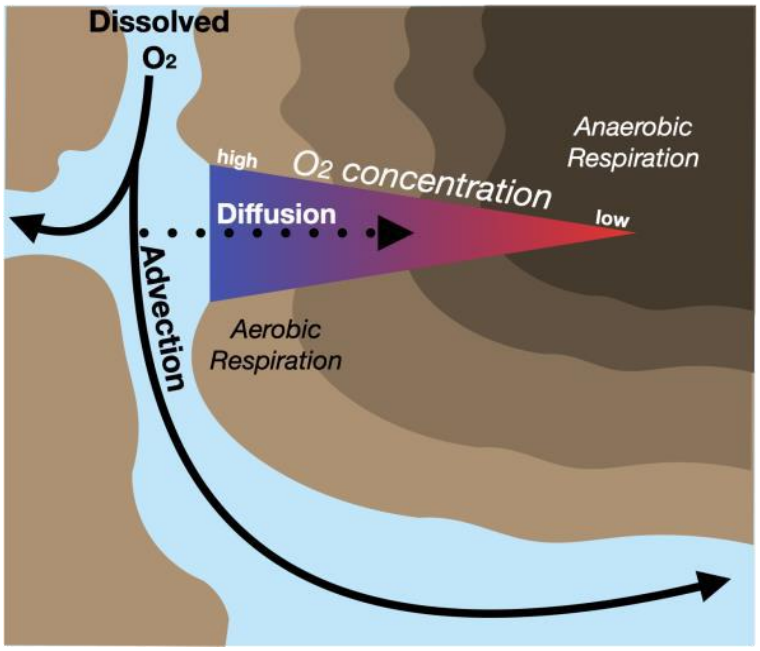

Figure 1. Dissolved oxygen is carried through large pore channels by advective flow between soil aggregates in well-aerated soil environments. Toward the interior of the soil aggregate, oxygen becomes increasingly limited due to diffusion-controlled transport, creating anoxic aggregate centers. Within the oxygen-limited and depleted interiors, microbial anaerobic respiration of organic carbon (i.e., oxidation of lower molecular weight organic acids) dominates. Image adapted from Keiluweit et al., 2016.

Neighboring zones within soils that favor anaerobic versus aerobic respiration creates redox interfaces that place highly reduced species, such as Fe(II), and oxidized species in close proximity (Pallud et al., 2010). Iron reduction, solubilization, and mineral transformation in a diffusion-controlled aggregate interior can determine the fate and transport of many contaminants and nutrients. Iron oxides and other iron-containing minerals are ubiquitous in soils and therefore its reduced product Fe(II) is pervasive throughout most soil profiles that do not have high sulfur content. As soluble Fe(II) diffuses out of an aggregate interior to an oxic zone near a an aerated flow channel, co-occurrence of Fe(II) and Fe(III) solid phases leads to Fe-driven contaminant redox transformations and contaminant mobilization into the aqueous phase (Pedersen et al., 2006; Frierdich and Catalano, 2012a, b), and incorporation of contaminants into mineral phases (Nico et al., 2009). Through consideration of both kinetic and transport limitations imposed by soil heterogeneity, we can more accurately characterize chemical and biological transformation of geogenic contaminants within soils.

The work covered in Chapter 2 investigates how the co-occurrence of Fe(II) and Cr(III) minerals in reduced zones of soil aggregates may inhibit Mn oxide catalyzed Cr(IV) formation within diffusion-limited systems. Altering the oxidation state and structure of Mn oxides impacts the oxidation of Cr(III), a non-toxic mineral, to Cr(VI), a mobile and highly toxic groundwater contaminant. Within this system, this may occur from the precipitation of Fe oxides on the surface of the Mn oxide, which blocks reactive sites (e.g., Postma, 1985; Krishnamurti and Huang, 1988; Schaefer et al., 2017; Mock et al., 2019). Simultaneously, the oxidation of Cr(III) and Fe(II) by Mn oxides also releases

Mn(II) through reductive dissolution which can react with the Mn oxides solids and result in lower mineral reactivity. By furthering our understanding on how various reductant concentrations and mineral crystallinities can control the mobility of redox active metals, such as chromium, we can better understand the net-transport of contaminants into groundwater.

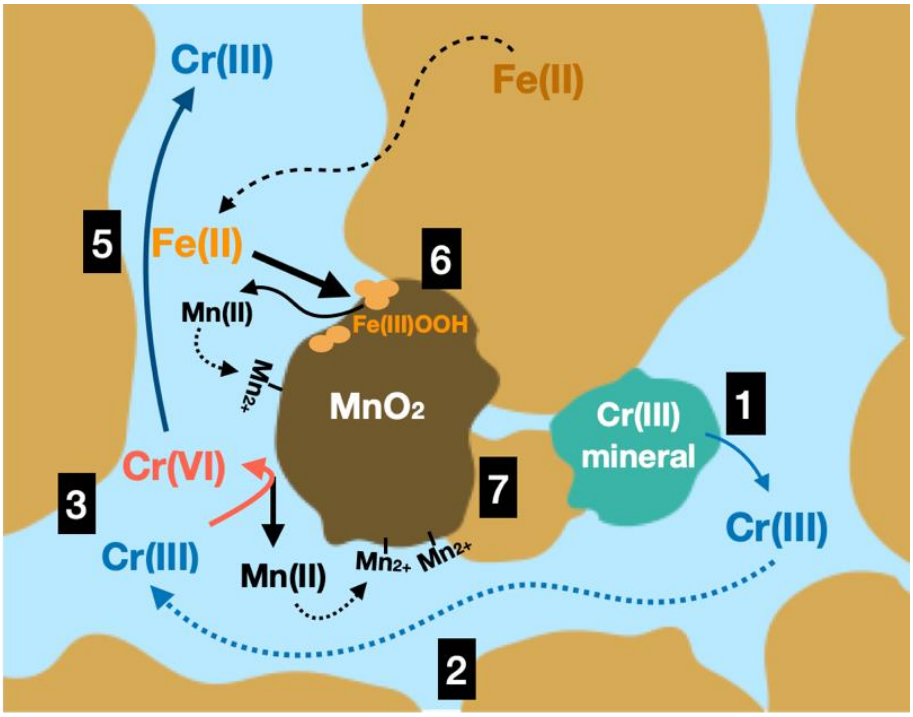

Figure 2. Overview of biogeochemical reaction networks involved in Cr(III) oxidation by Mn oxides in the presence of Fe(II). Cr(III) dissolution from $Cr(OH)_3$ (1) and subsequent diffusion to the surface of the Mn(III/IV) oxides (2) must occur before Cr(III) is rapidly oxidized to Cr(VI) on its surface (3). Fe(II) diffusion from anaerobic zones (4), can both directly reduce Cr(VI) (5) or precipitate as Fe oxide on the Mn(III/IV) oxide surface (6). Additionally, Mn(II) generated from the oxidation of Cr(III) or Fe(II) can react with the Mn(III/IV) oxides resulting in reductive transformation of the mineral surface (7).

5. Impact of field-scale redox conditions

Determining the spatial distribution of redox conditions within regional aquifer basins can aid with the prediction of groundwater contamination from redox active metals. Regional stratification of redox conditions driven by geology, hydrology, and climate can also be extremely localized (McMahon and Chapelle, 2008). Models created to predict redox conditions in aquifers include predictor variables including groundwater residence time, flow patterns, subsurface geology, biogeochemical parameters, and geographic location (Rosecrans et al., 2017; Erickson et al., 2021). The heterogeneous distribution of these factors within aquifers results in "hot-spots" of redox conditions favorable for the release of geogenic contaminants. Therefore, where and how users access these groundwater resources are key factors that determine the quality of water extracted

However, a challenge when addressing redox sensitive contaminant release is the contrasting behavior of toxic metals under a range of redox conditions. The behavior of Mn in the subsurface is driven by heterogeneous distribution of redox conditions and regional chemistry (Figure 3). For example, anaerobic conditions are favorable for microbial reductive dissolution of Mn and Fe oxides, which can mobilize adsorbed metals or metalloids, such as As (e.g., Fendorf et al., 2010; Neil et al., 2014). Soluble Mn(II) produced from reductive processes can then be re-immobilized through enzyme catalyzed oxidation with molecular oxygen to form Mn(III/IV) oxides (Tebo, 2004). Because abiotic Mn(II) oxidation is relatively slow, high concentrations of Mn may accumulate at relatively shallow aquifer depths over time (Gillispie et al., 2016). In

contrast, suboxic to anoxic conditions at deeper aquifer depths can lead to accumulation of carbonate from anaerobic microbial respiration, which can immobilize Mn(II) through precipitation of Mn(II) carbonates (Buschmann et al., 2007; Schaefer et al., 2020).

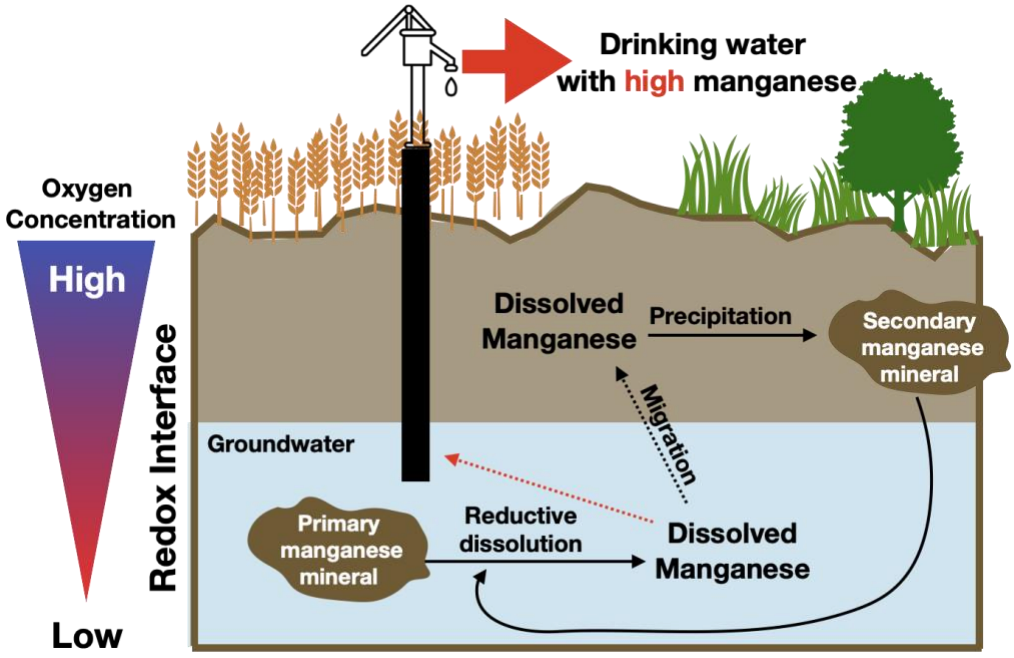

Figure 3. Redox, sorption, and precipitation processes controlling Mn mobility in groundwater aquifers, which determines soluble Mn contaminant levels in well water.

Previously Mn was only regarded as a nuisance contaminant; however, recently, regulatory agencies are reconsidering Mn exposure through drinking water as a threat to human health (World Health Organization, 2021; California State Water Resource Control Board, 2021). Therefore, increased attention to its release and distribution to users is greatly needed. In Chapter 3, monitoring data is used to quantify Mn occurrence in California's community water systems in both treated and untreated water. Community water systems were further sorted by system size based on user population to determine if disparities exist in Mn treatment within smaller systems with limited infrastructure.

Further consideration of co-occurring redox sensitive and primary contaminants was used to better understand the impact of redox conditions on Mn release into water accessed for domestic use. Since groundwater accessed by private wells is likely what is used at-tap, Chapter 4 investigates private well communities' risk of accessing groundwater with high Mn in California's Central Valley. Possible mitigation strategies, such as accessing deeper groundwater, were evaluated. Additionally, differences in poverty level within domestic well communities were investigated to determine areas where point-of-use treatment may be cost-prohibitive.

6. Barriers to addressing diminished groundwater quality

An improved understanding of the natural infrastructure – such as the controls on subsurface redox conditions – will provide communities and water managers with better tools to improve access to safe drinking water. By identifying geographic regions likely to have high contaminant levels caused by fine-scale biogeochemical processes, we can then design infrastructure, monitoring, and treatment to mitigate the impacts of their release on human health. However, a key tenet of the Human Right to Water initiative is that it extends to all individuals within the state, including those within disadvantaged or rural communities (State Water Resource Control Board, 2021). Barriers to accessing water treatment or infrastructure due to financial or political reasons may make these mitigation efforts difficult to obtain and result in inequitable access to safe drinking water. Therefore, full consideration of such barriers will allow improved allocation of resources to communities that need it the most.

7. Importance of interdisciplinary approach

To effectively evaluate the safety of our drinking water, it is critical that we understand the network of complex biogeochemical reactions that control geogenic metals cycling. The overarching goal of this work is to explore how redox conditions in the redox fluctuating zone influences the release of geogenic metals and threaten drinking water sources on various scales, from individual soil aggregates to entire aquifer basins, to better manage our groundwater resources. By considering how redox conditions and the contaminant co-occurrence may limit or contribute to the release of geogenic metals in our proposed work, we can better understand factors that control groundwater contamination and optimize groundwater management practices.

8. References

Balazs C. L. and Ray I. (2014) The Drinking Water Disparities Framework: On the Origins and Persistence of Inequities in Exposure. *Am J Public Health* **104**, 603–611.

Bangia K., August L., Slocombe A. and Faust J. (2020) Assessment of contaminants in California drinking water by region and system size. *AWWA Water Science* **2**, e1194.

Borch T., Kretzschmar R., Kappler A., Cappellen P. V., Ginder-Vogel M., Voegelin A. and Campbell K. (2010) Biogeochemical Redox Processes and their Impact on Contaminant Dynamics. *Environ. Sci. Technol.* **44**, 15–23.

Bouchard M. F., Sauvé S., Barbeau B., Legrand M., Brodeur M.-È., Bouffard T., Limoges E., Bellinger D. C. and Mergler D. (2011) Intellectual impairment in school-age children exposed to manganese from drinking water. *Environ Health Perspect* **119**, 138–143.

Buschmann J., Berg M., Stengel C. and Sampson M. L. (2007) Arsenic and manganese contamination of drinking water resources in Cambodia: coincidence of risk areas with low relief topography. *Environ Sci Technol* **41**, 2146–2152.

California Department of Water Resources (2015) California Water Plan - Groundwater Update. https://cawaterlibrary.net/wp-content/uploads/2017/05/GWU2013_Combined_Statewide_Final.pdf

California State Water Resource Control Board (2021) Drinking Water Notification Level for Manganese. https://www.waterboards.ca.gov/drinking_water/certlic/drinkingwater/Manganese

Coetzee D. J., McGovern P. M., Rao R., Harnack L. J., Georgieff M. K. and Stepanov I. (2016) Measuring the impact of manganese exposure on children's neurodevelopment: advances and research gaps in biomarker-based approaches. *Environ Health* **15**, 91.

Costa M. and Klein C. B. (2006) Toxicity and Carcinogenicity of Chromium Compounds in Humans. *Critical Reviews in Toxicology* **36**, 155–163.

Cranston R. E. and Murray J. W. (1980) Chromium species in the Columbia River and estuary1. *Limnology and Oceanography* **25**, 1104–1112.

Erickson M. L., Elliott S. M., Brown C. J., Stackelberg P. E., Ransom K. M., Reddy J. E. and Cravotta C. A. (2021) Machine-Learning Predictions of High Arsenic and

High Manganese at Drinking Water Depths of the Glacial Aquifer System, Northern Continental United States. *Environ. Sci. Technol.* **55**, 5791–5805.

Fakhreddine S., Dittmar J., Phipps D., Dadakis J. and Fendorf S. (2015) Geochemical Triggers of Arsenic Mobilization during Managed Aquifer Recharge. *Environ. Sci. Technol.* **49**, 7802–7809.

Fendorf S., Michael H. A. and van Geen A. (2010) Spatial and temporal variations of groundwater arsenic in South and Southeast Asia. *Science* **328**, 1123–1127.

Frierdich A. J. and Catalano J. G. (2012a) Controls on Fe(II)-Activated Trace Element Release from Goethite and Hematite. *Environ. Sci. Technol.* **46**, 1519–1526.

Frierdich A. J. and Catalano J. G. (2012b) Fe(II)-Mediated Reduction and Repartitioning of Structurally Incorporated Cu, Co, and Mn in Iron Oxides. *Environ. Sci. Technol.* **46**, 11070–11077.

Gerke H. H. (2006) Preferential flow descriptions for structured soils. *Journal of Plant Nutrition and Soil Science* **169**, 382–400.

Gillispie E. C., Austin R. E., Rivera N. A., Bolich R., Duckworth O. W., Bradley P., Amoozegar A., Hesterberg D. and Polizzotto M. L. (2016) Soil Weathering as an Engine for Manganese Contamination of Well Water. *Environ. Sci. Technol.* **50**, 9963–9971.

Hall S. J., McDowell W. H. and Silver W. L. (2013) When Wet Gets Wetter: Decoupling of Moisture, Redox Biogeochemistry, and Greenhouse Gas Fluxes in a Humid Tropical Forest Soil. *Ecosystems* **16**, 576–589.

Hausladen D. M. and Fendorf S. (2017) Hexavalent Chromium Generation within Naturally Structured Soils and Sediments. *Environ. Sci. Technol.* **51**, 2058–2067.

Jurinak J. J. (1957) The Effect of Clay Minerals and Exchangeable Cations on the Adsorption of Ethylene Dibromide Vapor 1. *Soil Science Society of America Journal* **21**, 599–602.

Keiluweit M., Nico P. S., Kleber M. and Fendorf S. (2016) Are oxygen limitations under recognized regulators of organic carbon turnover in upland soils? *Biogeochemistry* **127**, 157–171.

Khan K., Wasserman G. A., Liu X., Ahmed E., Parvez F., Slavkovich V., Levy D., Mey J., van Geen A., Graziano J. H. and Factor-Litvak P. (2012) Manganese exposure from drinking water and children's academic achievement. *NeuroToxicology* **33**, 91–97.

Krishnamurti G. S. R. and Huang P. M. (1988) Influence of Manganese Oxide Minerals on the Formation of Iron Oxides. *Clays Clay Miner.* **36**, 467–475.

Manceau A. and Charlet L. (1992) X-ray absorption spectroscopic study of the sorption of Cr(III) at the oxide-water interface: I. Molecular mechanism of Cr(III) oxidation on Mn oxides. *Journal of Colloid and Interface Science* **148**, 425–442.

McClain C. N., Fendorf S., Johnson S. T., Menendez A. and Maher K. (2019) Lithologic and redox controls on hexavalent chromium in vadose zone sediments of California's Central Valley. *Geochimica et Cosmochimica Acta* **265**, 478–494.

McMahon P. B. and Chapelle F. H. (2008) Redox processes and water quality of selected principal aquifer systems. *Ground Water* **46**, 259–271.

Mock R. P., Schaefer M. V., Pacheco J. L., Lake L., Lee I. and Ying S. C. (2019) Influence of Fe(II) on Arsenic(III) Oxidation by Birnessite in Diffusion-Limited Systems. *ACS Earth Space Chem.* **3**, 550–561.

Neil C. W., Yang Y. J., Schupp D. and Jun Y.-S. (2014) Water Chemistry Impacts on Arsenic Mobilization from Arsenopyrite Dissolution and Secondary Mineral Precipitation: Implications for Managed Aquifer Recharge. *Environ. Sci. Technol.* **48**, 4395–4405.

Nico P. S., Stewart B. D. and Fendorf S. (2009) Incorporation of Oxidized Uranium into Fe (Hydr)oxides during Fe(II) Catalyzed Remineralization. *Environ. Sci. Technol.* **43**, 7391–7396.

Oze C., Bird D. K. and Fendorf S. (2007) Genesis of hexavalent chromium from natural sources in soil and groundwater. *PNAS* **104**, 6544–6549.

Pallud C., Kausch M., Fendorf S. and Meile C. (2010) Spatial Patterns and Modeling of Reductive Ferrihydrite Transformation Observed in Artificial Soil Aggregates. *Environ. Sci. Technol.* **44**, 74–79.

Parsons C. T., Couture R.-M., Omoregie E. O., Bardelli F., Greneche J.-M., Roman-Ross G. and Charlet L. (2013) The impact of oscillating redox conditions: Arsenic immobilisation in contaminated calcareous floodplain soils. *Environmental Pollution* **178**, 254–263.

Parton W. J., Stewart J. W. B. and Cole C. V. (1988) Dynamics of C, N, P and S in grassland soils: a model. *Biogeochemistry* **5**, 109–131.

Pedersen H. D., Postma D. and Jakobsen R. (2006) Release of arsenic associated with the reduction and transformation of iron oxides. *Geochimica et Cosmochimica Acta* **70**, 4116–4129.

Postma D. (1985) Concentration of Mn and separation from Fe in sediments—I. Kinetics and stoichiometry of the reaction between birnessite and dissolved Fe(II) at 10°C. *Geochimica et Cosmochimica Acta* **49**, 1023–1033.

Puckett L. J. and Cowdery T. K. (2002) Transport and fate of nitrate in a glacial outwash aquifer in relation to ground water age, land use practices, and redox processes. *J Environ Qual* **31**, 782–796.

Rai D., Sass B. and Moore D. (1987) Chromitim(III) Hydrolysis Constants and Solubility of Chromium(III) Hydroxide. *Inorganic Chemistry* **26**, 345–349.

Rosecrans C. Z., Nolan B. T. and Gronberg J. M. (2017) Prediction and visualization of redox conditions in the groundwater of Central Valley, California. *Journal of Hydrology* **546**, 341–356.

Sass B. and Rai D. (1987) Solubility of Amorphous Chromium(III)-Iron(III) Hydroxide Solid Solutions. *Inorganic Chemistry* **26**, 2228–2232.

Schaefer M. V., Handler R. M. and Scherer M. M. (2017) Fe(II) reduction of pyrolusite (β-MnO2) and secondary mineral evolution. *Geochem Trans* **18**, 7.

Schaefer M. V., Plaganas M., Abernathy M., Aiken M. L., Garniwan A., Lee I. and Ying S. C. (2020) Manganese, arsenic, and carbonate interactions in model oxic groundwater systems. *Environ. Sci. Technol.*

Sexstone A. J., Revsbech N. P., Parkin T. B. and Tiedje J. M. (1985) Direct Measurement of Oxygen Profiles and Denitrification Rates in Soil Aggregates. *Soil Science Society of America Journal* **49**, 645–651.

Spangler A. H. and Spangler J. G. (2009) Groundwater Manganese and Infant Mortality Rate by County in North Carolina: An Ecological Analysis. *EcoHealth* **6**, 596–600.

State Water Resource Control Board (2021) Failing Water Systems: The Human Right to Water (HR2W) List Criteria. https://www.waterboards.ca.gov/water_issues/programs/hr2w/docs/hr2w_expanded_criteria.pdf

Stoiber T., Temkin A., Andrews D., Campbell C. and Naidenko O. V. (2019) Applying a cumulative risk framework to drinking water assessment: a commentary. *Environmental Health* **18**, 37.

Tebo B. M. (2004) Biogenic Manganese Oxides: Properties and Mechanisms of Formation. *Annual Review of Earth and Planetary Sciences* **32**, 287–328.

UNESCO World Water Assessment Programme (2020) The United Nations world water development report 2020: water and climate change. https://www.unwater.org/publications/world-water-development-report-2020/

United Nations Human Rights to Water and Sanitation. *UN-Water*. https://www.unwater.org/water-facts/human-rights/

World Health Organization (2021) Manganese in drinking water. https://www.who.int/docs/default-source/wash-documents/wash-chemicals/gdwq-manganese-background-document-for-public-review.pdf?sfvrsn=9296741f_5

Ying S. C., Schaefer M. V., Cock-Esteb A., Li J. and Fendorf S. (2017) Depth Stratification Leads to Distinct Zones of Manganese and Arsenic Contaminated Groundwater. *Environ. Sci. Technol.* **51**, 8926–8932.

Zausig J., Stepniewski W. and Horn R. (1993) Oxygen Concentration and Redox Potential Gradients in Unsaturated Model Soil Aggregates. *Soil Science Society of America Journal* **57**, 908–916.

Zhitkovich A. (2011) Chromium in Drinking Water: Sources, Metabolism, and Cancer Risks. *Chem. Res. Toxicol.* **24**, 1617–1629.

Chapter 2: Inhibition of chromium (III) oxidation through manganese (IV) oxide passivation and Fe(II) abiotic reduction

1. Abstract

Manganese (Mn) oxides are strong oxidants ubiquitous in soils and can oxidize redox active metals, such as chromium (Cr). In soil environments, trivalent chromium [Cr(III)] is benign, immobile micronutrient, whereas the hexavalent [Cr(IV)] form is present as a highly mobile, toxic chromate oxyanion. Although many studies have characterized the capacity of Mn(IV) oxides to oxidize Cr(III) to toxic Cr(VI), the oxidative capacity of Mn(IV) oxides in the presence of potentially passivating soil constituents, including reduced soluble iron [$Fe(II)_{aq}$], remains unresolved. It is hypothesized that at redox interfaces, such as diffusion-limited environments within soil aggregates, can lead to decreased Cr(VI) production from Mn(IV) oxides due to passivation by $Fe(II)_{aq}$.

A multi-chamber, diffusion-limited reactor was used to simulate transport at soil redox interfaces and investigate the capacity of poorly-crystalline and crystalline Mn(IV) oxides to oxidize solid Cr(III) minerals to Cr(VI) in the presence of $Fe(II)_{aq}$. Without $Fe(II)_{aq}$, Cr(VI) was generated at a rate controlled by the solubility of $Cr(OH)_3$. With $Fe(II)_{aq}$ in the Cr/Mn system, Cr(VI) generation decreased as a function of $Fe(II)_{aq}$ concentration, where high concentrations of $Fe(II)_{aq}$ completely inhibited Cr(VI) production likely through both Mn oxide passivation and Cr(VI) back reduction. At both $Fe(II)_{aq}$ concentrations iron oxide minerals hematite (Fe_2O_3)and goethite (a-FeOOH) formed on the Mn oxide surface as evidence that surface passivation likely plays a role in

decreasing Cr oxidation. Additionally, Cr(III) oxidation rate decreased with increasing crystallinity of the Mn oxides due to lower specific surface area of the Mn oxide.

2. Introduction

Chromium is both a naturally occurring and anthropogenically sourced redox-active soil and water contaminant that occurs predominantly in the Cr(III) and Cr(VI) oxidation states (Richard and Bourg, 1991; Ball and Nordstrom, 1998; Costa and Klein, 2006). Cr(III) is an essential trace micronutrient, however ingestion of Cr(VI) is linked to adverse human health outcomes including cancer (Zhitkovich, 2011). In the subsurface, trivalent chromium is commonly found as a sparingly soluble hydroxide precipitate that can form strong mineral complexes (Rai et al., 1987), whereas hexavalent chromium is present as a highly mobile, toxic chromate oxyanion found in groundwater sources including aquifers in California's Central Valley (Oze et al., 2007; Hausladen et al., 2018). Chromite, Cr-magnetite, and Cr-bearing silicates are common sources of geogenic Cr(III) in soils and sediments which can undergo *in situ* abiotic oxidation to Cr(VI) (Oze et al., 2004). Since Cr(III)-bearing minerals cover roughly 1% of the Earth's surface and along plate boundaries, understanding processes that enhance or inhibit abiotic oxidation of Cr(III) to Cr(VI) have implications for global groundwater quality and those who rely on this resource (Oze et al., 2004; Hausladen et al., 2018).

Prior to oxidation, dissolution of Cr(III) from Cr-bearing minerals and migration of Cr(III) to Mn oxide solids must occur. In well-mixed environments, Cr(III) oxidation is limited by the solubility of the Cr(III) mineral and the distance it must travel to the site of oxidation (Hausladen and Fendorf, 2017; Pan et al., 2017). Increasing iron substitution

in $Cr_xFe_{1-x}(OH)_3$ secondary minerals decreases the mineral solubility, and consequently Cr(VI) generation (Hausladen and Fendorf, 2017; Pan et al., 2017). Abiotic oxidation of Cr(III) in soils is dominantly catalyzed by manganese(III/IV) oxides (Eary and Rai, 1991; Fendorf and Zasoski, 1992; Oze et al., 2007). Manganese(III/IV) oxides in soils are generally biogenic poorly-crystalline, layered Mn(III/IV) minerals that are highly reactive due to their large surface area (Tebo, 2004). Under reducing conditions, anaerobic microbial respiration can produce reduced species such as Fe(II), Mn(II), and microbial metabolites which can decrease the oxidative capacity of Mn oxides (Ying et al., 2011; Wu et al., 2015; Mock et al., 2019), therefore, potentially inhibiting Mn oxide-driven Cr(VI) production. Simultaneously, Fe(II) can also directly reduce Cr(VI) to form very weakly soluble Cr(III)-Fe(III) hydroxides as a dominant abiotic mechanism of Cr immobilization under reducing conditions (Sass and Rai, 1987; Fendorf and Li, 1996).

Within soil environments exist complex, heterogeneous soil aggregate structures connected by complex pore networks. Dissolved oxygen moves through larger pore throats via advective flow, whereas diffusive transport dominates within finer pore throats including intra-aggregate pores (Gerke, 2006). Within the soil aggregate, the rate of oxygen consumption in the interior of aggregates can be greater than the rate of oxygen supplied by diffusion creating a redox gradient from the exterior to interior of aggregates (Sexstone et al., 1985; Zausig et al., 1993). These sustained anaerobic microsites within soil aggregates support microbial Fe(III) respiration, producing soluble Fe(II) that then diffuses to the oxygenated or more oxidizing aggregate exterior (Tokunaga et al., 2003; Ying et al., 2013; Masue-Slowey et al., 2013). Ying et al. (2013)

and Masue-Slowey et al. (2013) demonstrated that abiotic oxidation of Fe(II) with molecular oxygen and Mn oxides at the aggregate exterior leads to Fe(III) hydroxide precipitation which can act as a high affinity and capacity adsorbent for reduced metal contaminants, such as arsenic, co-transported outward from the aggregate center. Within the oxic exterior of soil aggregates, it has been demonstrated that Cr(VI) reduction occurs due to increased organic carbon and microbial activity which drives either direct reduction or the release of reactive reductants, such as Fe(II), that then reduces Cr(VI) (Tokunaga et al., 2001, 2003).

Though the aforementioned abiotic Cr oxidation and reduction pathways have been investigated individually, a systems approach is better representative of the environment where aqueous and solid phases of minerals are often physically separated, aqueous species movement may be limited by diffusion, and co-occurring elements may alter the oxidative potential of the system. Despite the rate limitations of geogenic Cr(VI) production in soils, Cr(VI) formation is observed in these highly-structured soil environments where it can then migrate into aquifers used as drinking water sources (Gonzalez et al., 2005; Ndung'u et al., 2009).

In this study, we investigate how the co-occurrence of Fe(II) and Cr(III) within a diffusion-controlled environment may alter the oxidative potential of Mn oxides and, therefore, the oxidation of Cr(III) to Cr(VI). To do this, we utilize a diffusion-limited reactor to model highly structured soil environments. We also examined the effect of two Mn oxides, pyrolusite and birnessite, of varying crystallinity to investigate the impact of Mn oxide reactivity on Cr(III) oxidation and two Fe(II) concentrations representative of

concentrations observed at the surface of constructed soil aggregates. We hypothesize Cr(III) oxidation will occur despite diffusion limitations, and Cr(VI) detection within the system will decrease as a function of increasing Fe(II) concentration.

3. Materials and Methods

A multi-chamber reactor was used to investigate the impact of high and low Fe(II) concentrations on the capacity of poorly-crystalline and crystalline Mn oxides (birnessite and pyrolusite, respectively) to oxidize Cr(III) from chromium hydroxides ($Cr(OH)_3$, moderate solubility) in a diffusion-controlled environment. The multi-chamber reactor has been described in detail previously (Ying et al., 2011; Mock et al., 2019). Aside from simulating transport-limited conditions, the multi-chamber reactor is uniquely designed to maintain physical separation of solid phases within their respective chambers for detailed solid phase analysis of individual mineral phases that is not possible within homogenous batch or synthetic aggregate reactor systems.

3.1. Mineral Synthesis

Chromium(III) hydroxides ($Cr(OH)_3$) were synthesized by titrating 50 mM solution of $CrCl_3$ to a pH of 6 with NaOH and stirred for 24 hours at room temperature, similar to the procedure described in Hansel et al. (2003). The solids were centrifuged, triple rinsed with double deionized water (DDI, 18 MΩ-cm), dried in a warm oven (30°C), and ground prior to experimental use. Birnessite was synthesized following the protocol described by McKenzie (1971). 63 g of $KMnO_2$ (Fisher Scientific) was dissolved into 1 L DDI water and heated to 90°C. While vigorously stirring, 66 mL of concentrated HCl was added to the heated $KMnO_2$ solution in a 4 L flask and maintained at

temperature for 10 minutes. After letting the slurry cool for 30 minutes, the oxides were filtered through 50 μm ashless filter paper (Whatman) and triple washed with DDI. Dried solids were ground with an agate mortar and pestle prior to experimental use. Pyrolusite was purchased from Sigma Aldrich. Mineral identities were confirmed using powder X-ray diffraction (XRD) analysis using a Siemens D500 diffractometer with a Cu Kα X-ray source operating at 40 kV. JADE software (Materials Data, Inc.) was used to analyze the data and peak positions and intensities were matched with data from RRUFF database (rruff.info). The surface area of minerals was determined with multi-surface BET and adsorption-desorption BJH methods using a Quantachrome Nova 2000e.

3.2. Multi-chamber Reactor

All experiments were conducted in an anoxic glove bag (95% N_2:5% H_2 atmosphere; COY) at ambient temperature (25^o C). The multi-chamber diffusion reactor was constructed using PVC pipes (ID 209-030, 7.6 cm internal diameter) separated by a 0.05-μm nitrocellulose isopore filter (Millipore) to simulate diffusion-controlled transport within soil aggregates.

Manganese oxides (3.5 g) were added to 750 mL deoxygenated solution (10 mM PIPES and 10 mM NaCl buffered at pH 7 to approximate average soil pore water pH and ionic strength) in one reaction chamber and allowed to equilibrate for 24 hours with continuous stirring at 400 rpm using overhead impellers. The experiment was initiated by suspending 2 g of Cr(III) hydroxides in the adjacent reactor chamber in 750 mL of buffer solution. To examine the effect of Fe(II) on Cr(VI) reduction and inhibition of Mn oxidation, $FeCl_2$ stock solution (3 M Fe(II)) was then added to the Cr(III) hydroxide

containing chamber to a final concentration of 14 µM or 100 µM in the Cr(III) hydroxide chamber. The reactions were run for 96 hours and sampled throughout the duration of the experiment.

3.3. Aqueous Phase Analysis

For aqueous analysis, 5 mL of slurry was withdrawn from each chamber and filtered through a 0.22-µm cellulose acetate filter (CVS) and acidified with concentrated trace metal grade HNO_3. Dissolved Cr, Fe, and Mn concentrations were measured using ICP-OES (PerkinElmer Optima 7300DV). Dissolved Cr(VI) was quantified following Bartlett and James (1973) using s-diphenyl carbazide (DPC) colorimetric assay. DPC reagent was made by dissolving 0.05 g DPC into 10 mL methanol and adding to 87.2 mL DDI water with 2.8 mL H_2SO_4 while minimizing light exposure. To determine Cr(VI), 0.125 mL of the DPC reagent was added to 1 mL of filtered sample and developed for 20 minutes (detection limit = 0.1 µM). Absorbance was measured at 540 nm on a spectrophotometer (Genesys 20 Thermo Spectronic).

3.4. Solid Phase Analysis

The total concentration of solid phase Mn, Fe, and Cr was determined by acid digestion. During sampling, 5 mL of slurry was collected from each chamber. All liquid was allowed to evaporate from the centrifuge tubes in a 90°C heat block. Dried solids were then resuspended in 3 mL of concentrated trace metal grade HNO_3 and agitated until dissolved. Acid dissolved samples were then diluted with DDI water and analyzed using ICP-OES for Mn, Fe, and Cr. Final solid concentrations were calculated by

subtracting the aqueous concentrations from the total digestions after accounting for dilutions.

3.5. Bulk X-Ray Absorption Spectroscopy

To determine Cr and Mn oxidation state and Fe oxide mineral formation and transformation over time, Mn oxide solids were collected by depositing solids from 5 mL of slurry onto a 0.22-μm cellulose acetate filter (CVS) and dried in an anoxic glove bag. All samples were stored anoxically until immediately before X-ray analysis. Samples were transported to Stanford Synchrotron Radiation Lightsource (SSRL) in an anoxic container (Mitsubishi) with O_2 scavenging AnaeroPacks (Mitsubishi). Prior to analysis, solids deposited onto the filter were sealed in 0.5-mil Kapton tape and mounted onto an aluminum sample holder.

XAS spectra were collected at SSRL beamlines 4-1, 4-3, and 11-2. Mn K-edge X-ray absorption near edge structure (XANES) spectra were collected at beamline 4-1 under liquid-N_2 cryostat (~77K) to limit Mn photoreduction. Fluorescence data were collected using a PIPS detector with soller slits and Cr filter (3 absorption lengths) placed 7.5 cm perpendicular to the beam path. Spectra were collected in 5 eV steps below the edge (6310-6520 eV), in 0.25 eV steps at the edge (6520-6570 eV), and in steps equivalent to 0.05 $Å^{-1}$ above the edge.

Bulk Fe K-edge EXAFS spectra were collected at beamline 11-2 at room temperature using a He purge box (<0.15% O_2). Fluorescence and transmission data were collected using a 7-channel silicon drift detector or a 100-element Ge detector. Fe spectra were collected from 6922 to 7712 eV, approximately to a k = 12. Different points

on each Fe sample were selected for the replicate scans (~5 scans) to prevent photooxidation. Comparison of the scans showed no indication of beam damage. Data processing and linear combination analysis (LCA) was performed in Athena software (Ravel and Newville, 2005). The pre- and post-edge regions were fit with linear and third order polynomial functions, respectively, and spectra were normalized to an edge step of 1. Goethite, ferrihydrite, hematite, magnetite, and lepidocrocite standards were used for the LCA fitting. Chromium K-edge XANES spectroscopic analysis was attempted on beamline 11-2 using a 100-element Ge detector, but because bulk concentrations were below detection limit, samples were analyzed using micro-X-ray fluorescence (μ-XRF) mapping to perform μ-XANES on Cr hotspots (details in Methods section 2.6).

Manganese average oxidation state (AOS) and proportion of Mn(II), Mn(III), and Mn(IV) were estimated by fitting sample spectra with a linear combination of Mn XANES reference standards ($MnSO_4$, manganite, and birnessite, respectively) following the standards library compiled and analysis procedure outlined by Manceau et al. (Manceau et al., 2012).

3.6. μ-XRF Imaging and Sample Preparation

Spatial distribution (e.g., co-location) of Cr and Fe on Mn oxide particles and Cr speciation was determined by performing micro-X-ray fluorescence (μ-XRF) imaging analysis at Stanford Synchrotron Radiation Lightsource beamline 2-3 on pyrolusite and birnessite particles collected at the end of the experiments. Chromium hotspots identified using μ-XRF images were then analyzed using μ-XANES analysis to determine Cr redox speciation.

To prepare samples for μ-XRF analysis, anoxically dried solid samples from the Mn oxide-containing chamber were embedded in Loctite 404 adhesive in a 1.5 mL centrifuge tube under anoxic conditions (O_2 < 1 ppmv, H_2 ~3.5%) and allowed to cure for >24 hours. Loctite is relatively free of impurities and μ-XRF analysis of the Loctite matrix revealed no noticeable background for Cr, Mn, or Fe. The bottom of the centrifuge tube and sample were cut and glued to 2 inch x 2 inch x 1 mm thick quartz slide (Ted Pella part no. 26012). The sample was then cut to ~1 mm thickness and polished to 100-200 microns depending on contact with the slide.

μ-XRF analysis was carried out at 6010 eV for total Cr, total Fe at 7500 eV or 7150 eV, and total Mn at 7500 eV or 7150 eV. The beam was calibrated to the pre-edge peak of Na_2CrO_4 at 5993 eV for Cr mapping. Multi-energy maps were collected on birnessite samples for Cr speciation (total Cr at 6010 eV and Cr(VI) at 5993 eV), Fe speciation [7122 eV intensity subtracted from intensity at 7130 eV representing Fe(III)] and Mn speciation [6559 eV subtracted from 6553 eV representing Mn(III), 6562 eV subtracted from 6559 eV representing Mn(IV)] and processed using map math in SMAK software (Webb, 2005). Chromium μ-XANES spectral points were chosen based on high Cr intensities detected in total Cr μ-XRF maps. μ-XANES spectra were then processed and analyzed using the same methods outlined for bulk XANES analysis. Total Mn, Fe, and Cr maps were generated using SMAK (Webb, 2005).

3.7. X-Ray Photoelectron Spectroscopy Oxidation States

X-Ray photoelectron spectroscopic (XPS) data was collected with a Kratos AXIS Ultra DLD XPS instrument with an Al Kα monochromated X-ray source and a 165 mm

electron energy hemispherical analyzer. All samples were collected under vacuum pressure below 3 x10^{-9} Torr during analysis. Spectra were calibrated using the C 1s peak at 284.8 eV and oxidation states were determined by comparing observed peaks with peaks at known energies.

3.8. Diffusion Modeling

The Thiele modulus (Thiele, 1939; Tokunaga et al., 2001; Ying et al., 2012) was used to determine if reactions were diffusion or reaction (i.e. chemical kinetics) limited within the multi-chamber experiments. To estimate systems with first-order reaction rates and constant diffusivities the following equations were used:

Equation 1.

$$\phi = R\sqrt{\frac{k}{D_e}}$$

R = radius of the aggregate (mm)
k = first-order rate constant (s^{-1})
D_e = effective diffusivity of the of the aggregate ($mm^2\ s^{-1}$)

If Φ is <0.3 then the reaction is assumed to be kinetically limited and if Φ is >3, then reactions are diffusion limited. The half-length of the reactor used in these experiments was 70 mm.

To determine the rate $Cr(OH)_3$ dissolution and subsequent diffusion of Cr(III) across the membrane, 2 g of $Cr(OH)_3$ was added to 750 mL of background solution in one reactor chamber and allowed to equilibrate between the two chambers in the absence of Mn oxides and Fe(II). Aqueous samples from the adjacent chamber were collected over time and dissolved Cr quantified using ICP-OES. Additional controls were

conducted to determine the diffusion rate of Fe(II) at both high and low concentrations across the membrane without Mn oxides or Cr. Control experiments showed that diffusion of dissolved Cr, Mn(II), Fe(II) were very similar (Figure S2-S5). By applying the effective diffusivity calculated using data acquired in diffusion controls to calculate the Thiele modulus, we determined that all experiments conducted within the multi-chamber reactor were diffusion rather than kinetically limited (Table S2).

4. Results

4.1. Aqueous Fe and Mn dynamics

We examined the chemical processes controlling Cr and Mn mobility at a diffusion-controlled redox interface simulating the transport of reduced species from the interior of soil aggregates to the oxidizing exterior. Specifically, we examined the reaction products after the diffusion of aqueous Fe(II) and Cr(III) solubilized from $Cr(OH)_3$ into a chamber containing Mn oxides (crystalline pyrolusite or poorly-crystalline birnessite) using a multi-chamber reactor (Figure S1).

Relatively low (14 µM) or high (100 µM) concentrations of Fe(II) were added into the $Cr(OH)_3$ chamber to simulate the concentrations of Fe(II), a prevalent abiotic reductant found in reducing zones of soil aggregates (Masue-Slowey et al., 2011, 2013). These concentrations were chosen because previous studies observed Fe(II) concentrations within soil aggregates ranging from 0-50 µM Fe(II) in the first 2 mm, 100-200 µM Fe(II) at 4 mm from the surface, and up to 250 µM within the center of the aggregate (Mansue-Slowey et al., 2011). Since Cr(VI) reduction in aggregates was observed toward the aggregate surface (Tokunaga et al., 2001), concentrations of Fe(II)

observed toward the surface were used as relatively low/high Fe(II) additions. Fe(II) concentrations decreased over the first 20 hours of reaction in the presence of low Fe(II) and remained below detection in both chambers for the remainder of the experiment (Figure 1). In the high Fe(II) treatment, steady state was reached after ~9 hours with 30±7 µM dissolved Fe remaining in both chambers for the remainder of the experiment.

Dissolved Mn (Mn_{aq}) in the pyrolusite chamber increased over the duration of the experiment under low and no Fe(II) treatment (Figure 1). Mn_{aq} at the end of the experiments were comparable between low Fe(II) (21.9 µM Mn_{aq}) and no Fe(II) (14.9 µM Mn_{aq}) treatments. Mn_{aq} concentrations increased more rapidly in the presence of high Fe(II), with Mn_{aq} ~10 times higher (213 µM) than with no Fe(II) or low Fe(II) at 100 hours of reaction. The final concentration of Mn_{aq} between the chamber containing $Cr(OH)_3$ and pyrolusite was similar for all Fe treatments demonstrating that the reaction proceeded until steady state had been reached.

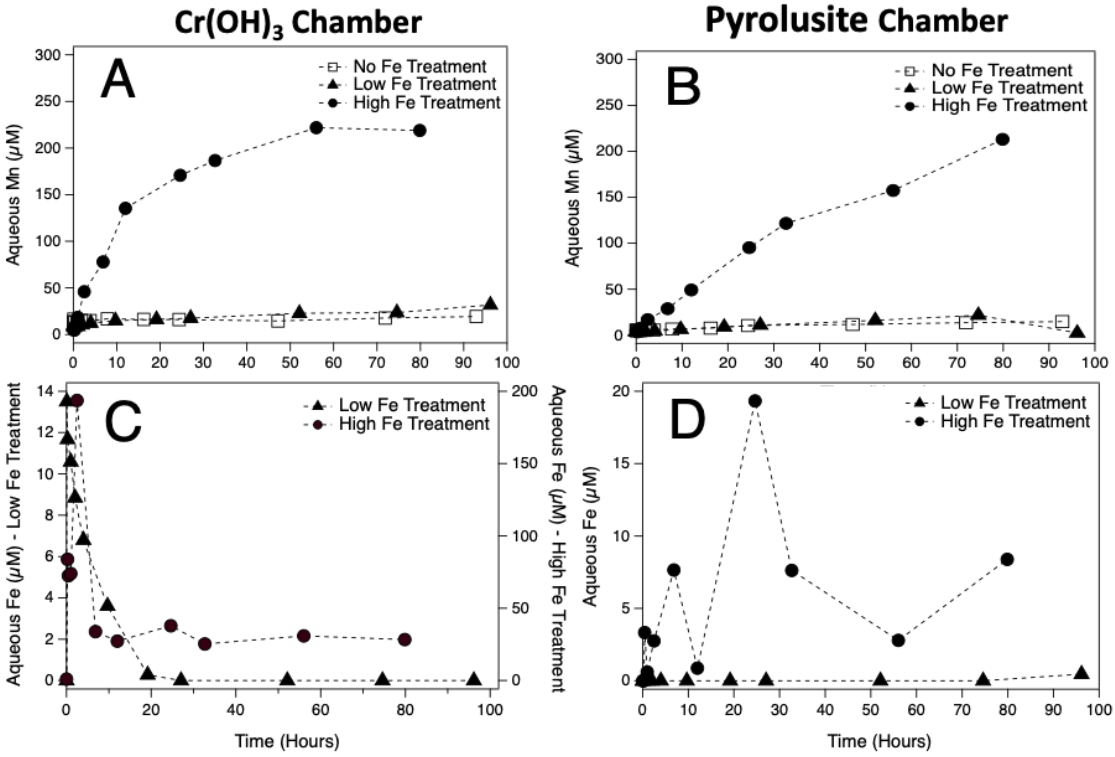

Figure 1. Concentration of dissolved Mn (A and B) and Fe (C and D) in the $Cr(OH)_3$ chamber where Fe(II) is injected to initiate the reaction (left panel) and pyrolusite chamber (right panel) without Fe(II) addition (open squares), low Fe(II) addition (14 µM, closed triangles), and high Fe(II) addition (100 µM, closed squares). Note that the y-axis range for aqueous Fe concentrations in panel C differ for high (right axis) versus low Fe treatment (left axis).

4.2. Aqueous Cr dynamics

Aqueous hexavalent chromium [Cr(VI)] generation was monitored in both chambers following the addition of Fe(II) to the $Cr(OH)_3$ containing chamber (Figure 2). Chromium(VI) dynamics with no Fe(II) and low Fe(II) treatments were similar in the pyrolusite chamber. During the first 20 hours of the experiment, the concentration of Cr(VI) without Fe(II) addition and with low Fe(II) increased from below detection to 0.36 µM and 0.47 µM Cr(VI), respectively, before decreasing to ~0.2 µM Cr(VI)

between 60 and 100 hours. In contrast, Cr(VI) was not detected in the presence of high Fe(II). Cr(VI) was below detection limit (0.1 µM) in the $Cr(OH)_3$ chamber for all experiments.

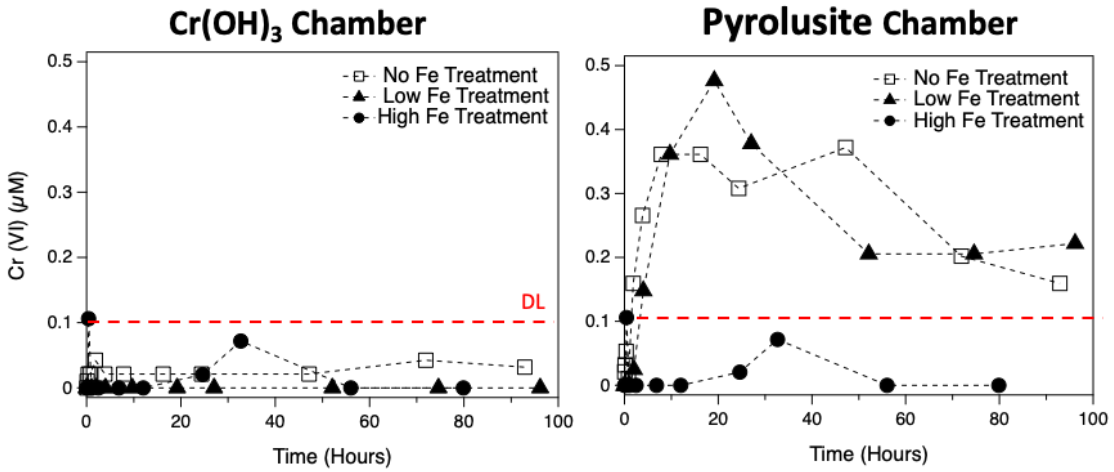

Figure 2. Aqueous concentration of Cr(VI) determined using s-diphenyl carbazide (DPC) colorimetric assay in the chromium hydroxide and Fe(II) injection chamber (right panel) and pyrolusite chamber (left panel) after the addition of no (white boxes), low (14 µM, black triangles), and high (100 µM, black circles) concentrations of Fe(II). Red dashed line represents the detection limit of the DPC colorimetric assay (0.1 µM).

4.3. Cr and Fe Sorption onto Mn oxides

Pyrolusite solids were collected over the duration of the experiment and analyzed for solid associated Fe and Cr. In the absence of Fe(II), 78-120 µmol Cr g^{-1} pyrolusite was detected on the pyrolusite solids after 60 hours. In the low Fe(II) treatment, pyrolusite-associated Cr was less than without Fe(II) (~7 µmol Cr g^{-1} pyrolusite) and remained similar throughout the duration of the experiment. Solid-associated Cr was not detected in the high Fe(II) treatment. Total iron was measured on the solids in the pyrolusite chamber in both the high and low Fe(II) treatments. In the low Fe(II) treatment, Fe was not detected on the pyrolusite solids until after 24 hours, when it

increased to ~21-31 µmol Fe g^{-1} pyrolusite. In the high Fe(II) treatments, Fe was detected less than an hour after its addition and increased to over 50 times (1220 µmol Fe per g pyrolusite) the solid associated iron in the low Fe(II) treatment despite only a 7-fold difference in initial Fe(II) concentration.

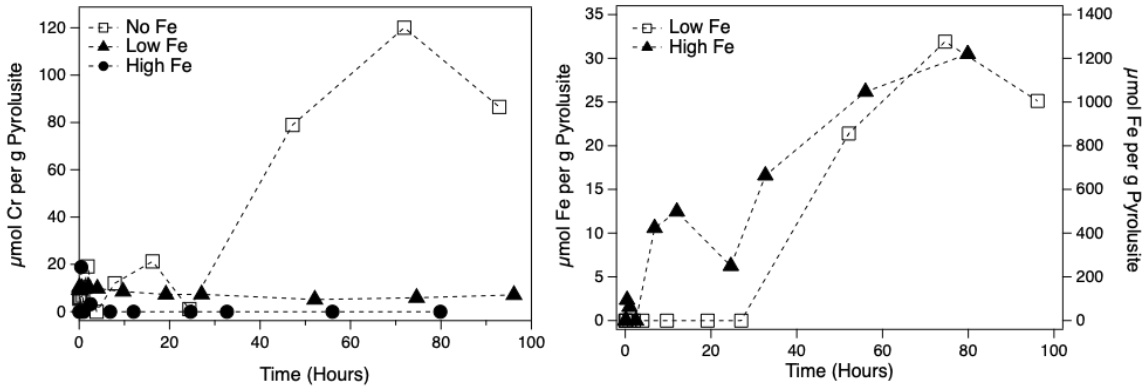

Figure 3. Solid concentration of chromium (right) and iron (left) per gram of pyrolusite after the addition of no (white boxes), low (14 µM, black triangles), and high (100 µM, black circles) concentrations of Fe(II) determined using acid digestion. Red dashed line represents the detection limit of the DPC colorimetric assay (0.1 µM).

XPS analysis was used to determine Fe, Mn, and Cr speciation at pyrolusite surfaces in addition to bulk solid phase speciation from XAS (Figures S7-S9). For both low and high Fe(II) treatments, Fe 2p3/2 peaks were observed at around 710.9 eV, indicating Fe(III). Mn 2p3/2 peaks were observed at around 642 eV, which suggests Mn(IV) of MnO_2 in pyrolusite. The sole Cr 2p3/2 peak at 576.5 eV is assigned to Cr(III) rather than Cr(VI) which has a peak at ~580 eV. XPS results indicate that surface-associated iron was oxidized Fe(III) and surface-associated chromium was reduced Cr(III) with no indication of Cr(VI) in XPS data. The relative atomic composition of the pyrolusite solids at the termination of the experiment in the low Fe(II) treatment was both

3% Fe(III) and 3% Cr(III). In comparison, the pyrolusite solids that received high Fe(II) injection, the percent of Fe increased to 5% in relation to the total atomic composition on the pyrolusite surface.

X-ray absorption spectroscopic analysis (XAS) of the pyrolusite solids at the termination of the experiment were used to identify the type of Fe (III) (oxyhydr)oxides present on the pyrolusite solids. In the low Fe(II) treatment, the iron solids were mostly goethite (75%) with a smaller portion identified as hematite (22%). The high Fe(II) treatment had less goethite (52%) and ferrihydrite (43%) (Table S1 and Figure S6). No solid-associated Fe(II) was detected in XAS measurements, consistent with XPS data indicating that the Fe on the solid surface was present as Fe(III) solids. Mn K-edge XANES spectra revealed no average oxidation state (AOS) or structural changes in the pyrolusite in the absence of Fe(II) and in the low Fe(II) reactors (AOS ~3.9). However, the AOS of pyrolusite changed from 3.9 to 3.7 in the presence of high Fe(II).

Table 1. Average oxidation state (AOS) of pyrolusite prior to initiation and at termination. Standards and fitting method from Manceau et al. (2012).

	AOS at initiation	**AOS at termination**	**Decrease in AOS**
No Fe	3.92	3.92	0
Low Fe	3.99	3.96	0.03
High Fe	3.93	3.71	0.22

To assess the spatial distribution of Mn, Fe, and Cr, solids from the Mn chambers containing both birnessite and pyrolusite each reacted with low and high Fe were analyzed using synchrotron μ-XRF and Cr K-edge μ-XANES. Iron and Mn were spatially

correlated in each treatment providing evidence of near-complete Fe surface coverage of Mn-oxide similar to previous observations (Schaefer et al., 2017; Mock et al., 2019) (Figure 4 and 5). Chromium had lower abundance and was more diffuse than Fe and Mn. However, Cr in the high Fe(II) treatments appeared to be more localized than in low Fe(II) treatments for both birnessite (Figure 4) and pyrolusite (Figure 5). XANES spectra of sample areas containing the highest concentrations of Cr indicated that only Cr(III) was associated with solids based on the absence of a pre-edge feature diagnostic of Cr(VI).

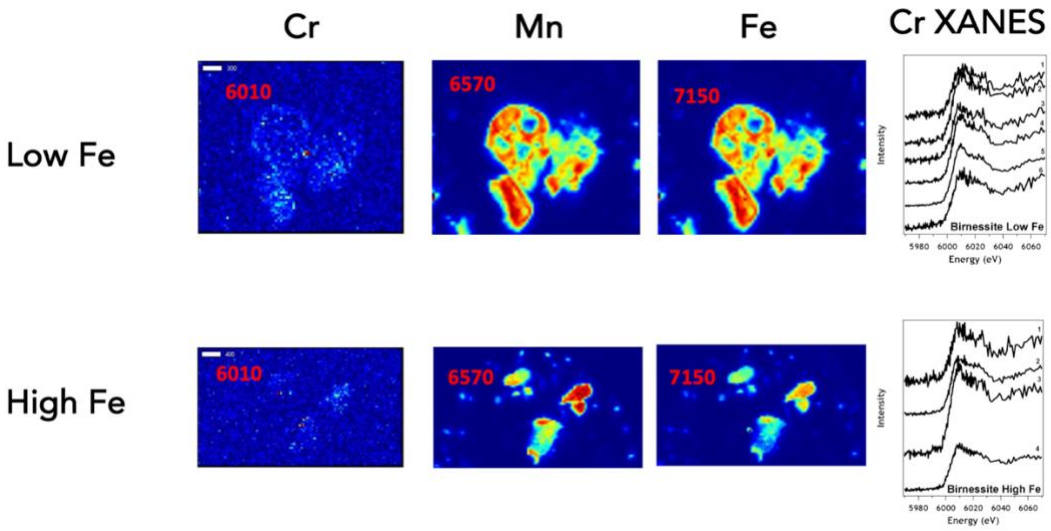

Figure 4. μ-XRF imaging and Cr K-edge μ-XANES spectra of birnessite particles collected after low Fe (top panels) and high Fe (bottom panels) was injected within the $Cr(OH)_3$ chamber. Numbers in red show the energy in eV at which XRF maps were collected. Cr K-edge XANES show that Cr(VI) was not detected on the surface of birnessite particles.

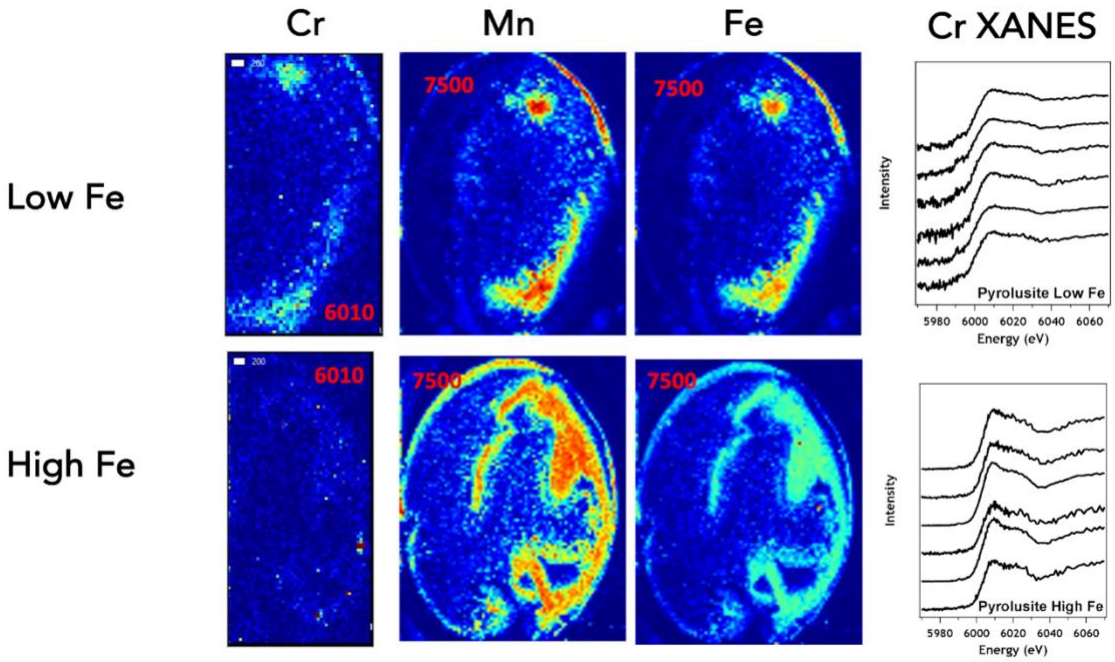

Figure 5. μ-XRF imaging and Cr K-edge μ-XANES spectra of pyrolusite particles collected after low Fe (top panels) and high Fe (bottom panels) was injected within the $Cr(OH)_3$ chamber. Numbers in red show the energy in eV at which XRF maps were collected. Cr K-edge XANES show that Cr(VI) was not detected on the surface of pyrolusite particles similar to results from birnessite experiments (Figure 4).

4.4. Effect of Mn oxide crystallinity on Cr and Fe dynamics

The effect of Mn oxide crystallinity on the oxidation of Cr and Fe in a diffusion-controlled environment was also observed (Figure 6 and 7). We replaced pyrolusite in reactors with birnessite, a more poorly crystalline Mn oxide that is representative of biogenic Mn oxides found in soils. In the absence of Fe(II), Cr(VI) concentrations peaked at ~20 hours at approximately 3.2 μM, and decreased to 1.7 μM after 60 hours (Figure 7). The measured concentration of Cr(VI) after 20 hours was 10 times higher than the Cr(VI) measured in the pyrolusite reactors in the absence of Fe(II). The initial rate of Cr(III) oxidation differed in the presence of the two minerals. In the absence of Fe(II),

oxidation of Cr(III) by birnessite had an initial rate of 0.4 µM h^{-1}, which was ~10 times more than by pyrolusite (Figure 7, Table S3).

When low concentrations of Fe(II) were injected into the reactor, changes in aqueous Cr(VI) concentrations within the birnessite chamber did not follow a similar pattern of Cr(VI) generation in the presence of pyrolusite. Aqueous Cr(VI) concentration peaked quickly at ~20 minutes (1.4 µM) and then decreased until ~20 hours before plateauing at ~ 0.25 µM Cr(VI), a concentration similar to the amount measured in the pyrolusite chamber in the low Fe(II) treatments (Figure 7). No Cr(VI) was detected in the $Cr(OH)_3$ chamber with low and high Fe(II) treatments for both birnessite and pyrolusite. Aqueous Fe(II) dynamics were similar between the two Mn oxides over the duration of the low Fe(II) experiments. When low Fe(II) was introduced, the concentration of Fe(II) in the Cr(OH)3 chamber peaked just after addition, decreased, and was no longer detected after 20 hours (Figure 6). Aqueous Fe was not detected in the Mn oxide chamber for the duration of the experiment for both Mn oxide types.

In the high Fe(II) and birnessite treatments, no Cr(VI) was detected in the birnessite chamber for the duration of the experiment (Figure 7). This is similar to the observed Cr(VI) dynamics in the presence of pyrolusite and high Fe(II). After the addition of high Fe(II), aqueous Fe concentration peaked in both chambers immediately after Fe addition and remained in solution for the duration of the experiment (Figure 6). Iron in solution was observed in both Mn oxide mineral treatments when treated with high Fe(II). Aqueous Mn concentrations were highly variable in the birnessite chamber, however, the aqueous Mn concentration in the $Cr(OH)_3$chromium hydroxide chamber

peaked at ~10 hours and then decreased for the remainder of the experiment. In comparison to the pyrolusite treatment, Mn concentration was approximately 10 times less than what was measured in the pyrolusite treatments.

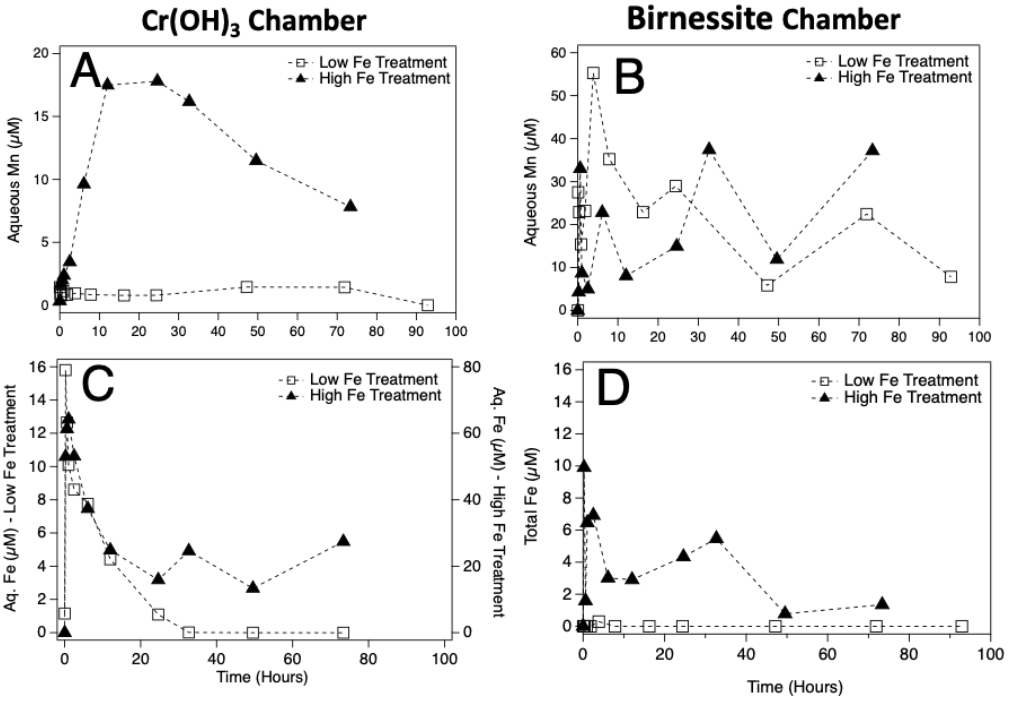

Figure 6. Concentration of dissolved Mn (A and B) and Fe (C and D) in the $Cr(OH)_3$ chamber where Fe(II) is injected to initiate the reaction (left panel) and birnessite chamber (right panel) without Fe(II) low Fe(II) addition (14 µM, open squares) and high Fe(II) addition (100 µM, closed triangles). Note that the y-axis range for aqueous Fe concentrations in panel C differ for high (right axis) versus low Fe treatment (left axis).

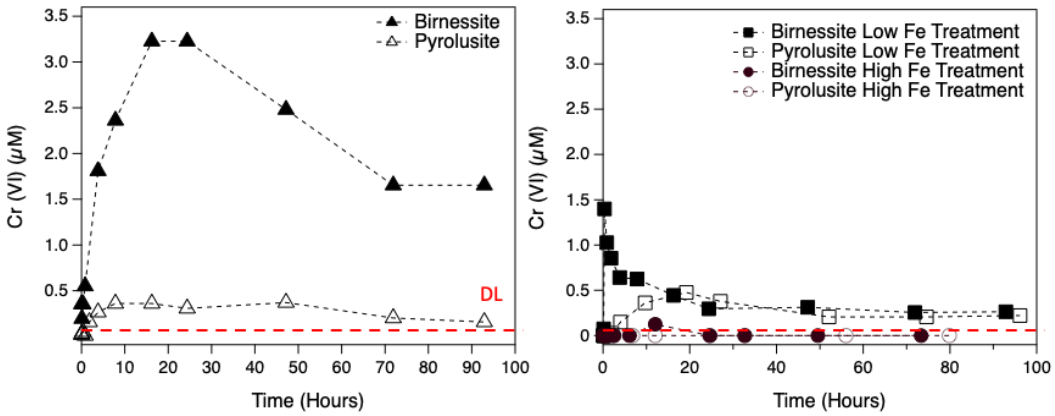

Figure 7. Aqueous concentration of Cr(VI) measured by DPC in the Mn oxide chamber when using highly-crystalline pyrolusite (black triangles) and poorly-crystalline birnessite (white boxes) after the addition of no (left) and low (14 µM; right) concentrations of Fe(II).

5. Discussion

5.1. Competing Redox Processes that Limit Cr(VI) Production

Our results indicate that Cr(III) oxidation by Mn(III/IV) oxide occurs in a diffusion controlled system without the direct physical interaction of the solid minerals. The reaction sequence began with the dissolution of $Cr(OH)_3$ and diffusion of aqueous Cr(III) across the semipermeable membrane, where Cr(III) was then oxidized by the Mn oxides (pyrolusite or birnessite) to Cr(VI). These observations are consistent with findings reported by Pan et al. (Pan et al., 2019), where oxidation of Cr(III) from $Cr(OH)_3$ by birnessite in a diffusion-limited environment was also observed. This study demonstrated that Mn oxide-driven Cr(III) oxidation was inhibited due to precipitation of $Cr(OH)_3$ on the Mn oxide surface or the precipitation of highly-reactive Mn oxides in ambient oxygen conditions. Further, no adsorbed Cr(VI) was detected on Mn oxides, but adsorbed Cr(VI) was found on $Cr_xFe_{1-x}(OH)_3$ minerals at lower pH.

Since Cr(VI) is also observed under reducing conditions (Johnson et al., 1992; Oze et al., 2016; Ao et al., 2022) we also investigated the fate of Cr in the presence of both oxidant (Mn oxide) and reductant [Fe(II)]. Aqueous Fe(II) added to the Cr chamber remained soluble in the presence of $Cr(OH)_3$ and diffused to the Mn chamber. In the diffusion controlled reactors, the oxidation of Cr(III) in the presence of 14 µM Fe(II) was similar to the Fe-free control, however oxidation of Cr(III) to Cr(VI) was not observed in the presence of 100 µM Fe(II). A combination of three possible mechanisms may explain the decrease of Cr(VI): (i) passivation of Mn oxide surfaces by oxidation of Fe(II) and precipitation of Fe(III) minerals, (ii) adsorption of aqueous species onto Mn oxide blocking reactive sites, or (iii) direct reduction of Cr(VI) by Fe(II) (Fendorf and Li, 1996; Buerge and Hug, 1997, 1999).

Solid phase analysis at the termination of the reactors indicates the formation of Fe(III) oxyhydroxides on Mn oxide surfaces and that more Fe(III) was associated with the high Fe(II) treatment. Prior studies have found that Fe(II) oxidation by Mn oxides and subsequent formation of Fe(III) oxyhydroxides on Mn oxide surfaces suppresses Mn oxide oxidative capacity toward reduced species such as arsenic (Mock et al., 2019). The Fe(III) oxyhydroxides formed on the surface of pyrolusite are primarily goethite, a higher-crystallinity Fe(III) oxyhydroxide (Table S1) due to the lower surface area of the pyrolusite and a more complete coverage of the available surface area. In previous work, the further reaction of the Fe(III) oxyhydroxides with remaining Fe(II) resulted in the formation of a more crystalline Fe(III) oxyhydroxides, goethite (Hansel et al., 2003, 2005). Schaefer et al. (2017) demonstrated that Fe oxide coatings formed through the

abiotic reaction of Fe(II) with pyrolusite results initially in lepidocrocite, but continued reaction with Fe(II) resulted in partial reduction of lepidocrocite to magnetite and release of additional aqueous Mn. Surface passivation by Fe(III) mineral precipitation likely contributed to suppressing Cr(III) oxidation through the blocking of reactive sites on the Mn oxide surface.

In the high Fe(II) treatments, high aqueous Mn(II) was detected due to reductive dissolution of the Mn oxide solid (Figure 1 and 6). Elzinga (2011) determined that aqueous Mn(II) sorption and comproportionation with structural Mn(IV) forms Mn(III) within the Mn oxide sheet. These overall changes in the crystalline structure of the mineral change its sorption and redox activity. While there was a small decrease in the AOS in the birnessite reactors, the AOS of the pyrolusite solids at the termination of the high Fe(II) treatment was lower due to the higher aqueous Mn(II) detected in the rectors and Mn(II) sorption onto the mineral. Since AOS is a measurement of solid-phase Mn speciation, Mn(II) dissolution may occur within a change in the AOS and would not be able to be measured (Elzinga et al., 2016). In turn, the decrease in average oxidation state may be due to either dissolved Mn(II) reacting back with the Mn oxide surface or Mn(IV) reduction without dissolution (Learman et al., 2011; Elzinga, 2016).

In addition, $Fe(II)_{aq}$ can directly reduce $Cr(VI)_{aq}$ through a homogeneous reaction (e.g., Fendorf and Li, 1996; Buerge and Hug, 1997, 1999; Ginder-Vogel et al., 2005). In the low $Fe(II)_{aq}$ treatments, after 20 hours Fe_{aq} was below detection in both chambers indicating that all of the initial Fe precipitated as Fe(III) oxides. However in the high Fe treatments $Fe(II)_{aq}$ remained in solution for the duration of the experiment (Figure 1 and

6). Past studies have shown that relatively low concentrations of $Fe(II)_{aq}$ (e.g 10 µM) can reduce $Cr(VI)_{aq}$ under environmental conditions (Fendorf and Li, 1996), which would inhibit Cr(VI) accumulation in the high Fe treatment. Sustained $Fe(II)_{aq}$ also indicated that Fe(II) had equilibrated with the initial Mn oxide solids.

The $Cr(VI)_{aq}$ generated in multiple experimental iterations was above the public health goal (PHG) of 0.05 µg L^{-1} for Cr(VI) set by the California Office of Environmental Health Hazard Assessment (Office of the Environmental Health Hazard Assessment, 2011). The Cr(VI) detected in the pyrolusite and birnessite reactors without Fe(II) was ~900 and ~8,000 times higher than the public health goal, respectively. Currently, an enforceable maximum contaminant level (MCL) only exists for total chromium. The World Health Organization sets its recommended guideline value for total chromium at 50 µg L^{-1} and the US Environmental Protection Agency MCL is set at 100 µg L^{-1} (US EPA, 2015; World Health Agency, 2020)

No primary or enforceable MCL exists for Mn despite increasing evidence of toxicity at high concentrations, however the World Health Organization has a provisional health-based guideline of 80 µg L^{-1} (Coetzee et al., 2016; World Health Organization, 2021). All pyrolusite treatments exceeded the exposure threshold linking Mn(II) exposure in drinking water to neurotoxic effects in children (120 µg L^{-1}, Wasserman et al., 2011; Khan et al., 2012; Oulhote et al., 2014). The highest $Mn(II)_{aq}$ was detected in the high Fe with pyrolusite treatment and was ~130 times higher than the WHO provisional guideline.

5.2. Impact of Mn Oxide Crystallinity

To evaluate the effect of Mn oxide crystallinity on Fe(II) and Cr(III) oxidation reactions we compared crystalline and low specific surface area (SSA) pyrolusite to poorly crystalline, high SSA birnessite. Both surface area and crystallinity influence Mn oxide reactivity and oxidative capacity (Post, 1999). Pyrolusite is the most thermodynamically stable Mn oxide representing an end-member case for Mn(IV) reduction by $Fe(II)_{aq}$ and if Cr(III) oxidation occurs with pyrolusite, it is likely to occur with other Mn oxides. However, birnessite was included as a comparison since it more closely resembles abundant biogenic Mn oxides in soils and aquifers (Oze et al., 2007; McClain et al., 2017; Hausladen and Fendorf, 2017). As expected from prior studies, Cr(III) reaction with birnessite generated higher concentrations of Cr(VI) than pyrolusite with similar initial conditions due to the higher surface area of birnessite (Kim et al., 2002). Both pyrolusite and birnessite oxidized aqueous Fe(II) resulting in Fe(III) (oxyhydr)oxide surface precipitation; however, the larger surface area of birnessite resulted in incomplete surface coverage. Similar results have been observed for complete surface coverage for pyrolusite at higher Fe(II) concentrations (Schaefer et al., 2017) and incomplete surface coverage for birnessite (Mock et al., 2019). In the low Fe(II) treatment with birnessite, cumulative Cr(VI) generation was ~3 times higher than pyrolusite treatment which may be attributed to the faster initial rate of Cr(III) oxidation in the first ~20 hours before more, but not total, surface coverage by Fe(III) oxyhydroxides precipitation on the birnessite surface.

The solubility of the Cr-bearing mineral also plays an important role in Cr(VI) production in diffusion-limited environments. In the environment, Fe(II)-mediated Cr(VI) reduction results in formation of a Cr(III)-Fe(III) coprecipitate, $Cr_xFe_{1-x}(OH)_3$, that is less soluble than pure $Cr(OH)_3$ (Oze et al., 2007; Rajapaksha et al., 2013; Hausladen and Fendorf, 2017; Pan et al., 2017). In studies investigating the impact of lower solubility Cr-bearing minerals, Cr(VI) generation was proportional to the mineral solubility (Oze et al., 2007; Rajapaksha et al., 2013; Hausladen and Fendorf, 2017; Pan et al., 2017). Although Fe substituted Cr-bearing minerals were not investigated in this study, the dissolution of $Cr(OH)_3$ and migration of $Cr(III)_{aq}$ to the Mn oxide surface is the initial, rate-limiting step in the production of Cr(VI) within this system (Table S2). Mineral substitution of Fe resulting in decreased Cr(III) mineral solubility would only further limit diffusive flux to Mn oxides and decrease Cr(VI) production rate.

5.3. Diffusion Controls on Redox Reactions

In the environment, reducing conditions may occur in the interior of soil aggregates where oxygen demand exceeds oxygen supplied via diffusion from the aggregate surface (Pallud et al., 2010). Reduced Fe(II) from anoxic, biotic reduction of Fe oxides in the aggregate interiors then diffuses toward zones of Cr(VI) generation (aggregate exterior) all while maintaining physical separation between the mineral solids (Tokunaga et al., 2001). Similarly, Cr(III) solids and Mn oxides may be physically separated in the environment so the reaction is also dependent on the rate of Cr(III) dissolution from the solid mineral and diffusion to the site of oxidation (Oze et al., 2007). All experiments presented herein were diffusion controlled based on Thiele modulus

calculations (Table S2). We were then able to observe the impacts of Fe(II) diffusion to zones of Cr(VI) generation while maintaining physical separation of $Cr(OH)_3$ and Mn oxides, similar to physical limitations observed in soil aggregates. Prior studies showed that the solubility of the Cr(III)-bearing minerals combined with the distance that dissolved Cr(III) must travel to reach Mn oxides determined the rate of the Cr(VI) production (Hausladen and Fendorf, 2017; Pan et al., 2017, 2019).

Physical separation, yet close proximity, of secondary Cr(III) minerals to Mn oxides has been observed in serpentine soils (McClain et al., 2017, 2019). Within these environments, dissolution of Cr(III) from Cr-bearing minerals and diffusion to oxidative minerals like Mn oxides play an important role in the net production and transport of Cr(VI) into groundwater. However, Cr(VI) measured in infiltrating water was attenuated during flow to surface water sources due to dilution by infiltration water or reduction via microbial activity or abiotic Fe(II) (McClain et al., 2017, 2019). In the absence of processes reducing Cr(VI), advection of Cr(VI) through the flow water may lead to groundwater contamination.

6. Conclusions

The processes controlling Cr cycling in soil environments are complex and site-specific. Manganese and Fe oxides commonly occur in many soil environments and, due to their redox activity, it is important to understand how both play a role in the oxidative release of toxic groundwater contaminants such as chromium. In our work, we have demonstrated that despite diffusion limitations, physical separation of solid minerals, and the introduction of competing reactants at environmentally relevant concentrations,

Cr(VI) and Mn(II) were still generated at concentrations exceeding regulatory levels. The release and outward diffusion of Fe(II) from anaerobic centers of soil aggregates represents a pathway for the release of a competing reactant in well-aerated soil environments that may fully disrupt the oxidation of Cr(III). However, the extent of Cr(III) oxidation by Mn oxides was observed to be dependent on Fe(II) concentration and Mn oxide mineralogy

Despite evidence of less Cr(III) oxidation occurring in the presence of co-occurring reactants, such as Fe(II), there is still evidence of large-scale Cr(VI) transport into groundwater (McClain et al., 2017, 2019; Hausladen et al., 2018). Therefore, it is important to note that transport of Cr(VI) into advecting water is highly scale dependent. The specific biogeochemical characteristics of local environments such as anoxic zones, microbial activity, and mineral solubilities must therefore be taken into consideration when investigating the potential for geogenic metal release into groundwater.

7. References

Ao M., Sun S., Deng T., Zhang F., Liu T., Tang Y., Li J., Wang S. and Qiu R. (2022) Natural source of Cr(VI) in soil: The anoxic oxidation of Cr(III) by Mn oxides. *Journal of Hazardous Materials* **433**, 128805.

Ball J. W. and Nordstrom D. K. (1998) Critical Evaluation and Selection of Standard State Thermodynamic Properties for Chromium Metal and Its Aqueous Ions, Hydrolysis Species, Oxides, and Hydroxides. *J. Chem. Eng. Data* **43**, 895–918.

Buerge I. J. and Hug S. J. (1999) Influence of Mineral Surfaces on Chromium(VI) Reduction by Iron(II). *Environ. Sci. Technol.* **33**, 4285–4291.

Buerge I. J. and Hug S. J. (1997) Kinetics and pH Dependence of Chromium(VI) Reduction by Iron(II). *Environ. Sci. Technol.* **31**, 1426–1432.

Coetzee D. J., McGovern P. M., Rao R., Harnack L. J., Georgieff M. K. and Stepanov I. (2016) Measuring the impact of manganese exposure on children's neurodevelopment: advances and research gaps in biomarker-based approaches. *Environ Health* **15**, 91.

Costa M. and Klein C. B. (2006) Toxicity and Carcinogenicity of Chromium Compounds in Humans. *Critical Reviews in Toxicology* **36**, 155–163.

Eary L. E. and Rai D. (1991) Chromate Reduction by Subsurface Soils under Acidic Conditions. *Soil Science Society of America Journal* **55**, 676–683.

Elzinga E. J. (2016) (54)Mn Radiotracers Demonstrate Continuous Dissolution and Reprecipitation of Vernadite (δ-MnO2) during Interaction with Aqueous Mn(II). *Environ Sci Technol* **50**, 8670–8677.

Elzinga E. J. (2011) Reductive Transformation of Birnessite by Aqueous Mn(II). *Environ. Sci. Technol.* **45**, 6366–6372.

Fendorf S. and Li G. (1996) Kinetics of Chromate Reduction by Ferrous Iron. *Environ. Sci. Technol.* **30**, 1614–1617.

Fendorf S. and Zasoski R. (1992) Chromium (III) oxidation by. delta.-manganese oxide (MnO2). 1. Characterization. *Environmental Science & Technology* **26**, 79–85.

Gerke H. H. (2006) Preferential flow descriptions for structured soils. *Journal of Plant Nutrition and Soil Science* **169**, 382–400.

Ginder-Vogel M., Borch T., Mayes M. A., Jardine P. M. and Fendorf S. (2005) Chromate Reduction and Retention Processes within Arid Subsurface Environments. *Environ. Sci. Technol.* **39**, 7833–7839.

Gonzalez A. R., Ndung'u K. and Flegal A. R. (2005) Natural Occurrence of Hexavalent Chromium in the Aromas Red Sands Aquifer, California. *Environ. Sci. Technol.* **39**, 5505–5511.

Hansel C. M., Benner S. G. and Fendorf S. (2005) Competing Fe(II)-Induced Mineralization Pathways of Ferrihydrite. *Environ. Sci. Technol.* **39**, 7147–7153.

Hansel C. M., Benner S. G., Neiss J., Dohnalkova A., Kukkadapu R. K. and Fendorf S. (2003) Secondary mineralization pathways induced by dissimilatory iron reduction of ferrihydrite under advective flow. *Geochimica et Cosmochimica Acta* **67**, 2977–2992.

Hausladen D. M., Alexander-Ozinskas A., McClain C. and Fendorf S. (2018) Hexavalent Chromium Sources and Distribution in California Groundwater. *Environmental Science & Technology*.

Hausladen D. M. and Fendorf S. (2017) Hexavalent Chromium Generation within Naturally Structured Soils and Sediments. *Environ. Sci. Technol.* **51**, 2058–2067.

Johnson C. A., Sigg L. and Lindauer U. (1992) The chromium cycle in a seasonally anoxic lake. *Limnology and Oceanography* **37**, 315–321.

Khan K., Wasserman G. A., Liu X., Ahmed E., Parvez F., Slavkovich V., Levy D., Mey J., van Geen A., Graziano J. H. and Factor-Litvak P. (2012) Manganese exposure from drinking water and children's academic achievement. *NeuroToxicology* **33**, 91–97.

Kim J. G., Dixon J. B., Chusuei C. C. and Deng Y. (2002) Oxidation of Chromium(III) to (VI) by Manganese Oxides Contribution from Texas Agriculture Experimental Station, Texas A&M University, College Station, TX. *Soil Science Society of America Journal* **66**, 306–315.

Learman D. R., Voelker B. M., Vazquez-Rodriguez A. I. and Hansel C. M. (2011) Formation of manganese oxides by bacterially generated superoxide. *Nature Geosci* **4**, 95–98.

Manceau A., Marcus M. A. and Grangeon S. (2012) Determination of Mn valence states in mixed-valent manganates by XANES spectroscopy. *American Mineralogist* **97**, 816–827.

Masue-Slowey Y., Kocar B. D., Bea Jofré S. A., Mayer K. U. and Fendorf S. (2011) Transport Implications Resulting from Internal Redistribution of Arsenic and Iron within Constructed Soil Aggregates. *Environ. Sci. Technol.* **45**, 582–588.

Masue-Slowey Y., Ying S. C., Kocar B. D., Pallud C. E. and Fendorf S. (2013) Dependence of arsenic fate and transport on biogeochemical heterogeneity arising from the physical structure of soils and sediments. *J Environ Qual* **42**, 1119–1129.

McClain C. N., Fendorf S., Johnson S. T., Menendez A. and Maher K. (2019) Lithologic and redox controls on hexavalent chromium in vadose zone sediments of California's Central Valley. *Geochimica et Cosmochimica Acta* **265**, 478–494.

McClain C. N., Fendorf S., Webb S. M. and Maher K. (2017) Quantifying Cr(VI) Production and Export from Serpentine Soil of the California Coast Range. *Environ Sci Technol* **51**, 141–149.

McKenzie R. M. (1971) The synthesis of birnessite, cryptomelane, and some other oxides and hydroxides of manganese. *Mineralogical Magazine* **38**, 493–502.

Mock R. P., Schaefer M. V., Pacheco J. L., Lake L., Lee I. and Ying S. C. (2019) Influence of Fe(II) on Arsenic(III) Oxidation by Birnessite in Diffusion-Limited Systems. *ACS Earth Space Chem.* **3**, 550–561.

Ndung'u K., Friedrich S., Gonzalez A. R. and Flegal A. R. (2009) Chromium oxidation by manganese (hydr)oxides in a California aquifer. *Applied Geochemistry* **25**, 377–381.

Office of the Environmental Health Hazard Assessment (2011) Final Public Health Goal for Hexavalent Chromium. , 3.

Oulhote Y., Mergler D., Barbeau B., Bellinger D. C., Bouffard T., Brodeur M.-È., Saint-Amour D., Legrand M., Sauvé S. and Bouchard M. F. (2014) Neurobehavioral Function in School-Age Children Exposed to Manganese in Drinking Water. *Environ Health Perspect* **122**, 1343–1350.

Oze C., Bird D. K. and Fendorf S. (2007) Genesis of hexavalent chromium from natural sources in soil and groundwater. *PNAS* **104**, 6544–6549.

Oze C., Fendorf S., Bird D. K. and Coleman R. G. (2004) Chromium Geochemistry of Serpentine Soils. *International Geology Review* **46**, 97–126.

Oze C., Sleep N. H., Coleman R. G. and Fendorf S. (2016) Anoxic oxidation of chromium. *Geology* **44**, 543–546.

Pallud C., Kausch M., Fendorf S. and Meile C. (2010) Spatial Patterns and Modeling of Reductive Ferrihydrite Transformation Observed in Artificial Soil Aggregates. *Environ. Sci. Technol.* **44**, 74–79.

Pan C., Liu H., Catalano J. G., Qian A., Wang Z. and Giammar D. E. (2017) Rates of Cr(VI) Generation from CrxFe1–x(OH)3 Solids upon Reaction with Manganese Oxide. *Environ. Sci. Technol.* **51**, 12416–12423.

Pan C., Liu H., Catalano J. G., Wang Z., Qian A. and Giammar D. E. (2019) Understanding the Roles of Dissolution and Diffusion in Cr(OH)3 Oxidation by δ-MnO2. *ACS Earth Space Chem.* **3**, 357–365.

Papassiopi N., Vaxevanidou K., Christou C., Karagianni E. and Antipas G. S. E. (2014) Synthesis, characterization and stability of Cr(III) and Fe(III) hydroxides. *Journal of Hazardous Materials* **264**, 490–497.

Post J. E. (1999) Manganese oxide minerals: Crystal structures and economic and environmental significance. *PNAS* **96**, 3447–3454.

Rai D., Sass B. and Moore D. (1987) Chromitim(III) Hydrolysis Constants and Solubility of Chromium(III) Hydroxide. *Inorganic Chemistry* **26**, 345–349.

Rajapaksha A. U., Vithanage M., Ok Y. S. and Oze C. (2013) Cr(VI) Formation Related to Cr(III)-Muscovite and Birnessite Interactions in Ultramafic Environments. *Environ. Sci. Technol.* **47**, 9722–9729.

Ravel B. and Newville M. (2005) ATHENA, ARTEMIS, HEPHAESTUS: data analysis for X-ray absorption spectroscopy using IFEFFIT. *J Synchrotron Rad* **12**, 537–541.

Richard F. C. and Bourg A. C. M. (1991) Aqueous geochemistry of chromium: A review. *Water Research* **25**, 807–816.

Sass B. and Rai D. (1987) Solubility of Amorphous Chromium(III)-Iron(III) Hydroxide Solid Solutions. *Inorganic Chemistry* **26**, 2228–2232.

Schaefer M. V., Handler R. M. and Scherer M. M. (2017) Fe(II) reduction of pyrolusite (β-MnO2) and secondary mineral evolution. *Geochem Trans* **18**, 7.

Sexstone A. J., Revsbech N. P., Parkin T. B. and Tiedje J. M. (1985) Direct Measurement of Oxygen Profiles and Denitrification Rates in Soil Aggregates 1. *Soil Science Society of America Journal* **49**, 645–651.

Tebo B. M. (2004) Biogenic Manganese Oxides: Properties and Mechanisms of Formation. *Annual Review of Earth and Planetary Sciences* **32**, 287–328.

Thiele E. W. (1939) Relation between Catalytic Activity and Size of Particle. *Ind. Eng. Chem.* **31**, 916–920.

Tokunaga T. K., Wan J., Firestone M. K., Hazen T. C., Schwartz E., Sutton S. R. and Newville M. (2001) Chromium Diffusion and Reduction in Soil Aggregates. *Environ. Sci. Technol.* **35**, 3169–3174.

Tokunaga T. K., Wan J., Hazen T. C., Schwartz E., Firestone M. K., Sutton S. R., Newville M., Olson K. R., Lanzirotti A. and Rao W. (2003) Distribution of Chromium Contamination and Microbial Activity in Soil Aggregates. *Journal of Environmental Quality* **32**, 541–549.

US EPA (2015) Chromium in Drinking Water. https://www.epa.gov/sdwa/chromium-drinking-water#standard

Wasserman G. A., Liu X., Parvez F., Factor-Litvak P., Ahsan H., Levy D., Kline J., van Geen A., Mey J., Slavkovich V., Siddique A. B., Islam T. and Graziano J. H. (2011) Arsenic and manganese exposure and children's intellectual function. *NeuroToxicology* **32**, 450–457.

Webb S. M. (2005) SIXpack: a graphical user interface for XAS analysis using IFEFFIT. *Phys. Scr.* **2005**, 1011.

Wielinga B., Mizuba M. M., Hansel C. M. and Fendorf S. (2001) Iron promoted reduction of chromate by dissimilatory iron-reducing bacteria. *Environ Sci Technol* **35**, 522–527.

World Health Organization (2021) Manganese in drinking water. https://www.who.int/publications/i/item/WHO-HEP-ECH-WSH-2021.5. WHO/HEP/ECH/WSH/2021.5

World Health Agency (2020) Chromium in drinking water. https://apps.who.int/iris/bitstream/handle/10665/338062/WHO-HEP-ECH-WSH-2020.3-eng.pdf?sequence=1&isAllowed=y. WHO/HEP/ECH/ESH/2020.3

Wu Y., Li W. and Sparks D. L. (2015) The effects of iron(II) on the kinetics of arsenic oxidation and sorption on manganese oxides. *Journal of Colloid and Interface Science* **457**, 319–328.

Ying S. C., Kocar B. D. and Fendorf S. (2012) Oxidation and competitive retention of arsenic between iron- and manganese oxides. *Geochimica et Cosmochimica Acta* **96**, 294–303.

Ying S. C., Kocar B. D., Griffis S. D. and Fendorf S. (2011) Competitive Microbially and Mn Oxide Mediated Redox Processes Controlling Arsenic Speciation and Partitioning. *Environ. Sci. Technol.* **45**, 5572–5579.

Ying S. C., Masue-Slowey Y., Kocar B. D., Griffis S. D., Webb S., Marcus M. A., Francis C. A. and Fendorf S. (2013) Distributed microbially- and chemically-mediated redox processes controlling arsenic dynamics within Mn-/Fe-oxide constructed aggregates. *Geochimica et Cosmochimica Acta* **104**, 29–41.

Zausig J., Stepniewski W. and Horn R. (1993) Oxygen Concentration and Redox Potential Gradients in Unsaturated Model Soil Aggregates. *Soil Science Society of America Journal* **57**, 908–916.

Zhitkovich A. (2011) Chromium in Drinking Water: Sources, Metabolism, and Cancer Risks. *Chem. Res. Toxicol.* **24**, 1617–1629.

Chapter 3: Assessment of manganese in California's community water systems and geochemical controls of release into groundwater

1. Abstract

In California, manganese (Mn) is currently regulated as a secondary contaminant due to aesthetic concerns. However, recent revisions of manganese regulatory guidelines in drinking water by the World Health Organization (WHO, 80 μg L^{-1}) and Health Canada (120 μg L^{-1}), have increased the regulatory attention of Mn in drinking water sources, primarily due to neurotoxic impacts observed in infants and young children. To better understand Mn occurrence in California's community water systems, Mn concentrations reported to the Safe Drinking Water Information System (SDWIS) were used to estimate the potentially exposed population. We estimate that between 2011-2021, over 525,000 users with reported Mn data are potentially exposed to average Mn concentrations exceeding the WHO health-based guideline and over 34,000 users are potentially exposed to Mn concentrations exceeding the US Environmental Protection Agency health-advisory limit (300 μg L^{-1}). We observed that water treatment significantly decreased Mn concentration when compared to the intake concentration, however smaller water systems may lack access to treatment.

To better understand the biogeochemistry of Mn release into groundwater, we investigated other water quality parameters at intake into community water systems. In line with our current understanding of Mn dissolution, we observed a slight positive correlation with other redox related groundwater quality parameters (dissolved organic

carbon and iron) with higher concentrations of Mn. Additionally, higher Mn concentrations were observed in systems with groundwater concentrations exceeding the arsenic and chromium maximum contaminant limits (10 μg L^{-1}), and the treatment of these primary contaminants may also treat high concentrations of Mn. Our work demonstrates that many community water system users may be potentially exposed to Mn in drinking water, however, treatment of water will considerably decrease Mn concentrations and represents a pathway to reduce exposure.

2. Introduction

Manganese (Mn) is a naturally occurring, redox sensitive mineral ubiquitous in soils and sediments globally. Its release into groundwater is primarily due to microbially mediated reductive dissolution of naturally occurring minerals controlled by local biogeochemical conditions (Gillispie et al., 2016; Ying et al., 2017; McMahon et al., 2019). In surface waters, seasonal redox stratification can result in anoxic conditions favorable to the release of Mn in surface water (Davison, 1993; Krueger et al., 2020), however previous analysis of Mn in surface and groundwater have demonstrated higher rates of exceedances in groundwater sources in the United States (Eaton, 2021). Although less common, Mn from anthropogenic sources, such as industrial or mining activities can be released into the environment (Harvey and Fuller, 1998) or exacerbate its geochemical release (Johnson et al., 2000; Gandy et al., 2007).

Extraction of freshwater from sources with high concentrations of Mn has previously only been regarded as an infrastructure challenge due to solid mineral

deposition or aesthetic issues (Gerke et al., 2016; US EPA, 2018). However, recent research has linked Mn overexposure to neurotoxic impacts. Exposure to Mn in drinking water exceeding 100 μg L^{-1} has been linked to lower intelligence quotient (IQ) scores (Bouchard et al., 2011; Oulhote et al., 2014; Kullar et al., 2019), increased risk of attention-deficit hyperactivity disorder (Schullehner et al., 2020) and decline in academic achievement (Khan et al., 2012). In addition, higher concentrations of Mn in groundwater (200 μg L^{-1}) were associated with higher infant mortality rates (Spangler and Spangler, 2009).

Clear evidence exists to indicate that the central nervous system is the target for Mn toxicity, but further research is needed to establish a clear mode of action (Aschner et al., 2007). Following ingestion and Mn uptake, Mn crosses the blood-brain barrier where it accumulates in the brain. Our current understanding indicates that Mn accumulation is involved in the formation of free radicals, neurotransmitter impairment, and mitochondrial dysfunction (Takeda, 2003). Disruption of the neurotransmitter dopamine, which is involved in regulating cognition and behaviors such as memory, learning, and attention was observed in previous epidemiological studies (Neal and Guilarte, 2013; Lin et al., 2020). Since infants and young children have both greater gastrointestinal absorption and immature excretion pathways, this population may be at greater risk of Mn toxicity. In addition, since dopamine pathways increase during development, cognitive impacts of Mn may be more prominent within this population (Valcke et al., 2018).

Currently, the United States Environmental Protection Agency (USEPA) has two guidelines for Mn: the secondary maximum contaminant limit (SMCL, 50 μg L^{-1}) and the health advisory limit (HAL, 300 μg L^{-1}). California State Water Resource Control Board (SWRCB) follows the SMCL and enforces a consumer notification limit of 500 μg L^{-1}. In California, SMCLs are enforceable (California State Water Resources Control Board, 2020). As of 2022, the California Division of Drinking Water has initiated the process of developing revised notification and response levels for Mn within the state. In 2021, the World Health Organization (WHO) issued a provisional guideline value of 80 μg L^{-1} Mn in drinking water. This guideline was based on cumulative evidence from epidemiological and animal-based studies indicating Mn neurotoxicity. The aim of the guideline is to be protective of vulnerable populations, especially bottle-fed infants at risk of high Mn consumption through both drinking water and infant formula (World Health Organization, 2021).

In California, approximately 39 million users are served by public, community water systems (Legislative Analyst's Office, 2020). These systems are responsible for the extraction, monitoring, treatment, and distribution of water to users. In 2012, the state passed AB 685, or the Human Right to Water, which clearly outlined the universal right to clean, safe, affordable, drinking water for all community water system (CWS) users (AB 685). Despite this legislation, many systems do not meet these standards (State Water Resource Control Board, 2021).

Currently, little is known about Mn in water delivered to California CWS users since it has yet to be regulated as a primary drinking water contaminant. The goal of our work is to use currently available data to (1) determine the extent of Mn in water delivered to CWSs through California and the number of users potentially exposed to concentration exceeding threshold values, (2) investigate if treatment has resolved issues of high Mn, and (3) explore co-occurring redox sensitive contaminants to elucidate biogeochemical controls of Mn release into groundwater sources accessed for domestic use.

3. Materials and Methods

To best estimate potential Mn exposure via drinking water delivered to CWS users, we integrated reported water quality parameters at point-of-entry, delineations defining those served by CWS, and estimates for population within each system. The impact of treatment was characterized by comparison of water quality parameters at intake versus point-of-entry. Further consideration of groundwater quality parameters, such as other primary contaminants and redox sensitive constituents, were used to best understand subsurface conditions most favorable to Mn release. A summary of publicly available data and data counts during processing is available in Table S1 and S2.

3.1. Data Sources

3.1.1. Water Quality Data

Water quality for CWSs was estimated using reported data collected from Safe Drinking Water Information System (SDWIS) between 2011 and 2021 (California State Water Resource Control Board, 2021). Mn and other primary contaminants (arsenic, chromium, and nitrate) were downloaded in addition to other collected groundwater quality data (pH, hardness reported as $CaCO_3$, sulfate, dissolved organic carbon [DOC], and iron). Information on how the data was collected is available here: https://www.waterboards.ca.gov/drinking_water/certlic/drinkingwater/documents/edtlibrary/data_dictionary.pdf.

Flow path data was accessed upon request from the Division of Drinking Water in August of 2020. These data include raw sources that flow into receiving sources, inducing treatment or distribution points. Data on the relative contribution of each flow source into the distribution point was not available.

3.1.2. Community Water System Boundaries

A CWS is defined as a system providing water for human consumption with 15 or more service connections or serving 25 or more people daily for at least 60 days per year (defined by the California State Water Resources Control Board). Community water system (CWS) boundaries were developed by Tracking California Water System Service Areas Tool (Tracking California). The “active” status of the community water system

was confirmed via the State Drinking Water Information System, wholesale systems were removed, and then the boundaries were cleaned. A total of 2,851 active community water system boundaries were included in the final layer and were obtained in March 2022 (Pace et al., 2020).

Information regarding the federal water system type, water source type, population (including transient and residential population), service connections (including agricultural, commercial, institutional, residential, and combined), fee code designation, treatment plant class, and distribution system class were obtained from SDWIS in April 2022 (Table S1).

CWSs were stratified by residential population into very small (<500 users), small (501-3,300 users), medium (3,301-10,000 users), large (10,001-100,000 users), and very large (100,000+ users) water systems (US EPA, 2022). CWS with no reported residential population or domestic service connections were excluded.

3.2. Data Handling

3.2.1. Estimating Contaminant Exposure in Community Water Systems

Mn and other contaminant data from SDWIS were used to estimate mean contaminant exposure in CWS between 2011-2021. All inactive or proposed facilities were removed from analysis. Systems with the classification of transient-noncommunity and non-public were excluded (definition of each is found here: https://www.waterboards.ca.gov/drinking_water/certlic/drinkingwater/docs/class_dec_tre

e.pdf). Non-detects were calculated to be the reporting limit divided by the square root of 2 (Lubin et al., 2004; Bangia et al., 2020).

Reported contaminant concentration was joined with flow path data and those with no reported flow path information were excluded. To estimate contaminant concentration at point-of-use, we retained the reported values that flowed directly into distribution systems (point-of-entry; Balazs et al., 2011; Sherris et al., 2021). To account for higher frequency sampling when in exceedance, samples collected on the same day from the same point were averaged. A 10-year mean was calculated for each water system to allow comparison since reporting frequency was highly heterogeneous. Summary of data after each vetting step is available in Table S2.

Population data from SDWIS Public Water System Information was used to estimate population exposure to concentrations above threshold values. Transient (e.g., recreation area, highway, rest area, hotel/motel) and non-transient (e.g. industrial/agricultural, medical facility, school) populations were not included in population calculations. All data sorting was done in Excel or RStudio (version 2022.02.1).

3.2.2. Potentially Exposed Population

To account for multiple sources within a distribution system, we calculated the potentially exposed population (PEP) similar to Balazs et al. (2011). The total population served by each CWS was apportioned into five Mn exposure categories based on the

proportion of sources for that CWS with mean reported Mn concentrations falling within each category. The population assigned each exposure category was then summed across all CWS to estimate the exposed population. For example, to calculate the PEP for small CWS we used the following equation:

Equation 1.

$$PEP = \sum_{i=1}^{822} \left(X_i \times \frac{S_L}{S_T}\right) + \left(X_i \times \frac{S_{LM}}{S_T}\right) + \left(X_i \times \frac{S_M}{S_T}\right) + \left(X_i \times \frac{S_{MH}}{S_T}\right) + \left(X_i \times \frac{S_H}{S_T}\right)$$

Where X_i is the total population served by the CWS, $s_{L,LM,M,MH,H}$ is the number of sources for the CWS with a mean reported Mn concentration classified as low, medium-low, medium, medium-high, or high, and S_T is the total number of point-of-entry sources for each community water system with reported data. For example, if a CWS was served by two point-of-entry sources with one source classified as low and the other medium-high, half of the population served by this CWS would be classified as potentially exposed to low Mn and the other, medium-high Mn. Since no relative flow proportion for each source was provided, it was assumed that flow between each source was equal.

3.2.3. Impact of Treatment Status on Contaminant Exposure

To determine the impact of treatment on Mn concentration, the mean Mn concentrations at initial intake were compared to Mn concentrations at point-of-entry. Since no treatment designation was provided with reported values, the initial reported

value in the flow path was considered as the intake concentration. If the initial reported value flowed into point-of-entry (e.g. only one value was reported), it was excluded from analysis.

3.2.4. Geochemical Controls of Mn Release

To elucidate how groundwater quality parameters (pH, hardness, sulfate, and iron) or co-occurrence with other primary groundwater contaminants (As, Cr, and nitrate) was associated with groundwater Mn, water quality parameters were collected with reported Mn concentration. To account for potential temporal variation in sample collection, all data that did not have an associated water quality parameter sample on the same date were excluded. Data was further separated from water source (groundwater or surface water) and treatment status (untreated or treated). All data sorting and vetting was done in Excel or RStudio (version 2022.02.1).

3.3. Statistical Analysis

Due to the non-normality of our data, non-parametric comparisons were used to test for significant differences in reported chemical data. The Kruskal-Wallis test with the Benjamini & Hochbert adjustment (Helsel and Hirsch, 1992) was used to determine significant differences in Mn concentration between CWS of different sizes (Table S4). The Mann-Whitney test was used to compare Mn concentration pre-and post-treatment (Table S5) and Mn concentration with co-occurring groundwater contaminant data above and below threshold values (Table S6). Spearman correlation analysis was also applied to

examine the relationship between Mn concentration and various other reported water quality data (Table S7 and S8). An alpha level of 0.05 was used for each statistical test and all tests were performed in RStudio (version 2022.02.1).

4. Results

4.1. Occurrence of Mn in Community Water Systems within California

From our analysis of reported Mn concentrations at CWS point-of-entry, many CWS users are accessing drinking water with mean reported concentrations exceeding those that are linked to negative health-impacts. About 39 million California residents rely on 2,851 active CWS as their primary source of drinking water, 1,284 of which reported Mn concentrations at point-of-entry between 2011-2021. Over 61.5% of users are connected to very large CWS (>100,0001 users) that more frequently report Mn concentration at point-of-entry than all other systems size classifications (Table 1). Consistently, very small systems have the largest percentage of the user population accessing water with higher reported Mn concentrations at point-of-entry, yet they serve 0.7% of the total user population (Figure 1). Overall, we estimate that 525,972 (2.2%) users within our analysis are potentially exposed to Mn concentration exceeding the WHO provisional guideline (80 μg L^{-1}) and 34,454 (0.1%) exceeding the health-advisory-limit (300 μg L^{-1}). However, this is likely to be an underestimate since over a third (35.3%) of CWSs within California did not report Mn concentrations at point-of-use and were therefore unable to be included in our estimates.

Table 1. Total population with no Mn data and the potentially exposed population (PEP)[a] to Mn in drinking water. CWS size designation is as follows: very small (<500 users), small (501-3,300 users), medium (3,301-10,000 users), large (10,001-100,000 users), and very large (100,000+ users).

	Very Small	Small	Medium	Large	Very Large	Total
Total population	257,836	559,439	1,333,204	12,838,022	23,922,533	38,911,034
Total population with no reported Mn at point-of-use	143,032 (55.5%)	371,284 (60.9%)	824,735 (61.9%)	6,724,378 (52.4%)	5,679,342 (23.7%)	13,742,721 (35.3%)
Total population with Mn data at point-of-use	114,804	238,155	508,469	6,113,644	18,243,191	25,218,262
Low (<50 µg L^{-1})	92,646 (80.7%)	220,434 (92.6%)	4,837,772 (95.1%)	5,851,886 (95.7%)	17,852,744 (97.9%)	24,501,482 (97.2%)
Low-Medium (50-80 µg L^{-1})	4,775 (4.2%)	5,182 (2.2%)	18,197 (3.6%)	43,663 (0.7%)	118,992 (0.7%)	190,809 (0.8%)
Medium (80-120 µg L^{-1})	3,856 (3.4%)	7,648 (3.2%)	0 (0%)	104,513 (1.7%)	235,373 (1.3%)	351,390 (1.4%)
Medium high (120-300 µg L^{-1})	9,606 (8.4%)	876 (0.4%)	0 (0%)	93,563 (1.5%)	36,083 (0.2%)	140,128 (0.6%)
High (> 300 µg L^{-1})	3,921 (2.4%)	4,014 (1.7%)	6,500 (1.3%)	20,019 (0.3%)	0 (0%)	34,454 (0.1%)

[a]Potentially exposed population (PEP) was calculated by multiplying the total CWS user population by the number of distribution point-of-entry falling within one of four Mn levels divided by the total number of distribution point-of-entries (Balazs et al. 2011).

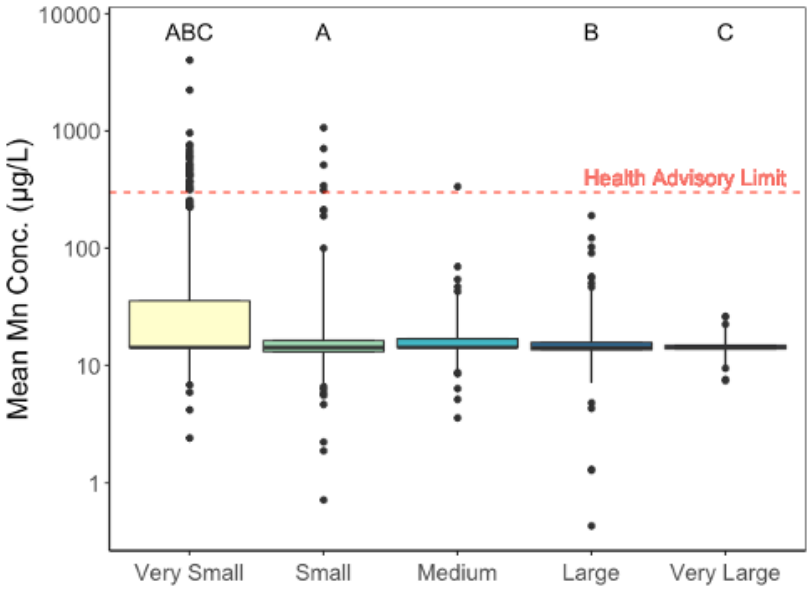

Figure 1. Mean Mn concentration from 2011 to 2021 measured at points leading directly into distribution systems. Boxes represent the 25th, 50th, and 75th percentile of concentrations and whiskers represent 5th and 95th percentiles. Outliers are represented as points. Red dashed line is the health-advisory limit for Mn (300 ug/L). Letters represent significant differences ($p<0.05$). Very Small = <500 users (n=822 CWS), Small = 501-3,300 users (n=170 CWS), Medium = 3,301-10,000 users (n =86 CWS), Large = 10,001-100,000 users (n=150 CWS), Very Large = >100,000 users (n=56 CWS).

Most CWS are along the coastal region of California. Spatial analysis of mean Mn concentration at intake and after available treatment at point-of-entry, do not demonstrate any spatial patterns of Mn occurrence at intake or after any available treatment (Figure 2).

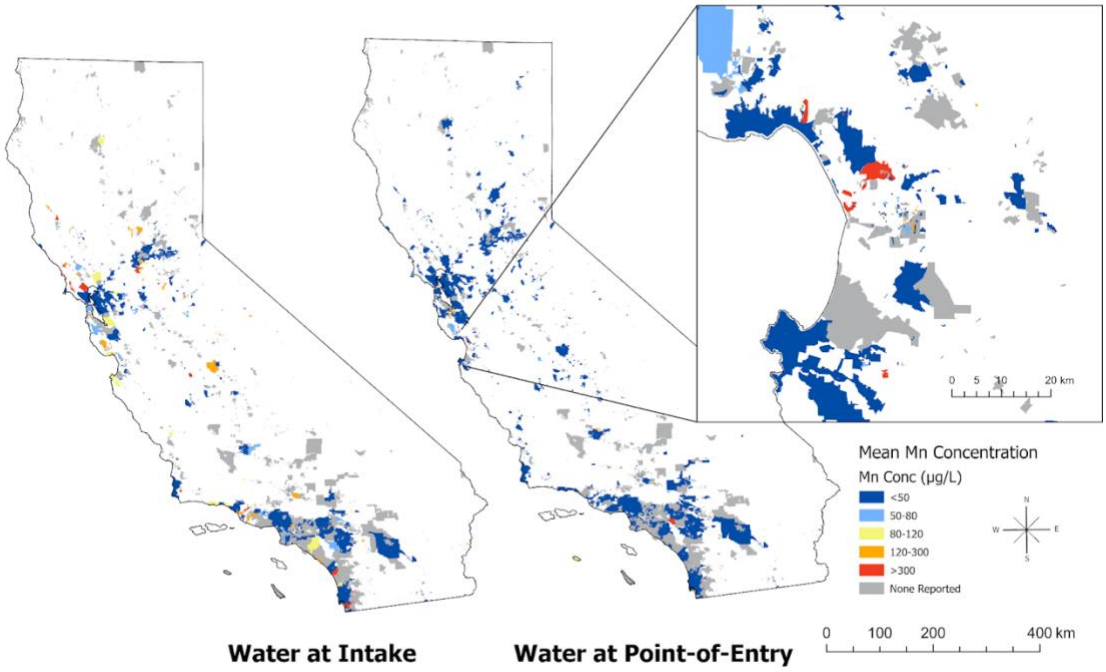

Figure 2. Mean Mn concentration in CWS between 2011-2021 at intake (left) and point-of-entry (right). Inlay zooms in on the Central Coast region to demonstrate that there is fine-scale heterogeneity in Mn contamination when considering very small and small community water systems.

4.2. Impact of treatment on Mn at point-of-use

Analysis of reported Mn data at intake versus point-of-entry revealed that treatment of surface or groundwater following withdrawal greatly impacts Mn concentrations (Figure 2 and 3). The median concentration of Mn prior to treatment in small systems was 147.7 µg L^{-1} Mn, but following treatment it was 17.3 µg L^{-1}, which is below the SMCL and WHO health-based guidelines. Although a smaller difference was observed in very large systems in comparison to smaller systems, a significant difference was observed between pre- (median of 27.7 µg L^{-1}) and post-treatment (median of 14.3 µg L^{-1}) Mn concentrations (Table S5).

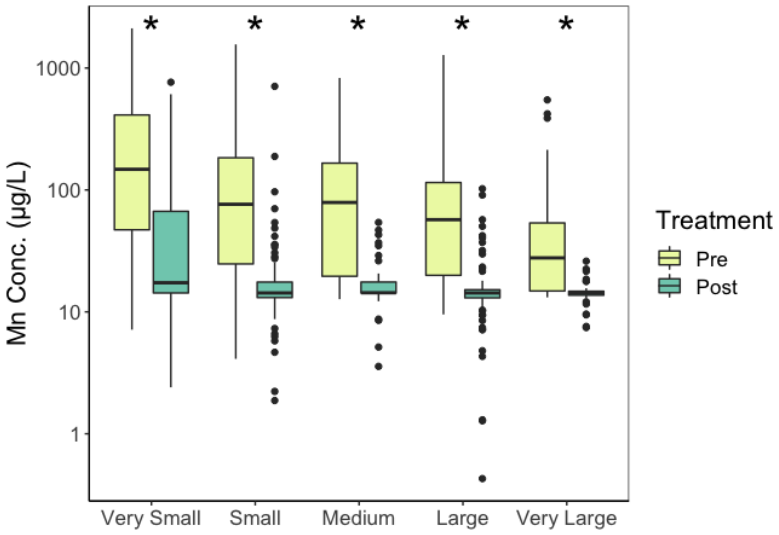

Figure 3. Impact of treatment on Mn concentration within CWS stratified by size. Pre-treatment is the mean of the first reported value in the flow path and post-treatment is the mean of reported value at point-of-entry between 2011-2021. All data that did not have reported values for pre/post-treatment are excluded from analysis. Boxes represent the 25th, 50th, and 75th percentile of concentrations and whiskers represent 5th and 95th percentiles. Outliers are represented as points. Very Small = <500 users (n=134 CWS) , Small = 501-3,300 users (n=69 CWS), Medium = 3,301-10,000 users (n =48 CWS), Large = 10,001-100,000 users (n=96 CWS), Very Large = >100,000 users (n=50 CWS). * Designates significant difference in median pre- and post-treatment between each system size classification (p>0.000, Table S5).

4.3. Co-occurrence of Mn with other contaminants

To better understand the co-occurrence of Mn with other contaminants we analyzed As and Cr data collected concurrently with Mn. We observed that raw groundwater extracted by CWSs that exceeded the maximum contaminant level for As or Cr (10 μg L^{-1}), are also likely to have higher median Mn concentrations than water with As or Cr below the MCL (Figure 4). The median Mn concentration for groundwater with As below the As MCL (75 μg L^{-1} Mn) was significantly lower than when As concentration exceeded the MCL (115 μg L^{-1}, $p<0.000$, Table S6) in untreated groundwater. Similarly, Mn concentration measured in groundwater below the Cr MCL had a significantly lower median concentration (26.7 μg L^{-1} Mn) than when extracted groundwater exceeded the Cr MCL (40 μg L^{-1}, $p<0.000$, Table S7). However, Cr does not correlate with Mn in raw groundwater ($r=0.08$, $p < 0.000$) whereas there was a slight positive correlation between As and Mn concentration in raw groundwater ($r=0.15$, $p < 0.000$, Table S7).

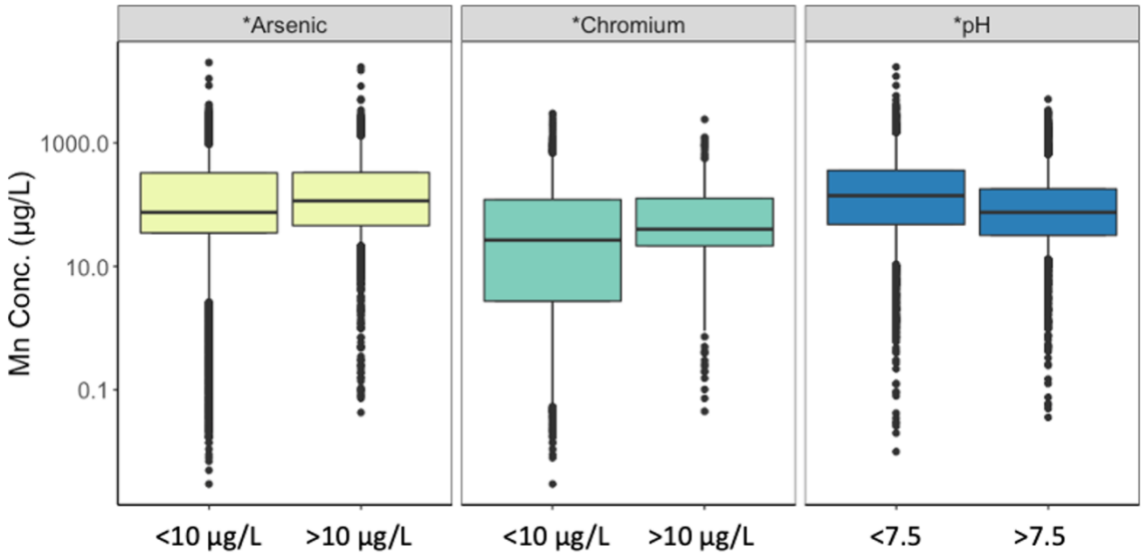

Figure 4. Raw groundwater Mn concentration in relation to primary groundwater contaminants As and Cr, and water pH from samples collected on the same day and sampling location. Boxes represent the 25th, 50th, and 75th percentile of concentrations and whiskers represent 5th and 95th percentiles. Outliers are represented as points. *= significantly different median Mn values between concurrently measured co-contaminant or water quality values listed as categories at the bottom of the plot ($p<0.000$, Table S6). Count of all samples analyzed are listed in Table S6.

4.4. Co-occurrence with other redox sensitive groundwater constituents

Since Mn is a redox sensitive groundwater contaminant, we also gathered all available ancillary chemical data for other redox sensitive groundwater contaminants including concentrations of nitrate, Fe, and sulfate, along with dissolved organic carbon (DOC) which fuels microbial metals reduction. A positive correlation was found between Mn and Fe ($r = 0.43$, $p < 0.000$) and DOC ($r = 0.46$, $p < 0.000$), whereas a slight positive correlation was observed with sulfate ($r = 0.28$, $p < 0.000$) in raw groundwater (Table S7). Following a similar pattern to the observed correlations, higher median Mn concentrations were observed in raw groundwater samples with Fe (SMCL = 200 µg L^{-1}) and sulfate (SMCL = 250µg L^{-1}) exceeding set SMCL values (Figure 5, Table S6).

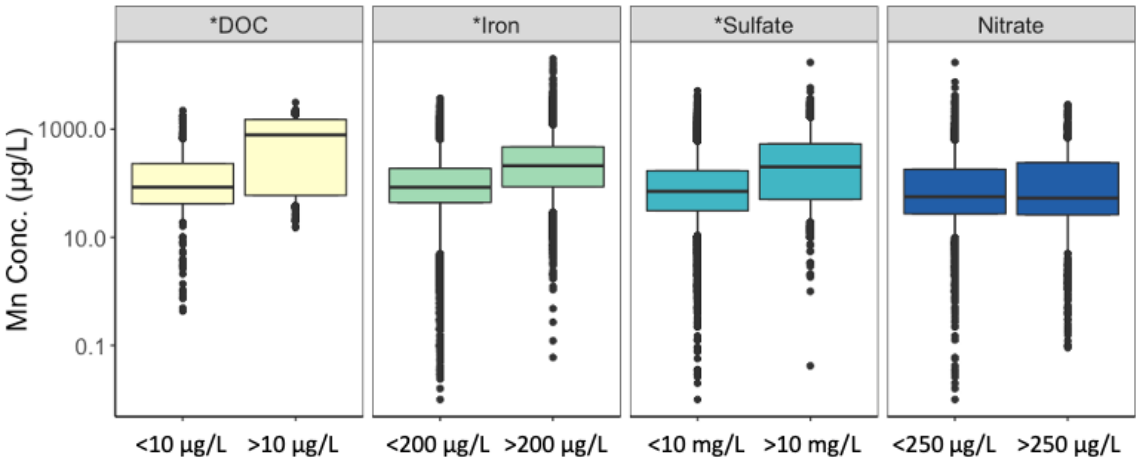

Figure 5. Raw groundwater Mn concentration in relation to other redox sensitive groundwater constituents sampled on the same day and sampling location. Boxes represent the 25th, 50th, and 75th percentile of concentrations and whiskers represent 5th and 95th percentiles. Outliers are represented as points. *= significantly different median Mn values between concurrently measured co-contaminant or water quality values listed as categories at the bottom of the plot ($p<0.000$, Table S6). Count of all samples analyzed are listed in Table S6.

Additional controls over Mn fate in the subsurface, such as pH and calcium carbonate ($CaCO_3$), was also investigated. A slight positive correlation was observed between Mn and sulfate ($n = 0.28$, $p < 0.000$), whereas Mn was slightly negatively correlated with pH ($n = -0.22$, $p < 0.000$, Table S7).

5. Discussion

5.1. Mn distribution and reporting in CWS

From our analysis, we observed less reporting of Mn values at point-of-use within very small or small systems (55.5% and 60.9%) than very large systems (23.7%). Additionally, we found a higher percentage of very small system users (14.2%) potentially exposed to Mn concentrations exceeding the WHO guideline value at point-of-use than very large systems (2.1%). Previous analyses of primary contaminant

violation in community water systems have also demonstrated higher instances of primary contaminant violations in smaller systems and have attributed this difference to the challenges faced by smaller systems when accessing treatment options (Balazs et al., 2011; Rubin, 2013; Schaider et al., 2019; Bangia et al., 2020; Pace et al., 2022). Larger systems have better economy-of-scale and can easily distribute costs of management and treatment across the larger user base. In contrast, since small systems serve less users, costs of additional treatment may no longer meet user affordability requirements (Balazs and Ray, 2014; Pierce et al., 2020; Glade and Ray, 2022).

In an analysis of the USEPA's Unregulated Contaminant Monitoring Rule (UCMR) dataset which included monitoring of Mn in finished water of public systems, it was observed that 12.8% of public water systems exceeded 50 μg L^{-1} Mn and 2.1% of public water systems reported Mn concentrations exceeding 300 μg L^{-1} (Eaton, 2021; U.S. Environmental Protection Agency, 2022). Within our study, approximately 15.2% of CWS with reported mean Mn concentrations exceeded the SMCL (50 μg L^{-1} Mn) and 3.1% exceeded the HAL (300 μg L^{-1}), most of which were small or very small systems. This is similar to the national average, yet slightly higher due to the inclusion of more very small or small systems in comparison to larger systems. While smaller systems are required to be included in UCMR sampling events, only 800 small systems were included out of over 10,000 sampled systems (U.S. Environmental Protection Agency, 2022). Since smaller systems may lack monitoring and treatment infrastructure due to associated costs, their inclusion in large scale monitoring events is critical to identify populations accessing water in excess of Mn or other contaminants.

Observed differences in contaminant concentrations between CWSs based on size can be attributed to diminished technical, managerial, and financial (TMF) capacity of smallers systems which limits consistent monitoring and adjustments in treatment. These disparities can be further exacerbated by a range of sociopolitical barriers including proximity to polluting sources, lack of political power, and limited access to financial resources (Balazs and Ray, 2014). Often, larger systems have better economy-of-scale and can easily distribute costs of management and treatment across its larger user base. However, since small systems serve less users, costs of additional treatment may no longer meet user affordability requirements (Balazs and Ray, 2014; Pierce et al., 2020; Glade and Ray, 2022). Smaller systems often rely on fewer surface or groundwater intake points than larger systems, and if the source water violates water quality standards, they are unable to switch to a different intake source (Logar et al., 2019). Drought conditions likely exacerbates user affordability issues in smaller systems due to depletion of long-term water storage (Piper, 2003; Klasic et al., 2022).

5.2. Mn and impact of treatment

Outside of the UCMR 5 monitoring event, previous analysis of potential drinking water Mn contamination has largely focused on untreated, raw groundwater concentrations (Homoncik et al., 2010; McArthur et al., 2012; Palmucci et al., 2016; Rosecrans et al., 2017; McMahon et al., 2019; Erickson et al., 2019; Bondu et al., 2020; Kousa et al., 2021) which may not be representative of Mn concentrations at CWS point-of-entry. Our analyses show that Mn concentrations are significantly lower across all system sizes following associated treatment (Figure 2 and 3). In larger systems that have

more resources for treatment, treatment of Mn may occur for aesthetic reasons since water with Mn concentrations greater than 50 μg L^{-1} can appear discolored or have a metallic taste (Sain et al., 2014). Common treatments used to remove Mn include oxidation/precipitation, physical treatment, biological treatment, and infrastructure management.

5.2.1. Co-treatment of primary contaminants

Despite smaller economies of scale, very small and small systems Mn concentrations were significantly lower following available treatment (Figure 3) potentially due to the required treatment of primary contaminants to meet state-wide, enforceable standards. For example, our results show that median Mn concentration was higher in raw groundwater that also exceeded the MCL for arsenic for all system sizes (Figure 4, Table S9). Therefore, treatment of groundwater is required to meet state drinking water standards. Common treatments for As in groundwater is oxidation/filtration via ozone, chlorine dioxide, or other oxidants, and followed by membrane filtration, which will also result in the oxidation and removal of aqueous Mn (Wong, 1984; Knocke et al., 1987; Bissen and Frimmel, 2003). Treatment of other primary contaminants, such as nitrate, through processes such as ion exchange, reverse osmosis, or electrodialysis, may also result in the removal of Mn (Kapoor and Viraraghavan, 1997; Breda et al., 2017). However, in our analysis and others (Burow et al., 2008; Erickson et al., 2019, 2021; Riedel et al., 2022), Mn and nitrate were not co-located in groundwater extracted for domestic use most likely due to predominant

groundwater redox conditions at the time of extraction. Therefore, systems with high concentrations of Mn, may not have high nitrate requiring treatment.

Reporting of available water treatments within individual CWS is minimal, making it difficult to quantitatively assess whether treatment of primary contaminants is sufficient for Mn removal in CWSs of different sizes. Further inquiry and analysis of systems that are effective or ineffective at removal of Mn is required to better understand the impact of specific treatments on Mn prior to distribution. Specific attention must also be paid to small systems where treatment may be prioritized for enforced, primary contaminants, but not for Mn.

5.2.2. Treatment options and feasibility

A common removal technique is to facilitate the oxidation of dissolved Mn(II) followed by the removal of the Mn(III/IV) particulates via filtration. Common oxidants used are oxygen, chlorine dioxide, ozone, and permanganate (Wong, 1984; Knocke et al., 1987). It is well known that Mn(II) can precipitate in well-oxygenated water, however, the process is slow at circumneutral pH and may require a longer residence time or stronger oxidants to facilitate a quicker removal (Morgan, 2005). Additional water quality parameters, such as DOC or the presence of other reactive metals, such as iron, that could inhibit Mn oxidation must also be considered (Li et al., 2021). Once precipitation occurs the suspended Mn(III/IV) oxides must be removed via filtration. Conventional media filtration is often sufficient to remove the suspended particles, but if direct oxidation results in the formation of ultrafine particles, membrane microfiltration or ultrafiltration may be required (Ellis et al., 2000). Removal of Mn via filtration is also

possible without prior chemical oxidation by the adsorption of Mn directly on the filtration media, such as “greensand” filters (Knocke et al., 1988, 1991) or direct ion exchange (Carrière et al., 2011). Biofiltration, or filtration media that supports the growth of biofilms, has also been demonstrated to remove Mn in drinking water without any chemical additions. Three pathways of Mn removal are possible using this method: direct intracellular oxidation, extracellular adsorption, or oxidation by biofilms produced by microorganisms (Breda et al., 2017).

Although the above methods are effective at Mn removal, various other water quality parameters, such as DOC, Fe, and dissolved oxygen, must also be considered when assessing removal effectiveness. Within our work, we observed higher concentrations of Mn co-occurring with higher concentration of DOC and Fe (Figure 5) which may limit the effective removal of Mn using these methods. Constant monitoring not only of Mn, but of other water quality parameters, is required to ensure removal. Smaller systems that lack infrastructure support may not have access to consistent monitoring to determine if break-through is occurring prior to distribution.

Infrastructure management may also represent a path to minimizing Mn user exposure. If the water system contains multiple wells, then it is possible to mix water from one with high Mn with a low Mn well prior to treatment or distribution to meet water quality standards. This management method, known as water blending, may be possible for municipal or small water systems, however, may not be feasible for small water systems that rely on one intake source (Logar et al., 2019). The most direct and cost-effective method to reduce Mn consumption is to simply remove the well from use if

it exceeds regulatory standards. However, this is not a viable option for private well users that rely solely on their well for water use within their household.

Further management options, such as consolation of small water systems with larger systems may also be a feasible mitigation solution. Approximately 66% of very small or small CWSs are in close proximity (4.8 km) to larger systems where consolidation is considered a viable option (London, 2021). Consolidation will improve the economy-of-scale since smaller systems will now have access to the improved infrastructure and management provided to larger systems. In addition, the cost of increased monitoring and treatment will then be shared among a larger user base which would increase water affordability. Despite evidence of the effectiveness of consolidation for water quality improvement (London et al., 2018; Logar et al., 2019), there are associated risks such as loss of local autonomy and the large initial financial investment (Logar et al., 2019). Further allocation of state-funding to support consolidation is required to enhance feasibility and ensure effectiveness of this management method (Nylen et al., 2018).

Within our work, we found that a higher percentage of very small and small systems exceeded the health-based threshold for Mn in drinking water and targeted mitigation measures within these communities are needed. Further consideration of other factors preventing access to infrastructure, such as within rural or disadvantaged communities, will also improve equitable distribution of state-sponsored funds.

5.3. Mn Geochemistry of Release

Manganese mobility in subsurface environments is predominantly controlled by biotic and abiotic redox transformations that result in either Mn immobilization through precipitation and adsorption reactions (Tebo, 2004; Farnsworth et al., 2012; Gillispie et al., 2016) or mobilization via microbially-driven reductive dissolution during anaerobic respiration (Gounot, 1994; Stumm and Morgan, 1996). Within our work, Mn in raw groundwater was positively correlated with Fe which is similar to findings in other studies (e.g., McArthur et al., 2012; McMahon et al., 2019; Kousa et al., 2021). Although a less favorable electron acceptor than Mn, Fe is often observed in groundwater under similar conditions as Mn due to the natural overlap of reducing zones (Ying et al., 2017) and the mixing of water from different zones during well screening (McMahon and Chapelle, 2008).

During reductive dissolution of Mn and Fe, sorbed metal contaminants, such as As and Cr, may be released into groundwater. Globally, the dissolution of sorbed metals to metal oxides often drives As contamination in groundwater sources (e.g., Fendorf et al., 2010; Neidhardt et al., 2014; Fakhreddine et al., 2015). Similarly, studies investigating redox controls on Cr(VI) contamination of groundwater in California's Central Valley observed higher Cr(VI) production co-located with Mn oxide staining in the subsurface (Manning et al., 2015; McClain et al., 2019). Since Cr(III) oxidation to Cr(VI) is primarily driven by Mn oxides and Mn(II) is released during oxidation, the location of these two minerals within the subsurface plays an important role in the release of these groundwater contaminants (see Ch. 2).

Another important factor driving the release of redox sensitive contaminants is the presence of carbon. Areas with higher DOC, and therefore higher microbial activity, often more rapidly deplete available oxygen and nitrate, leading to the reductive dissolution of available Mn and Fe oxides (Puckett and Cowdery, 2002; McMahon and Chapelle, 2008; Neidhardt et al., 2014; McMahon et al., 2019). Therefore, the positive correlation observed between DOC and Mn in raw groundwater supports our conclusion that reductive dissolution of Mn minerals is a primary driver of Mn mobilization into groundwater accessed for domestic use. Higher concentrations of DOC near riverbanks or infiltrating surface water often drive nearby reducing zones and the release of Mn and Fe into groundwater (Farnsworth and Hering, 2011; McMahon et al., 2019).

Within our work, we observed no correlation between Mn and nitrate concentrations. Previous work has outlined a redox framework where Mn reduction predominates over oxygen and nitrate below threshold values (Burow et al., 2008; McMahon and Chapelle, 2008). Periodic influxes of nitrate driven by infiltration or agricultural use has been demonstrated to also temporarily suppress Mn reducing since it is more thermodynamically favored during microbial respiration (Puckett and Cowdery, 2002; Kedziorek and Bourg, 2009). Increased rates of Mn and Fe release being observed at similar depths where nitrate concentrations were low further supports that Mn mobilization is redox controlled.

From spatial analysis of Mn in raw intake water and following treatment, no spatial patterns emerged in the distribution of Mn water accessed for use in CWS. Analysis of subsurface geochemical conditions favorable for Mn dissolution have

demonstrated the formation of "hot-spots" for Mn release into groundwater (Gillispie et al., 2016; Rosecrans et al., 2017; Erickson et al., 2021), but this may occur at a spatial resolution unable to be captured in this analysis due to the spatial heterogeneity of CWS boundaries. Rosecrans et al. (2017) applied machine learning techniques to model redox conditions and dissolved Mn in California's Central Valley. Regional characteristics such as lateral position within the Valley, depth to water table, and portion of poorly drained soils were the most important predictor variables of Mn concentration within groundwater and are consistent with our understanding of hydrological processes governing anoxic locations within the subsurface that drive Mn release. However, no such model currently exists for the entire state of California where other subsurface characteristics may govern Mn precipitation and dissolution. These models improve our understanding of groundwater accessed by CWS and also areas where groundwater accessed by private wells may exceed regulatory standards.

6. Data Limitations

6.1. Other water type users

State small systems (less than 14 service connections) and domestic well users were not considered in this study due to infrequent water quality reporting for these populations across the state. An estimated 1.3 million individuals within California rely on domestic wells as their main source of water (Pace et al., 2022). Since these systems lack regular reporting or treatment, raw groundwater is more likely to be what is used at tap. In previous analyses comparing Mn concentration from domestic, public wells, McMahon et al. (2019) observed more Mn exceeding the 300 $\mu g\ L^{-1}$ health advisory limit

in domestic wells (7.2%) than public wells (5.2%) due to the impact of land surface-soil-aquifer connections on Mn release and the depth of drilled wells. However, treatment of Mn was not taken into consideration within this study, which may further exacerbate differences in exposure between these two communities since treatment reduces Mn in extracted groundwater (Figure 3).

6.2. Modification of Mn concentration from point-of-use to tap

Within our study, we rely on reported water quality at the point-of-entry, or the point at which the water enters the distribution system. However, once in the distribution system, Mn concentration may be further modified prior to use. Residence time in the distribution system has been linked to lower concentration of Mn at the tap due to precipitation of Mn by oxidizing bacteria in biofilms, residual chlorine, or oxygen (Cerrato et al., 2010; Li et al., 2019; Zhang et al., 2021). Although these represent reduction in the overall concentration of Mn, physical disruption of the biofilms or precipitates within pipes through hydraulic disturbances (flushing or change in flow) or water chemistry (pH, sulfate, or temperature) may disrupt previous Mn deposition and increase exposure at-tap (Zhang et al., 2021). All of this may occur after entry into the distribution system and was unable to be captured within this study. Further consideration of water quality at tap is needed to assess the impact of residence time within the distribution system and how that may impact potential exposure.

Aversion behavior may also limit exposure to Mn. Particulate Mn as low as 50 μg L^{-1} is visually detected in drinking water. However, dissolved Mn does not have any visual deterrents and does not impart a metallic taste within water below 7,500 μg L^{-1}

(Sain et al., 2014). Since dissolved Mn does not impart any obvious visual deterrents, users may unknowingly consume water exceeding the WHO provisional guideline or the health advisory limit (Sain et al., 2014). If visually detected in tap water, users are more likely to rely on purchased water or further treat water prior to drinking, therefore reducing exposure. Further studies are needed to assess whether aversion behavior is a potential contribution to decreased Mn exposure particularly in small systems and domestic well communities with limited treatment options.

7. Future Implications

Mn is currently undergoing further consideration as a primary groundwater contaminant. Between 2019-2022, Mn was relisted as a groundwater contaminant by the WHO, received a maximum acceptable concentration in drinking water by Health Canada, and its status as a secondary contaminant is undergoing review within the state of California. As our perspective in the U.S. shifts from regarding Mn as a nuisance chemical to one of health concern, we need to simultaneously understand potential routes of exposure. Current treatment methods within large water systems have demonstrated effective removal of Mn prior to point-of-entry, however, increased attention needs to be given to smaller water systems without similar economies of scale. Funding treatment within these smaller systems may not only help address existing water quality problems, but also address issues with high concentrations of Mn such as increased access to water treatment, consolidation of smaller systems, or more frequent monitoring. Since Mn is on the cusp of being regulated as a primary contaminant, more consideration of the occurrence of Mn in all system sizes is needed to assess the magnitude of the issue.

Further, our understanding of Mn as a redox active contaminant will add to ongoing considerations as to where to drill new wells. In future work, additional consideration will need to be given to state small systems and private wells where water quality and treatment access may not be available to users.

8. References

Aschner M., Guilarte T. R., Schneider J. S. and Zheng W. (2007) Manganese: Recent advances in understanding its transport and neurotoxicity. *Toxicology and Applied Pharmacology* **221**, 131–147.

Balazs C. L. and Ray I. (2014) The Drinking Water Disparities Framework: On the Origins and Persistence of Inequities in Exposure. *Am J Public Health* **104**, 603–611.

Balazs C., Morello-Frosch R., Hubbard A. and Ray I. (2011) Social disparities in nitrate-contaminated drinking water in California's San Joaquin Valley. *Environ. Health Perspect.* **119**, 1272–1278.

Bangia K., August L., Slocombe A. and Faust J. (2020) Assessment of contaminants in California drinking water by region and system size. *AWWA Water Science* **2**, e1194.

Bissen M. and Frimmel F. H. (2003) Arsenic — a Review. Part II: Oxidation of Arsenic and its Removal in Water Treatment. *Acta hydrochimica et hydrobiologica* **31**, 97–107.

Bondu R., Cloutier V., Rosa E. and Roy M. (2020) An exploratory data analysis approach for assessing the sources and distribution of naturally occurring contaminants (F, Ba, Mn, As) in groundwater from southern Quebec (Canada). *Applied Geochemistry* **114**, 104500.

Bouchard M. F., Sauvé S., Barbeau B., Legrand M., Brodeur M.-È., Bouffard T., Limoges E., Bellinger D. C. and Mergler D. (2011) Intellectual impairment in school-age children exposed to manganese from drinking water. *Environ Health Perspect* **119**, 138–143.

Breda I. L., Ramsay L. and Roslev P. (2017) Manganese oxidation and bacterial diversity on different filter media coatings during the start-up of drinking water biofilters. *Journal of Water Supply: Research and Technology-Aqua* **66**, 641–650.

Burow K. R., Shelton J. L. and Dubrovsky N. M. (2008) Regional Nitrate and Pesticide Trends in Ground Water in the Eastern San Joaquin Valley, California. *Journal of Environmental Quality* **37**, S-249-S-263.

California State Water Resource Control Board (2021) EDT Library and Water Quality Analyses Data and Download Page. https://www.waterboards.ca.gov/drinking_water/certlic/drinkingwater/EDTlibrary.html

California State Water Resources Control Board (2020) Drinking Water Notification Level for Manganese. https://www.waterboards.ca.gov/drinking_water/certlic/drinkingwater/Manganese.html

Carrière A., Brouillon M., Sauvé S., Bouchard M. F. and Barbeau B. (2011) Performance of point-of-use devices to remove manganese from drinking water. *Journal of Environmental Science and Health, Part A* **46**, 601–607.

Cerrato J. M., Falkinham J. O., Dietrich A. M., Knocke W. R., McKinney C. W. and Pruden A. (2010) Manganese-oxidizing and -reducing microorganisms isolated from biofilms in chlorinated drinking water systems. *Water Research* **44**, 3935–3945.

Davison W. (1993) Iron and manganese in lakes. *Earth-Science Reviews* **34**, 119–163.

Eaton A. (2021) Assessment of Manganese Occurrence in Drinking Water in the United States. *ACS EST Water* **1**, 2450–2458.

Ellis D., Bouchard C. and Lantagne G. (2000) Removal of iron and manganese from groundwater by oxidation and microfiltration. *Desalination* **130**, 255–264.

Erickson M. L., Elliott S. M., Brown C. J., Stackelberg P. E., Ransom K. M., Reddy J. E. and Cravotta C. A. (2021) Machine-Learning Predictions of High Arsenic and High Manganese at Drinking Water Depths of the Glacial Aquifer System, Northern Continental United States. *Environ. Sci. Technol.* **55**, 5791–5805.

Erickson M. L., Yager R. M., Kauffman L. J. and Wilson J. T. (2019) Drinking water quality in the glacial aquifer system, northern USA. *Science of The Total Environment* **694**, 133735.

Fakhreddine S., Dittmar J., Phipps D., Dadakis J. and Fendorf S. (2015) Geochemical Triggers of Arsenic Mobilization during Managed Aquifer Recharge. *Environ. Sci. Technol.* **49**, 7802–7809.

Farnsworth C. E. and Hering J. G. (2011) Inorganic Geochemistry and Redox Dynamics in Bank Filtration Settings. *Environ. Sci. Technol.* **45**, 5079–5087.

Farnsworth C. E., Voegelin A. and Hering J. G. (2012) Manganese Oxidation Induced by Water Table Fluctuations in a Sand Column. *Environ. Sci. Technol.* **46**, 277–284.

Fendorf S., Michael H. A. and van Geen A. (2010) Spatial and temporal variations of groundwater arsenic in South and Southeast Asia. *Science* **328**, 1123–1127.

Gandy C. J., Smith J. W. N. and Jarvis A. P. (2007) Attenuation of mining-derived pollutants in the hyporheic zone: A review. *Science of The Total Environment* **373**, 435–446.

Gerke T. L., Little B. J. and Barry Maynard J. (2016) Manganese deposition in drinking water distribution systems. *Science of The Total Environment* **541**, 184–193.

Gillispie E. C., Austin R. E., Rivera N. A., Bolich R., Duckworth O. W., Bradley P., Amoozegar A., Hesterberg D. and Polizzotto M. L. (2016) Soil Weathering as an Engine for Manganese Contamination of Well Water. *Environ. Sci. Technol.* **50**, 9963–9971.

Glade S. and Ray I. (2022) Safe drinking water for small low-income communities: the long road from violation to remediation. *Environ. Res. Lett.* **17**, 044008.

Gounot A. M. (1994) Microbial oxidation and reduction of manganese: consequences in groundwater and applications. *FEMS Microbiol Rev* **14**, 339–349.

Harvey J. W. and Fuller C. C. (1998) Effect of enhanced manganese oxidation in the hyporheic zone on basin-scale geochemical mass balance. *Water Resources Research* **34**, 623–636.

Helsel D. R. and Hirsch R. M. (1992) *Statistical Methods in Water Resources*., Elsevier.

Homoncik S. C., MacDonald A. M., Heal K. V., Ó Dochartaigh B. É. and Ngwenya B. T. (2010) Manganese concentrations in Scottish groundwater. *Science of The Total Environment* **408**, 2467–2473.

Johnson R. H., Blowes D. W., Robertson W. D. and Jambor J. L. (2000) The hydrogeochemistry of the Nickel Rim mine tailings impoundment, Sudbury, Ontario. *Journal of Contaminant Hydrology* **41**, 49–80.

Kapoor A. and Viraraghavan T. (1997) Nitrate Removal From Drinking Water—Review. *Journal of Environmental Engineering* **123**, 371–380.

Kedziorek M. A. M. and Bourg A. C. M. (2009) Electron trapping capacity of dissolved oxygen and nitrate to evaluate Mn and Fe reductive dissolution in alluvial aquifers during riverbank filtration. *Journal of Hydrology* **365**, 74–78.

Khan K., Wasserman G. A., Liu X., Ahmed E., Parvez F., Slavkovich V., Levy D., Mey J., van Geen A., Graziano J. H. and Factor-Litvak P. (2012) Manganese exposure from drinking water and children's academic achievement. *NeuroToxicology* **33**, 91–97.

Klasic M., Fencl A., Ekstrom J. A. and Ford A. (2022) Adapting to extreme events: small drinking water system manager perspectives on the 2012–2016 California Drought. *Climatic Change* **170**, 26.

Knocke W., Benschoten J. V., Kearney M. J., Soborski A. W. and Reckhow D. (1991) Kinetics of Manganese and Iron Oxidation by Potassium Permanganate and Chlorine Dioxide.

Knocke W. R., Hoehn R. C. and Sinsabaugh R. L. (1987) Using Alternative Oxidants to Remove Dissolved Manganese From Waters Laden With Organics. *Journal AWWA* **79**, 75–79.

Knocke W. R., Ramon J. R. and Thompson C. P. (1988) Soluble Manganese Removal on Oxide-Coated Filter Media. *Journal (American Water Works Association)* **80**, 65–70.

Kousa A., Komulainen H., Hatakka T., Backman B. and Hartikainen S. (2021) Variation in groundwater manganese in Finland. *Environ Geochem Health* **43**, 1193–1211.

Krueger K. M., Vavrus C. E., Lofton M. E., McClure R. P., Gantzer P., Carey C. C. and Schreiber M. E. (2020) Iron and manganese fluxes across the sediment-water interface in a drinking water reservoir. *Water Research* **182**, 116003.

Kullar S. S., Shao K., Surette C., Foucher D., Mergler D., Cormier P., Bellinger D. C., Barbeau B., Sauvé S. and Bouchard M. F. (2019) A benchmark concentration analysis for manganese in drinking water and IQ deficits in children. *Environment International* **130**, 104889.

Legislative Analyst's Office (2020) Expanding Access to Safe and Affordable Drinking Water in California—A Status Update. , 22.

Li G., Chen R., Ma X. and Shi B. (2021) Critical Factors Affecting the Level of Dissolved Manganese in Different Raw Water and its Removal at Water Treatment Plants. *ACS EST Water* **1**, 2259–2268.

Li G., Ma X., Chen R., Yu Y., Tao H. and Shi B. (2019) Field studies of manganese deposition and release in drinking water distribution systems: Insight into deposit control. *Water Research* **163**, 114897.

Lin M., Colon-Perez L. M., Sambo D. O., Miller D. R., Lebowitz J. J., Jimenez-Rondan F., Cousins R. J., Horenstein N., Aydemir T. B., Febo M. and Khoshbouei H. (2020) Mechanism of Manganese Dysregulation of Dopamine Neuronal Activity. *J Neurosci* **40**, 5871–5891.

Logar N., Salzman J. and Horowitz C. (2019) Ensuring Safe Drinking Water in Los Angeles County's Small Water Systems. *Tulane Environmental Law Journal* **32**, 205–237.

London J., Fencl A., Watterson S., Jarin J., Aranda A., King A., Pannu C., Seaton P., Firestone L., Dawson M. and Nguyen P. (2018) The Strugle for Water Justice in California's San Joaquin Valley: A Focus on Disadvantaged Unincorporated Communities.

London J. K. (2021) Disadvantaged Unincorporated Communities and the Struggle for Water Justice in California. **14**, 26.

Lubin J. H., Colt J. S., Camann D., Davis S., Cerhan J. R., Severson R. K., Bernstein L. and Hartge P. (2004) Epidemiologic Evaluation of Measurement Data in the Presence of Detection Limits. *Environ Health Perspect* **112**, 1691–1696.

Manning A. H., Mills C. T., Morrison J. M. and Ball L. B. (2015) Insights into controls on hexavalent chromium in groundwater provided by environmental tracers, Sacramento Valley, California, USA. *Applied Geochemistry* **62**, 186–199.

McArthur J. M., Sikdar P. K., Nath B., Grassineau N., Marshall J. D. and Banerjee D. M. (2012) Sedimentological Control on Mn, and Other Trace Elements, In Groundwater of the Bengal Delta. *Environ. Sci. Technol.* **46**, 669–676.

McClain C. N., Fendorf S., Johnson S. T., Menendez A. and Maher K. (2019) Lithologic and redox controls on hexavalent chromium in vadose zone sediments of California's Central Valley. *Geochimica et Cosmochimica Acta* **265**, 478–494.

McMahon P. B., Belitz K., Reddy J. E. and Johnson T. D. (2019) Elevated Manganese Concentrations in United States Groundwater, Role of Land Surface–Soil–Aquifer Connections. *Environ. Sci. Technol.* **53**, 29–38.

McMahon P. B. and Chapelle F. H. (2008) Redox processes and water quality of selected principal aquifer systems. *Ground Water* **46**, 259–271.

Morgan J. J. (2005) Kinetics of reaction between O2 and Mn(II) species in aqueous solutions. *Geochimica et Cosmochimica Acta* **69**, 35–48.

Neal A. P. and Guilarte T. R. (2013) Mechanisms of lead and manganese neurotoxicity. *Toxicology Research* **2**, 99–114.

Neidhardt H., Berner Z. A., Freikowski D., Biswas A., Majumder S., Winter J., Gallert C., Chatterjee D. and Norra S. (2014) Organic carbon induced mobilization of iron and manganese in a West Bengal aquifer and the muted response of groundwater arsenic concentrations. *Chemical Geology* **367**, 51–62.

Nylen N. G., Pannu C. and Kiparsky M. (2018) Learning from California's Experience with Small Water Systems.

Oulhote Y., Mergler D., Barbeau B., Bellinger D. C., Bouffard T., Brodeur M.-È., Saint-Amour D., Legrand M., Sauvé S. and Bouchard M. F. (2014) Neurobehavioral Function in School-Age Children Exposed to Manganese in Drinking Water. *Environ Health Perspect* **122**, 1343–1350.

Pace C., Balazs C., Bangia K., Depsky N., Renteria A., Morello-Frosch R. and Cushing L. J. (2022) Inequities in Drinking Water Quality Among Domestic Well Communities and Community Water Systems, California, 2011–2019. *Am J Public Health* **112**, 88–97.

Pace C., Balazs C., Cushing L. and Morello-Frosch R. (2020) Locating Domestic Well Communities in California: A Methodological Overview.

Palmucci W., Rusi S. and Di Curzio D. (2016) Mobilisation processes responsible for iron and manganese contamination of groundwater in Central Adriatic Italy. *Environ Sci Pollut Res Int* **23**, 11790–11805.

Pierce G., Chow N. and DeShazo J. R. (2020) The case for state-level drinking water affordability programs: Conceptual and empirical evidence from California. *Utilities Policy* **63**, 101006.

Piper S. (2003) Impact of water quality on municipal water price and residential water demand and implications for water supply benefits. *Water Resources Research* **39**.

Puckett L. J. and Cowdery T. K. (2002) Transport and fate of nitrate in a glacial outwash aquifer in relation to ground water age, land use practices, and redox processes. *J Environ Qual* **31**, 782–796.

Riedel T., Kübeck C. and Quirin M. (2022) Legacy nitrate and trace metal (Mn, Ni, As, Cd, U) pollution in anaerobic groundwater: Quantifying potential health risk from "the other nitrate problem." *Applied Geochemistry* **139**, 105254.

Rosecrans C. Z., Nolan B. T. and Gronberg J. M. (2017) Prediction and visualization of redox conditions in the groundwater of Central Valley, California. *Journal of Hydrology* **546**, 341–356.

Rubin S. J. (2013) Evaluating violations of drinking water regulations. *Journal AWWA* **105**, E137–E147.

Sain A. E., Griffin A. and Dietrich A. M. (2014) Assessing taste and visual perception of Mn(II) and Mn(IV). *Journal AWWA* **106**, E32–E40.

Schaider L. A., Swetschinski L., Campbell C. and Rudel R. A. (2019) Environmental justice and drinking water quality: are there socioeconomic disparities in nitrate levels in U.S. drinking water? *Environmental Health* **18**, 3.

Schullehner J., Thygesen M., Kristiansen S. M., Hansen B., Pedersen C. B. and Dalsgaard S. (2020) Exposure to Manganese in Drinking Water during Childhood and Association with Attention-Deficit Hyperactivity Disorder: A Nationwide Cohort Study. *Environmental Health Perspectives* **128**, 097004.

Sherris A. R., Baiocchi M., Fendorf S., Luby S. P., Yang W. and Shaw G. M. (2021) Nitrate in Drinking Water during Pregnancy and Spontaneous Preterm Birth: A Retrospective Within-Mother Analysis in California. *Environ Health Perspect* **129**, 57001.

Spangler A. H. and Spangler J. G. (2009) Groundwater Manganese and Infant Mortality Rate by County in North Carolina: An Ecological Analysis. *EcoHealth* **6**, 596–600.

State Water Resource Control Board (2021) Failing Water Systems: The Human Right to Water (HR2W) List Criteria.

Stumm W. and Morgan J. J. (1996) *Aquatic chemistry: chemical Equilibria and rates in natural waters*., Wiley.

Takeda A. (2003) Manganese action in brain function. *Brain Research Reviews* **41**, 79–87.

Tebo B. M. (2004) Biogenic Manganese Oxides: Properties and Mechanisms of Formation. *Annual Review of Earth and Planetary Sciences* **32**, 287–328.

U.S. Environmental Protection Agency (2022) The Fourth Unregulated Contaminant Monitoring Rule (UCMR 4): Data Summary, January 2022.

US EPA (2022) Analyze Trends: EPA/State Drinking Water Dashboard. https://echo.epa.gov/trends/comparative-maps-dashboards/drinking-water-dashboard

US EPA (2018) Drinking Water Criteria Document for Manganese. https://www.epa.gov/ccl/regulatory-determination-1-support-documents-manganese

Valcke M., Bourgault M.-H., Haddad S., Bouchard M., Gauvin D. and Levallois P. (2018) Deriving A Drinking Water Guideline for A Non-Carcinogenic Contaminant: The Case of Manganese. *International Journal of Environmental Research and Public Health* **15**, 1293.

Wong J. M. (1984) Chlorination-Filtration for Iron and Manganese Removal. *Journal AWWA* **76**, 76–79.

World Health Organization (2021) Manganese in drinking water. https://www.who.int/publications/i/item/WHO-HEP-ECH-WSH-2021.5. WHO/HEP/ECH/WSH/2021.5

Ying S. C., Schaefer M. V., Cock-Esteb A., Li J. and Fendorf S. (2017) Depth Stratification Leads to Distinct Zones of Manganese and Arsenic Contaminated Groundwater. *Environ. Sci. Technol.* **51**, 8926–8932.

Zhang S., Tian Y., Guo Y., Shan J. and Liu R. (2021) Manganese release from corrosion products of cast iron pipes in drinking water distribution systems: Effect of water temperature, pH, alkalinity, SO42- concentration and disinfectants. *Chemosphere* **262**, 127904.

Chapter 4: Predicting manganese in drinking water accessed by domestic well communities and community water systems in Central Valley, California

1. Abstract

The United States Environmental Protection Agency has a secondary notification limit of 50 μg L^{-1} and a health advisory limit of 300 μg L^{-1} for Mn in drinking water, yet 1.3 million Californians rely on unmonitored domestic wells where Mn concentrations may exceed regulatory standards or concentrations neurotoxic to infants and young children. Existing probability estimates of groundwater Mn concentrations, population estimates, and sociodemographic data were integrated with spatial data delineating domestic well communities to predict the probability of high Mn concentrations in extracted groundwater in California's Central Valley, an area with both considerable reliance on domestic wells and disproportionate socioeconomic burden. Additional Mn concentration data representing water delivered to community water systems was used to estimate populations that may access water with Mn concentrations that exceed public health guidelines. We estimate that 0.4% of the population served by domestic wells in California's Central Valley rely on groundwater with Mn concentrations predicted to exceed concentration linked to neurotoxic effects. In community water systems, 2.4% of users in small community water systems and 0.4% of users for medium community water systems reported mean point-of-entry Mn concentrations more than the health-based guideline. Despite prior evidence that Mn concentration decreases with groundwater depth, we did not observe differences in estimated Mn concentration between groundwater serving shallow and deep domestic wells in the Central Valley. This

suggests that drilling deeper domestic wells would not lower Mn concentrations in their drinking water. These analyses demonstrate the need for additional well-monitoring programs that evaluate Mn and increased access to point-of-use treatment for domestic well users disproportionately burdened by associated costs.

2. Introduction

Manganese (Mn) is a ubiquitous groundwater constituent resulting from the solubilization of naturally occurring mineral sources (Gillispie et al., 2016; McMahon et al., 2019). While manganese concentrations in the range of 0.4 to 550 μg L^{-1} are common in untreated groundwater, levels as high as 28,200 μg L^{-1} have been reported in the United States (Groschen et al., 2009; McMahon et al., 2019). Currently, Mn has a federal secondary maximum contaminant level (SMCL) of 50 μg L^{-1} (US EPA, 2013), a federal health advisory limit (HAL) of 300 μg L^{-1} (US EOA, 2003), and in California, a customer notification limit of 500 μg L^{-1} for community water systems (California SWRCB, 2020). In 2021, the World Health Organization reissued a provisional guideline of 80 μg L^{-1} for Mn in drinking water (WHO, 2021).

A growing body of evidence suggests that concentrations previously considered safe may pose health threats to vulnerable populations, such as children. Studies of school-aged children consuming drinking water with naturally elevated concentrations of Mn have demonstrated lower academic achievement scores when drinking water with Mn concentrations exceeded 400 μg L^{-1} (Khan et al., 2012) and poor memory, attention, and increased risk of attention deficit hyperactivity disorder when Mn concentrations exceeded 100 μg L^{-1} in drinking water (Bouchard et al., 2011; Oulhote et al., 2014; Schullehner et

al., 2020). Despite these studies, the US EPA maintains a secondary contaminant status for Mn on the strength of adult cohort studies that did not observe neurotoxic endpoints (US EPA, 2003). In 2020, Mn was sampled in a subset of small and large public water systems in compliance with the unregulated contaminant monitoring (UCMR4). Approximately 2.1% of the water systems sampled reported Mn concentrations greater than the federal HAL (US EPA, 2022) and exposure to Mn through drinking water represents a potential health risk to vulnerable populations.

Domestic well communities reliant on unregulated groundwater face potentially greater risks of contaminant exposure than users served by community water systems potentially due to the relative lack of regulatory oversight of these systems by state and federal drinking water agencies (Pace et al., 2022). Domestic wells are generally drilled to a shallower depth than public wells and therefore have redox conditions that favor Mn dissolution (Ying et al., 2017; McMahon et al., 2019; Gailey, 2020). Shallow aquifers are more likely susceptible to drought leading to well failure and an increased concentration of redox sensitive contaminants as groundwater levels continue to decline (Pauloo et al., 2020; Levy et al., 2021). Several recent studies show that communities served by domestic wells in California disproportionately serve disadvantaged communities that face financial challenges in testing and treating groundwater (London, 2021; Pace et al., 2022). For these reasons, private wells drilled within shallow aquifers deserve further consideration when assessing groundwater quality, quantity, and mitigation efforts.

We focused on California's Central Valley, a region which is recognized as one of the most productive and economically important agricultural regions in the United States

and is currently home to one-third of domestic well users in the state (Pauloo et al., 2020). Mn concentrations above 500 μg L^{-1} were reported in untreated groundwater in 47 out of 58 counties in California between 2011-2019 (California SWRCB, 2020). Intense agricultural activity and a projected population growth of 1.1 million by 2040 is likely to increase demand for water resources (State of California Department of Finance, 2019). Most groundwater basins in the Central Valley are defined as "critically over drafted" by the California Sustainable Groundwater Management Act (SGMA) and are currently undergoing sustainability planning to address continued overdraft while meeting strict water quality standards for users (California Department of Water Resources, 2015; Faunt et al., 2016).

Our specific objectives in this study were to (1) characterize community water system users relying on water with Mn concentrations above threshold values after extraction and available treatment using reported Mn concentrations at point-of-entry, (2) characterize domestic well users at risk of the risk of unsafe levels of Mn in ambient groundwater extracted for use without treatment using secondary data on the geographic and sociodemographic characteristics of domestic well communities and probability estimates for groundwater Mn exceedances, and (3) investigate the availability and effectiveness of mitigation measures such as increased well depth, point-of-use treatment, and consolidation of water systems for domestic well users relying on groundwater with Mn exceeding threshold values.

3. Materials and Methods

To best characterize the population served by DWC accessing groundwater with high Mn concentrations, we integrated data defining water source type (i.e., CWS or DWC), estimates for the population served by each water source, poverty estimates, and water quality predictions. Since CWS rely on treated water, reported water quality data at point-of-use was integrated with available spatial delineations of water use type boundaries. A summary of spatial resolution of available data is listed in Table 1 and links to all publicly available data sets are listed in Table S1.

3.1. Community Water Systems

Community water system (CWS) boundaries were developed by Tracking California Water System Service Areas Tool (Tracking California) and obtained from the drinking water tool in March 2020. A CWS is defined as a system providing water for human consumption with 15 or more service connections or serving 25 or more people daily for at least 60 days per year (HSC § 116275). The active status of the CWS was confirmed within the State Drinking Water Information System (SDWIS) and wholesaler CWSs were removed because they do not distribute directly to consumers. The final geospatial layer contained 2,851 active CWSs within California and 667 within the Central Valley alluvial boundary (Pace et al., 2020). CWSs were stratified by number of service connections into small (15-199 connections), medium (200-9,999 connections), and large (10,000+ connections) water systems (Bangia et al., 2020; Pace et al., 2022).

3.2. Domestic Well Communities

Domestic well communities were defined as populated Public Land System Survey (PLSS) grids that were (1) outside the boundaries of community water system service areas, (2) intersected with at least 1 domestic well according to the Department of Water Resources Online System for Well Completion Reports (OSWCR) database, and (3) intersected with at least one residential parcel (Pace et al., 2020). Some uncertainties in the dataset include the absence of small water systems due to lack of publicly available data, missing/non-classified wells in the OSWCR database, and limitations in aerial apportionment of census data from census blocks to PLSS section geography in rural areas with large census blocks and low population. DWC data were retrieved in March 2020.

3.3. Groundwater Mn Concentration Prediction Model

Due to lack of reported water quality values for domestic wells within Central Valley, California (Table S4), we used predicted probability grids of groundwater Mn concentrations at multiple depths and 1 km^2 resolution developed for California's Central Valley to estimate the likelihood that untreated groundwater exceeded threshold concentration of Mn (Rosecrans et al., 2017). In brief, this model generated probability of groundwater Mn concentration using a Boosted Regression Tree (BRT) method (Nolan et al., 2015) by using over 60 subsurface geochemical and hydrological variables (e.g., regional soil properties, soil chemistry, land use, aquifer textures, and aquifer hydrology) within the Central Valley alluvial boundary. The resulting raster grids estimate the probability of Mn concentration exceeding 50 μg L^{-1} (SMCL) or 300 μg L^{-1} (HAL) at

depths of 33 m (corresponding with average domestic well depth; Gailey, 2020), 67 m (predicted well depth during times of drought; Pauloo et al., 2020), and 100 m (corresponding to average public supply well depth; Gailey, 2020). Additional discussion of the BRT model methods, output, other assumptions, and limitations are provided in Rosecrans et al. (2017).

3.4. Water quality estimation in Community Water Systems

Since groundwater is most likely treated in Community Water Systems prior to distribution, reported Mn concentrations were used to estimate Mn exposure within these communities. Water quality for CWSs was estimated using reported data collected from Safe Drinking Water Information System (SDWIS) over the most recent regulatory cycle of 2011-2019 (California SWRCB, 2021b). All inactive/proposed facilities or with the classification of transient-noncommunity and non-public were excluded from analysis (California SWRCB, 2021). Non-detects were calculated to be the reporting limit divided by the square root of 2 (Lubin et al., 2004; Bangia et al., 2020).

To best estimate contaminant concentration at point-of-use, only reported values that flowed directly into distribution systems (point-of-entry) were retained. Flow path data available by request from the Division of Drinking Water was used to identify location of reported values within the flow path from extraction of raw water, treatment, and point-of-entry. Any data sampled from a source that did not flow directly into the distribution system or did not have reported flow path data were excluded from further analysis (Balazs et al., 2011; Sherris et al., 2021). To account for higher frequency sampling when in

exceedance, samples collected on the same day and sampling location were averaged. A 9-year mean was calculated for each water system to allow comparison since reporting frequency was highly heterogeneous between systems.

3.5. Population estimates and sociodemographics

Population data from SDWIS Public Water System Information was used to estimate population exposure to concentrations above threshold values (California SWRCB, 2020a). Transient (e.g., recreation area, highway, rest area, hotel/motel) and non-transient (e.g., industrial/agricultural, medical facility, school) populations were not included in population calculations. Any CWS with less than 15 service connections were assumed to be state small systems and excluded from analysis. The population within CWS service area boundaries were assumed to exclusively access public water. To estimate populations reliant on CWS with mean Mn concentrations exceeding threshold values, the reported user population within these systems was summed. Population within domestic well communities was estimated via aerial apportionment of 2010 United State Census block population by Pace et al. (2020) and retained for our analysis.

We estimated poverty using 2011-2015 American Community Survey (ACS) data and methods developed by Office of Environmental Health and Hazard Assessment for CalEnviroScreen 4.0 (California OEHHA, 2021). We estimated the percentage of individuals falling below 200% of the Federal Poverty Level (2FPL). This translates to an income of $25,760 for an individual and $53,000 for a family of 4. Individuals or families with incomes less than twice the FPL are eligible for many social assistance programs such

as Medicaid. Census tract boundaries were overlaid with the DWC delineations to compare poverty rates between DWCs within and outside of the Central Valley. If DWC delineations overlapped with multiple census tract boundaries, a poverty value was assigned based on area-weighted apportionment.

We assigned disadvantaged community (DAC) status at the county level using the 2017 designation by CalEPA (California EPA, 2017). These communities face the top 25th percentile environmental, socioeconomic, and health burdens throughout the state and are eligible for access to additional state funding to address these disparities.

Table 1. Summary of spatial integration of available data.

Purpose	Description	Initial Spatial Resolution	Integration	Final Spatial Resolution
Water System	Likely DWC Boundaries[A]	PLSS Grid	CWS boundaries, unpopulated areas, and areas without wells were removed	DWC boundary
	CWS Boundary [A]	CWS boundary	Wholesaler systems and inactive systems removed	CWS boundary
Water Quality	Groundwater Mn Predictive Model (33 m, 67 m, 100 m)[B]	1 km^2 Raster	Mean predicted probability of groundwater Mn exceeding within CWS or DWC polygon boundaries calculated at depth	DWC or CWS boundary
	Reported Mn Concentrations at Point of Entry	CWS boundary	System reported values matched with spatial delineation	CWS boundary
Population	US Census population	Census Block	Ariel apportionment of 2010 US Census population[A]	DWC boundary
	CWS user population	CWS Boundary	Reported values from SDWIS	CWS boundary
Socioeconomics	Percentage below 2FPL (OEHHA)	Census tracts	Ariel weighted apportionment of reported values	DWC boundary
	Disadvantaged Community Designation	County	Retained designation if >50% of DWC boundary was within DAC community	DWC boundary

[A] From Pace et al. (2020)
[B] From Rosecrans et al. (2017)

3.6. Statistical Analysis

We compared the probability of Mn exceeding the SMCL and HAL within DWCs at the current average depth versus two deeper depths (drought conditions and deep wells), using a set of paired t-tests. Using Welch t-tests, we examined if there is evidence for the hypothesis that poverty rates (i.e., the share of population living below 2FPL) in DWCs within the Central Valley are higher than poverty rates in DWCs elsewhere in the state of California. Similarly, to test for significant differences in predicted Mn concentration in groundwater between Central Valley DWC users within or outside of disadvantaged communities, we used a Welch t-test. An alpha value of 0.05 is used for each test and all analyses were performed in RStudio (v 2022.02.1).

4. Results

4.1. Measured water quality in community water systems

Our results show that small water systems reported Mn concentration less frequently than larger systems and have a higher percentage of total population relying on water with Mn concentration greater than the health advisory limit. An estimated 8.7 million residential customers in the Central Valley rely on water delivered by the 667 CWS. Of these systems, 421, 193, and 53 are categorized as small, medium, and large, respectively. However, only 373 CWS systems reported Mn concentrations between 2011-2019 despite regulation of secondary contaminants requiring reporting every 1-3 years (Table 2, 22 CCR § 64449). Previous studies demonstrate less frequent reporting of primary contaminants by water system size, with smaller systems reporting less frequently

than larger systems (Balazs et al., 2012; Rubin, 2013; Bangia et al., 2020). In the present study, we similarly found large water systems reported Mn concentration at the point-of-entry 18.9 times per year compared to just 1.1 annual reports by small water systems. Less than half of small water systems reported one or more Mn measurement at the point-of-entry over the entire 9-year study period. Data availability was slightly better for medium and large water systems, 45.1% of medium and 77.4% of large water systems reported at least one point-of-entry Mn measurement between 2011-2019. Across all CWS sizes the mean Mn concentration exceeded the secondary notification limit of 50 ug/L for approximately 80,184 users and exceeded the health limit of 300 ug/L for 3,976 users. Although a larger number of users accessing water exceeding the SMCL and HAL are in medium and large systems, a larger percentage of smaller CWS were distributing water exceeding regulatory standards (Figure 1).

Table 2. Mn concentration data in groundwater serving DWCs and delivered by CWS and predicted population exposed to concentrations exceeding threshold values between 2011-2019.

	DWC[A]	**Small CWS[B]**	**Medium CWS[B]**	**Large CWS[B]**
Service connections[C]	1 to 4	15 to 200	200 to 9,999	10,000+
Total CWS or wells in Central Valley	69,733 wells	421 CWS	193 CWS	53 CWS
Total CWS with reported point-of-entry Mn values (% of total) [D]	-	245 (58.2) CWS	87 (45.1) CWS	41 (77.4) CWS
Count of reported Mn values at point-of-entry[D]	-	2,323	4,736	6,054
Observations per CWS per year	-	1.1	6.9	18.9
Total population with reported values	-	38,424	848,497	6,116,365
Population (%) <50 ug/L	-	31,558 (82.1)	810,809 (95.5)	6,080,735 (99.4)
Population (%) 50-300 ug/L	-	5,962 (15.5)	34,616 (4.1)	35,630 (0.6)
Population (%) >300 ug/L	-	904 (2.4)	3,072 (0.4)	0 (0)
Total population with predictive model values	554,436	-	-	-
Population (%) >80% probability of exceeding 50 µg/L Mn	22,670 (4.1)	-	-	-
Population (%) <80% probability of exceeding 50 µg/L Mn	531,765 (95.9)	-	-	-
Population (%) >80% probability of exceeding 300 µg/L Mn	2,342 (0.4)	-	-	-
Population (%) <80% probability of exceeding 300 µg/L Mn	552,094 (99.6)	-	-	-

[A]DWC = Domestic Well Communities
[B]CWS = Community Water Systems
[C]Size cutoffs are from Pace et al. (2022), Bangia et al. (2019)
[D]Total reported Mn values state-wide and before point-of-entry are available in Table S2

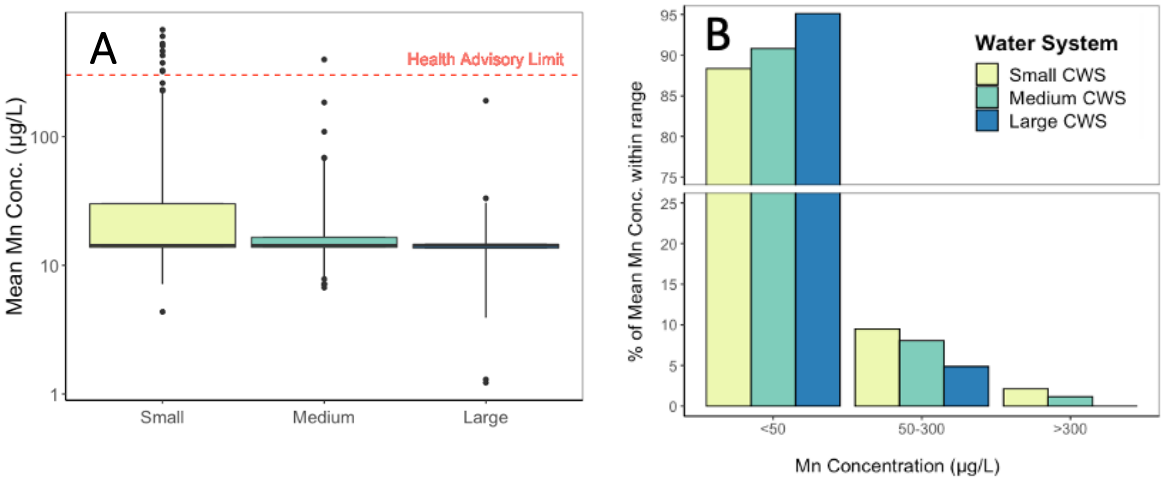

Figure 1. (A) Distribution of mean Mn concentrations at point-of-entry between 2011-2019 for small, medium, and large CWSs using data from EPA Safe Drinking Water Information System (SDWIS). Boxes represent the 25th, 50th, and 75th percentile of concentrations and whiskers represent 5th and 95th percentiles. Outliers are represented by points. Red dashed line is the health advisory limit (300 ug L^{-1}). (B) Percentage of mean Mn concentration between 2011-2019 that were in exceedances of threshold values. CWS = community water system. Small CWS = 15-199 service connections (n=421); Medium CWS = 200-9,999 service connections (n=193); Large CWS > 10,000 service connections (n=53). Data from SDWIS.

4.2. Predicted water quality in domestic wells

We do not report groundwater Mn concentration for DWCs in Table 2, and instead reported population with probability above or below 80% likelihood of withdrawing groundwater in exceedance of secondary notification limit (50 µg L^{-1}Mn) or health advisory limit (300 µg L^{-1}Mn) due to a paucity of data on reported Mn concentrations in supplying domestic wells (Table S4). Rosecrans et al. (2017) provides probability of Mn exceeding a threshold concentration for 93.4% of the area served by domestic wells in the Central Valley and 90.1% of the domestic well population within this region. We estimate that between 554,436 individuals in the Central Valley alluvial boundary region rely on domestic wells (Table 2). This is within the range of other domestic well user estimates at

the county-level within the region (452,450-686,000 users), however our study area size is in between previous estimates, and may account for differences in population estimates (Johnson et al., 2019; Pace et al., 2022).Within the total area served by DWCs in the Central Valley with predicted Mn in groundwater (15,092 km^2), 645 km^2 has >80% chance of groundwater extracted exceeding 50 µg L^{-1}Mn and 179 km^2 has >80% chance of groundwater extracted exceeding 300 µg L^{-1} Mn (Figure 2). Since DWCs are less likely to be drinking treated drinking water, DWCs that overlap with areas of high probability are likely accessing that water directly.

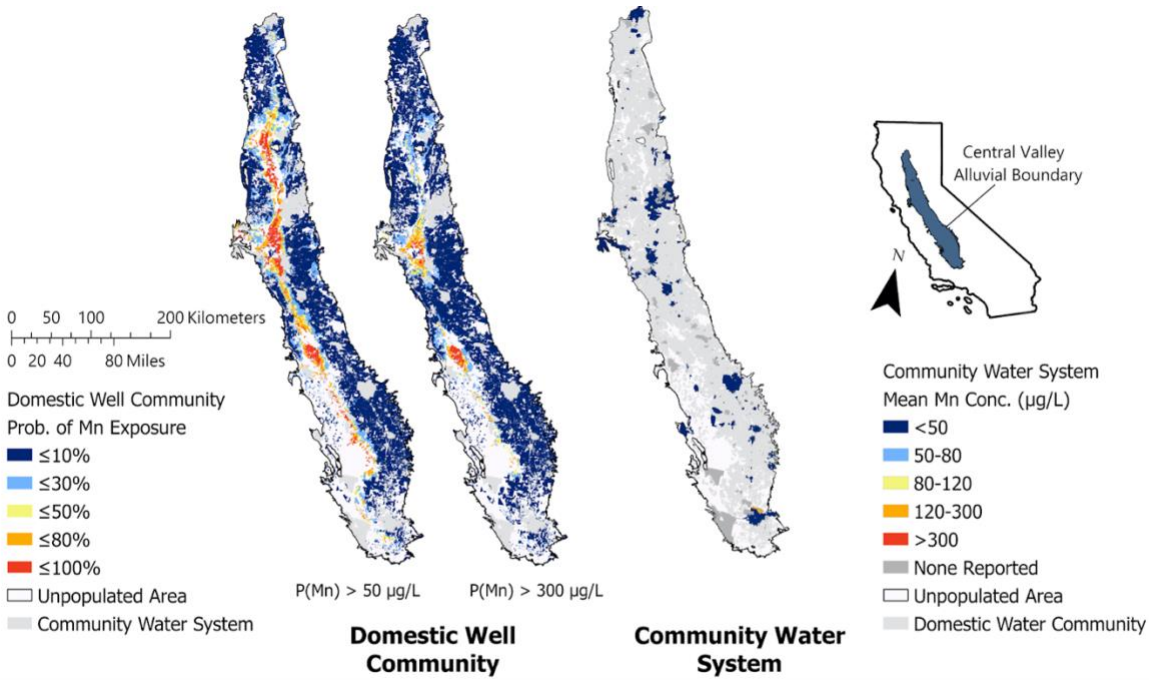

Figure 2. Probability map of groundwater Mn >50 µg L^{-1} (SMCL) or >300 µg L^{-1} (HAL) in domestic well communities and reported 2011-2019 mean Mn values at community water systems point-of-entry.

The most frequent domestic well depth in the Central Valley is between 33-50 m (Gailey et al. 2020). We compared predicted Mn concentrations at an average depth of 33 m and 67 m representative of wells drilled to deeper aquifer depth in response to drought-related water shortage (Pauloo et al., 2020). Our analyses demonstrated a significant difference between depths in probability of Mn exceeding the SMCL and HAL, however the effect size was negligible. The mean probability of exceeding the SMCL at 33 m is 12.8% while the mean probability of an exceedance at 67 m is 13.9% (Table S5).

In comparison to DWC, CWSs are regularly monitored for MCL violations and are required to manage or treat groundwater until brought into compliance which may unintentionally treat for manganese. For example, in the Central Valley, where nitrate or arsenic contamination is a major concern, treatment methods such as ion exchange, reverse osmosis, or electrodialysis may also result in the removal of Mn (Jensen et al., 2011). However, small CWSs often lack treatment for primary contaminants and receive more MCL violations than larger systems in California (Bangia et al., 2020; Pace et al., 2022). In some cases, shallow domestic well users may live within a CWS boundary or rely on smaller CWS that lack treatment. To capture predicted Mn concentration for those users, we mapped the probability of shallow untreated groundwater concentrations exceeding threshold values in areas that serve CWS (Figure S2).

4.3. Poverty in DWCs

By overlaying DWC boundaries with socioeconomic characteristics, our findings show that DWCs within the Central Valley region have higher instances of poverty then

domestic well communities outside of this region (Figure 3). The mean poverty rate in DWCs within the Central Valley is 42.3% and is significantly different ($p<0.000$) than the DWC outside of the Central Valley (32.4%, effect size = 0.72, Table S7). The distribution of poverty throughout the Central Valley is highly heterogeneous, with higher poverty rates in the southern San Joaquin Valley region (Figure 3). Community water systems users may have access to municipal monitoring and treatment, but out-of-pocket costs for domestic well communities may be a considerable financial burden, particularly for those below the poverty line.

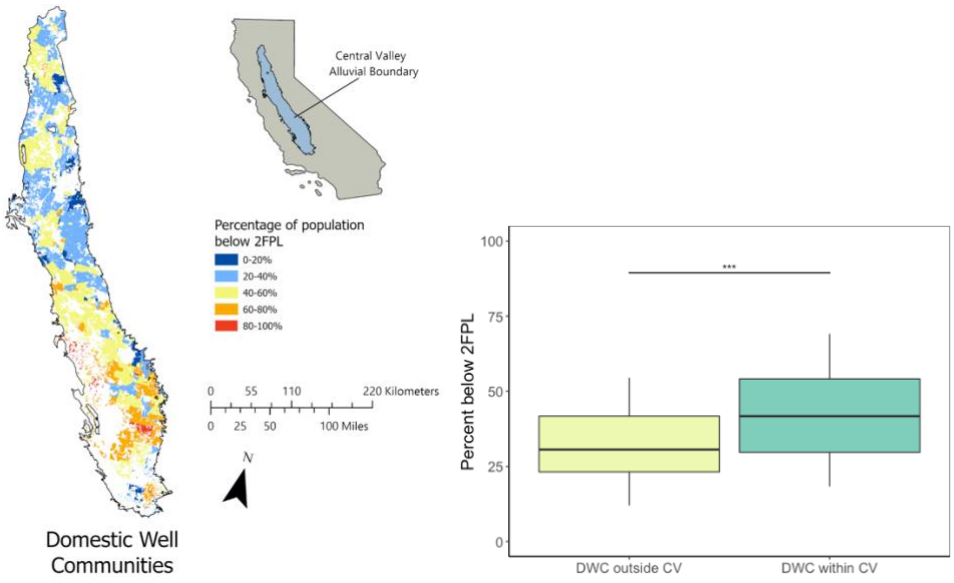

Figure 3. (A) Percentage of domestic well community (DWC) population below 2 times the federal poverty level (2FPL) outside of the Central Valley (CV) and within the CV. Boxes represent the 25th, 50th, and 75th percentile of concentrations and whiskers represent 5th and 95th percentiles. Outliers were excluded. Bracket shows denotes that a significant difference (*** indicates that $p < 0.001$) in the mean percentage of the population below 2FPL. DWC outside of CV: n=6,953, DWC within CV: n=19,528. (B) Spatial distribution of DWCs within the Central Valley with population below 2FPL.

Disadvantaged communities (DAC) were identified by CalEPA as communities over-burdened by pollution, socioeconomic, and health challenges and funding to address these disparities within these areas is prioritized (SB 535; California EPA, 2017). About 48% of domestic well users in the Central Valley live within DAC (Figure S4). However, 88.8% of the DWC user population with a high (>80%) probability of extracting groundwater with Mn more than the HAL live within a DAC (Table S9). Individuals within DAC communities may face further challenges in addressing water quality disparities driven by water access including associated treatment costs or larger pollution burden.

4.4. Possible Mn mitigation strategies

For communities that rely on domestic wells and CWS users lacking treatment, we have investigated three possible mitigation strategies for Mn overexposure: drilling of deeper wells, point-of-use treatment, or consolidation of DWCs into an existing CWSs.

4.4.1. Changing Well Depth in DWCs

Our results within this study do not demonstrate that drilling deeper wells is an effective mitigation strategy for Mn concentration in groundwater used for drinking within the Central Valley region. We observed a significantly greater chance of exceeding the SMCL and HAL in wells drilled deeper (100 m) than those relying on wells drilled at shallow aquifer depths (33 m), however the effect size was negligible (Figure S3). The mean probability of exceeding the HAL at 33.3 m is 6.0% while the mean probability of an exceedance at 100 m is 6.1% (Table S6). Although significantly different, drilling

deeper wells is not protective against higher Mn concentrations in groundwater extracted for drinking and any the costs associated with drilling deeper would also minimize any possible benefit.

This contrasts with our original hypothesis and previous studies demonstrating more favorable geochemical conditions for Mn mobilization at shallow depths. Manganese mobility in subsurface environments is predominantly controlled by biotic and abiotic redox transformations that result in Mn immobilization through precipitation and adsorption reactions (Tebo, 2004; Farnsworth et al., 2012; Gillispie et al., 2016; McClain et al., 2019) or mobilization via microbially-driven reductive dissolution during anaerobic respiration (Gounot, 1994). This kinetic constraint can result in high concentrations of Mn in shallow, oxic groundwaters (Tebo, 2004; Groschen et al., 2009; Farnsworth et al., 2012; Ying et al., 2017) and accumulation of Mn at relatively shallow aquifer depths over time (Gillispie et al., 2016; Schaefer et al., 2017). In addition, anoxia at deeper aquifer depths can lead to accumulation of carbonate from anaerobic microbial respiration which can immobilize Mn(II) through precipitation of Mn(II) carbonates (Buschmann et al., 2007; Schaefer et al., 2020).

Despite prior work demonstrating higher Mn concentrations within shallow aquifer zones, we may not have observed this within our study since wells are drilled below the fluctuation redox zone within the shallow aquifer. Wells are drilled to depths that ensure the screened portion is installed deeper than the variably saturated zone to ensure water supply is not seasonally affected. In an analysis of groundwater Mn concentrations in wells

throughout the US, the highest concentrations were measured in observation wells, which are shallower than the domestic wells, and a smaller difference was observed between domestic and private wells (McMahon et al., 2019). Within the Central Valley, studies investigating redox controls on chromium(VI) contamination of groundwater observed the highest rate of Mn oxide staining in the shallow aquifer zone between 10-20 m, which is shallower than the average domestic well in the region (Manning et al., 2015; McClain et al., 2019). Since the average well depths for DWCs were below depths where Mn accumulation was observed in the region, drilling deeper will not be beneficial. Further regional consideration of the depth to the shallow aquifer zone or area of Mn accumulation may be needed to determine if well depth could be protective in other areas.

4.4.2. Point-of-use treatment

Several point-of-use (POU) treatment technologies can be used to treat Mn, although their accessibility can be limited by the cost and maintenance of the unit. POU treatments through chemical, biological, and physical means can result in the effective removal of Mn (e.g., Patil et al., 2016; Tobiason et al., 2016). All methods include regular monitoring to ensure the treatment continues to remove Mn and does not require additional maintenance. Water monitoring can range from US$100-US$400 and treatment of water outside of compliance can range from US$70-US$400 per year or more depending on choice of treatment method and installation cost (Table S10).

Many low-income communities within San Joaquin Valley pay 4-10% of household income for water related expenses (Moore et al., 2011; Balazs and Ray, 2014).

When including expenses related to purchasing bottled water, up to 95% of households exceed the USEPA water affordability threshold of 1.5% of median household income (Moore et al., 2011). For individuals below 2FPL (US$25,760), monitoring and treatment for high Mn may account to 0.5-4% of an individual's household income, excluding additional costs associated with purchased water or treating for additional contaminants. In our analysis, a majority of DWC users at risk of withdrawing groundwater with concentrations exceeding the HAL occur within a disadvantaged community (Table S9). This predicted "hot-spot" of groundwater Mn contamination warrants further investigation, mitigation, and funding allocation to ensure access to safe, clean, and affordable drinking water.

Legislative changes to primary contaminant regulation may have co-benefits upon secondary contaminant remediation. It has been reported that decrease in arsenic concentrations in DWCs and CWSs was correlated with implementation of stricter regulation of As (Final Arsenic Rule which decreased the MCL from 50 to 10 μg L^{-1}) most likely due to increased As treatment of groundwater in CWSs (Spaur et al., 2021). Treatment of As within CWS may also treat for and remove Mn from groundwater within CWSs, but still does not address high Mn concentrations in DWCs that do not receive treatment (Jensen et al., 2011). The Final Arsenic Rule legislation made a direct change in concentrations in drinking water and demonstrates that stricter regulation of groundwater contamination is a pathway to limit exposure (Spaur et al., 2021). Legislation of other contaminants, such as Mn, may also be used to limit exposure within CWSs, but not unregulated domestic wells. Further investigation is needed to target domestic well

communities at high risk of Mn exposure through drinking water and in areas characterized by high rates of poverty to understand the burden of cost disparities and target areas for effective distribution of grants and funding.

4.4.3. Consolidation of DWCs

Consolidation of domestic well communities and small state water systems represents an additional option to decrease high Mn and other primary contaminants in drinking water. In our analysis, DWCs had extremely low monitoring data availability (Table S2). Consolidation onto an existing CWS may result in treated water and better monitoring/reporting of water quality parameters. In an analysis of disadvantaged unincorporated communities relying on domestic wells or small water systems, 66% were within 4.8 km of an existing system where consolidation is considered feasible (London, 2021). Though the state cannot force consolidation, financial incentivization has led to successful subsumption of domestic wells and small systems by the SWRCB for communities in the Tulare and Kings County and successfully resolved MCL violations and well failures issues (London et al., 2018).

Consolidation is a resource intensive process and allocation of funds to support consolidation projects is used to justify cities reluctance to consolidate. The Safe and Affordable Drinking Water Fund (SB 200) was passed in 2019 and allocates $130 million per year to improve water infrastructure in disadvantaged communities, including consolidation projects (California SWRCB, 2021b). In addition, consolidation of smaller systems onto larger systems may help bring down the cost of treatment due to improved

economies of scale. Since larger systems serve more users, they may distribute the cost of operation, treatment, and maintenance among many users whereas similar improvements in smaller systems may significantly increase user costs (Nylen et al., 2018). Applying for consolidation funding and construction is a multi-year project and interim treatment or alternative water source is needed for communities currently experiencing drinking water quality violations.

4.5. Limitations of Available Data

4.5.1. Spatial and Temporal Limitations of Mn Groundwater Model

The probability model used in this paper considers Mn concentrations predominantly from shallow groundwater monitoring wells and relatively deeper public supply wells which do not necessarily reflect the chemistry of finished water that is delivered to users dependent on shallow, private wells (Rosecrans et al., 2017). Further, shifts in subsurface geochemical conditions caused by environmental and human activity (e.g., seasonal variations and increased groundwater pumping possibly exacerbated by increasing drought frequencies) may influence contaminant release and were not considered here when assessing probability of groundwater concentrations exceeding threshold values (Gillispie et al., 2016).

The depths used in this study to represent domestic wells (33.3 m) and community wells (100 m) are calculated based on 29,379 domestic and 973 municipal well depths in the Central Valley (Gailey, 2020). Approximately 4.4% of domestic wells included in our investigation were drilled to a similar average depth (100-115 m) as the community wells

(100 m), and therefore their likelihood of exceeding a threshold concentration may be better represented by the deeper groundwater Mn predictive map that is predictive of CWS groundwater source chemistry (Figure S3). Further consideration of the heterogeneity of well depth within DWCs is important for understanding redox sensitive contaminants release into drinking water when applying depth resolved contaminant models.

4.5.2. Data Availability Limitations

A major limitation to better understanding groundwater Mn concentrations is the lack of publicly available data on Mn occurrence and concentration in domestic wells collected and managed by federal agencies (US EPA and USGS) and state regulatory agencies (California SWRCB).

4.5.2.1 US EPA and USGS

The US EPA is responsible for setting regulatory standards, monitoring frequency, and information on exceedances. Private water systems, including groundwater wells, are not monitored or regulated by the Federal Safe Drinking Water Act, nor are any standards or recommended criteria set for individual wells by the US EPA. The US EPA Unregulated Contaminant Monitoring Rule (UCMR) is responsible for collecting nation-wide data on suspected contaminants yet to be regulated with a health-based standard. Manganese was measured in the fourth UCMR between 2018-2020 for over 5,000 CWS (US EPA, 2022). However, only a subset of small systems (>10,000 users) are required to report and no collection from domestic water users is required. To better assess potential exposure on

vulnerable communities, more data on water quality from places that are less likely to have the resources to treat the source water, such as small systems or domestic well users, is important.

The USGS is responsible for monitoring state-wide water quality in the National Water-Quality Assessment (NAWQA), including a subset of domestic wells. The most recent assessment on domestic wells was from 1991-2004 and included about 2,100 wells throughout the entire US (DeSimone et al., 2015). Regional groundwater assessments throughout California are also conducted by USGS in cooperation with state agencies and may be used as a proxy for domestic well water quality.

4.5.2.2 State Regulatory Agencies

Currently, each CWS must monitor secondary contaminants in its groundwater sources on a 3-years basis or its surface water sources annually (22 CCR § 64449). Yet despite this regulatory monitoring framework, 44.1% of the CWS population in the Central Valley has no reported Mn concentration at point-of-entry in SDWIS between 2011-2019 and we are unable to assess water quality within these CWS (Table 2). Therefore, the estimated population accessing water with high Mn is likely an underestimate.

The Groundwater Ambient Monitoring Assessment (GAMA) program was established by the California SWRCB in 2000 to monitor and assess groundwater quality in areas that have high reliance on groundwater resources. Since its inception, the program has monitored over 2,300 domestic wells for water quality throughout the state, however

only ~5% of the wells were within the Central Valley and reported both well depth and Mn concentration (Table 2, California State Water Resource Control Board, 2020). Such low availability of water quality information for DWCs may considerably underestimate populations accessing water exceeding acceptable contaminant concentrations. Collecting current and accurate water quality information from active wells is critical to both confirming large scale predictive models and building more models for other drinking water contaminants.

4.5.3. Underrepresented Communities

Additional underrepresented communities within our study and others are disadvantaged, unincorporated communities (DUCs) which rely on informal or small water systems. These communities may live within CWS boundaries but lack infrastructure to access formal CWSs and associated monitoring/treatment infrastructure (London et al., 2018; London, 2021). Previous studies have assumed the entire population within CWS boundaries are supplied by CWSs (Bangia et al., 2020; Pace et al., 2020), but no study has investigated the infrastructure available within DUCs and the population served by such infrastructure throughout the entire state. These communities therefore warrant additional attention in future studies addressing water quality disparities driven by resource or infrastructure disparities.

5. Future Implications

This current work is an exploratory analysis but demonstrates a deep need for better quality and publicly available data to further investigate and understand Mn contamination for domestic well communities and community water systems. California has made clear its commitment to providing safe, clean, affordable, and accessible drinking water to those that live within the state, but more monitoring of domestic drinking water wells and support of domestic well users need to be prioritized not just for Mn, but all contaminants.

Many non-profits and community advocacy groups are already asking for increased attention paid to domestic wells and their users. These groups already have trusted relationships within the local community and access to well locations previously inaccessible to government agencies. When building large scale monitoring or mitigation projects, attention to what is already being done by these groups will be required. In addition, increased funding and collaborations with these groups will also increase access to users' ability to mitigate water quality issues at a more individual level.

6. References

Balazs C. L., Morello-Frosch R., Hubbard A. E. and Ray I. (2012) Environmental justice implications of arsenic contamination in California's San Joaquin Valley: a cross-sectional, cluster-design examining exposure and compliance in community drinking water systems. *Environmental Health* **11**, 84.

Balazs C. L. and Ray I. (2014) The Drinking Water Disparities Framework: On the Origins and Persistence of Inequities in Exposure. *Am J Public Health* **104**, 603–611.

Balazs C., Morello-Frosch R., Hubbard A. and Ray I. (2011) Social disparities in nitrate-contaminated drinking water in California's San Joaquin Valley. *Environ. Health Perspect.* **119**, 1272–1278.

Bangia K., August L., Slocombe A. and Faust J. (2020) Assessment of contaminants in California drinking water by region and system size. *AWWA Water Science* **2**, e1194.

Bouchard M. F., Sauvé S., Barbeau B., Legrand M., Brodeur M.-È., Bouffard T., Limoges E., Bellinger D. C. and Mergler D. (2011) Intellectual impairment in school-age children exposed to manganese from drinking water. *Environ Health Perspect* **119**, 138–143.

Buschmann J., Berg M., Stengel C. and Sampson M. L. (2007) Arsenic and manganese contamination of drinking water resources in Cambodia: coincidence of risk areas with low relief topography. *Environ Sci Technol* **41**, 2146–2152.

California Department of Water Resources (2015) California Water Plan - Groundwater Update 2013. https://data.cnra.ca.gov/dataset/california-water-plan-groundwater-update-2013/resource/40b189fa-33ee-4ec2-9eff-555ec5296c5b

California Environmental Protection Agency (2017) Designation of Disadvantaged Communities Pursuant to Sentate Bill 535. https://calepa.ca.gov/wp-content/uploads/sites/6/2017/04/SB-535-Designation-Final.pdf

California Office of Environmental Health Hazard Assessment (2021) CalEnviroScreen 4.0 - Update to the California Communities Environmental Health Screening Tool. https://oehha.ca.gov/media/downloads/calenviroscreen/report/ces3report.pdf

California State Water Resource Control Board (2021a) Decision tree for classification of water systems. https://www.waterboards.ca.gov/drinking_water/certlic/drinkingwater/docs/class_dec_tree.pdf

California State Water Resource Control Board (2020a) Drinking Water - Public Water System Information - California Open Data. https://data.ca.gov/dataset/drinking-water-public-water-system-information

California State Water Resource Control Board (2021b) EDT Library and Water Quality Analyses Data and Download Page. https://www.waterboards.ca.gov/drinking_water/certlic/drinkingwater/EDTlibrary.html

California State Water Resource Control Board (2020b) Groundwater Ambient Monitoring and Assessment (GAMA). https://www.waterboards.ca.gov/water_issues/programs/gama/docs/gama_eval_2020.pdf

California State Water Resource Control Board (2021c) Safe and Affordable Funding for Equity and Resilience. https://www.waterboards.ca.gov/water_issues/programs/grants_loans/sustainable_water_solutions/safer.html

California State Water Resources Control Board (2020) Drinking Water Notification Level for Manganese. https://www.waterboards.ca.gov/drinking_water/certlic/drinkingwater/Manganese.html

DeSimone L. A., McMahon P. B. and Rosen M. R. (2015) *The quality of our Nation's waters: Water quality in principal aquifers of the United States, 1991-2010*., U.S. Geological Survey.

Farnsworth C. E., Voegelin A. and Hering J. G. (2012) Manganese Oxidation Induced by Water Table Fluctuations in a Sand Column. *Environ. Sci. Technol.* **46**, 277–284.

Faunt C. C., Sneed M., Traum J. and Brandt J. T. (2016) Water availability and land subsidence in the Central Valley, California, USA. *Hydrogeol J* **24**, 675–684.

Gailey R. (2020) California Supply Well Impact Analysis for Drinking Water Vulnerability Webtool. https://drinkingwatertool.communitywatercenter.org/wp-content/uploads/2020/01/Gailey_2020_Final-CWC-Report.pdf

Gillispie E. C., Austin R. E., Rivera N. A., Bolich R., Duckworth O. W., Bradley P., Amoozegar A., Hesterberg D. and Polizzotto M. L. (2016) Soil Weathering as an Engine for Manganese Contamination of Well Water. *Environ. Sci. Technol.* **50**, 9963–9971.

Gounot A. M. (1994) Microbial oxidation and reduction of manganese: consequences in groundwater and applications. *FEMS Microbiol Rev* **14**, 339–349.

Groschen G. E., Arnold T., Morrow W. S. and Warner K. L. (2009) Occurrence and Distribution of Iron, Manganese, and Selected Trace Elements in Ground Water in the Glacial Aquifer System of the Northern United States., *U.S. Geological Survey*.

Jensen V. B., Darby J. L. and Seidel C. (2011) Drinking Water Treatment for Nitrate - Report for the State Water Resources Control Board. *Technical Report*, 198.

Johnson T. D., Belitz K. and Lombard M. (2019) Estimating domestic well locations and populations served in the contiguous U.S. for years 2000 and 2010. *Science of the Total Environment* **687**, 1261–1273.

Khan K., Wasserman G. A., Liu X., Ahmed E., Parvez F., Slavkovich V., Levy D., Mey J., van Geen A., Graziano J. H. and Factor-Litvak P. (2012) Manganese exposure from drinking water and children's academic achievement. *NeuroToxicology* **33**, 91–97.

Levy Z. F., Jurgens B. C., Burow K. R., Voss S. A., Faulkner K. E., Arroyo-Lopez J. A. and Fram M. S. (2021) Critical Aquifer Overdraft Accelerates Degradation of Groundwater Quality in California's Central Valley During Drought. *Geophysical Research Letters* **48**, e2021GL094398.

London J., Fencl A., Watterson S., Jarin J., Aranda A., King A., Pannu C., Seaton P., Firestone L., Dawson M. and Nguyen P. (2018) The Struggle for Water Justice in California's San Joaquin Valley: A Focus on Disadvantaged Unincorporated Communities. *UC Davis Center for Regional Change.*

London J. K. (2021) Disadvantaged Unincorporated Communities and the Struggle for Water Justice in California. **14**, 26.*Water Alternatives.*

Lubin J. H., Colt J. S., Camann D., Davis S., Cerhan J. R., Severson R. K., Bernstein L. and Hartge P. (2004) Epidemiologic Evaluation of Measurement Data in the Presence of Detection Limits. *Environ Health Perspect* **112**, 1691–1696.

Manning A. H., Mills C. T., Morrison J. M. and Ball L. B. (2015) Insights into controls on hexavalent chromium in groundwater provided by environmental tracers, Sacramento Valley, California, USA. *Applied Geochemistry* **62**, 186–199.

McClain C. N., Fendorf S., Johnson S. T., Menendez A. and Maher K. (2019) Lithologic and redox controls on hexavalent chromium in vadose zone sediments of California's Central Valley. *Geochimica et Cosmochimica Acta* **265**, 478–494.

McMahon P. B., Belitz K., Reddy J. E. and Johnson T. D. (2019) Elevated Manganese Concentrations in United States Groundwater, Role of Land Surface–Soil–Aquifer Connections. *Environ. Sci. Technol.* **53**, 29–38.

Moore E., Matalon E., (2011) The human costs of nitrate-contaminated drinking water in the San Joaquin Valley., *Pacific Institute*, Oakland, CA.

Nolan B. T., Fienen M. N. and Lorenz D. L. (2015) A statistical learning framework for groundwater nitrate models of the Central Valley, California, USA. *Journal of Hydrology* **531**, 902–911.

Nylen N. G., Pannu C. and Kiparsky M. (2018) Learning from California's Experience with Small Water Systems. *Berkeley Law.*

Oulhote Y., Mergler D., Barbeau B., Bellinger D. C., Bouffard T., Brodeur M.-È., Saint-Amour D., Legrand M., Sauvé S. and Bouchard M. F. (2014) Neurobehavioral Function in School-Age Children Exposed to Manganese in Drinking Water. *Environ Health Perspect* **122**, 1343–1350.

Pace C., Balazs C., Bangia K., Depsky N., Renteria A., Morello-Frosch R. and Cushing L. J. (2022) Inequities in Drinking Water Quality Among Domestic Well Communities and Community Water Systems, California, 2011–2019. *Am J Public Health* **112**, 88–97.

Pace C., Balazs C., Cushing L. and Morello-Frosch R. (2020) Locating Domestic Well Communities in California: A Methodological Overview. *Water Equity Science Shop.*

Patil D. S., Chavan S. M. and Oubagaranadin J. U. K. (2016) A review of technologies for manganese removal from wastewaters. *Journal of Environmental Chemical Engineering* **4**, 468–487.

Pauloo R. A., Escriva-Bou A., Dahlke H., Fencl A., Guillon H. and Fogg G. E. (2020) Domestic well vulnerability to drought duration and unsustainable groundwater management in California's Central Valley. *Environ. Res. Lett.* **15**, 044010.

Rosecrans C. Z., Nolan B. T. and Gronberg J. M. (2017) Prediction and visualization of redox conditions in the groundwater of Central Valley, California. *Journal of Hydrology* **546**, 341–356.

Rubin S. J. (2013) Evaluating violations of drinking water regulations. *Journal AWWA* **105**, E137–E147.

Schaefer M. V., Guo X., Gan Y., Benner S. G., Griffin A. M., Gorski C. A., Wang Y. and Fendorf S. (2017) Redox controls on arsenic enrichment and release from aquifer sediments in central Yangtze River Basin. *Geochimica et Cosmochimica Acta* **204**, 104–119.

Schaefer M. V., Plaganas M., Abernathy M., Aiken M. L., Garniwan A., Lee I. and Ying S. C. (2020) Manganese, arsenic, and carbonate interactions in model oxic groundwater systems. *Environ. Sci. Technol.* 57, 10621-10629

Schullehner J., Thygesen M., Kristiansen S. M., Hansen B., Pedersen C. B. and Dalsgaard S. (2020) Exposure to Manganese in Drinking Water during Childhood and Association with Attention-Deficit Hyperactivity Disorder: A Nationwide Cohort Study. *Environmental Health Perspectives* **128**, 097004.

Sherris A. R., Baiocchi M., Fendorf S., Luby S. P., Yang W. and Shaw G. M. (2021) Nitrate in Drinking Water during Pregnancy and Spontaneous Preterm Birth: A Retrospective Within-Mother Analysis in California. *Environ Health Perspect* **129**, 57001.

Spaur M., Lombard M. A., Ayotte J. D., Harvey D. E., Bostick B. C., Chillrud S. N., Navas-Acien A. and Nigra A. E. (2021) Associations between private well water and community water supply arsenic concentrations in the conterminous United States. *Sci Total Environ* **787**, 147555.

State of California Department of Finance (2019) Population Projections.

Tebo B. M. (2004) Biogenic Manganese Oxides: Properties and Mechanisms of Formation. *Annual Review of Earth and Planetary Sciences* **32**, 287–328.

Tobiason J. E., Bazilio A., Goodwill J., Mai X. and Nguyen C. (2016) Manganese Removal from Drinking Water Sources. *Curr Pollution Rep* **2**, 168–177.

U.S. Environmental Protection Agency (2003) Health Effects Support Document for Manganese. EPA 822-R-03-003. https://www.epa.gov/sites/default/files/2014-09/documents/support_cc1_magnese_healtheffects_0.pdf

U.S. Environmental Protection Agency (2022) The Fourth Unregulated Contaminant Monitoring Rule (UCMR 4): Data Summary. EPA 815-S-22-001. https://www.epa.gov/sites/default/files/2018-10/documents/ucmr4-data-summary.pdf

U.S. Environmental Protection Agency (2013) Secondary Drinking Water Standards: Guidance for Nuisance Chemicals. https://www.epa.gov/sdwa/secondary-drinking-water-standards-guidance-nuisance-chemicals

World Health Organization (2021) Manganese in drinking water. https://www.who.int/publications-detail-redirect/WHO-HEP-ECH-WSH-2021.5

Ying S. C., Schaefer M. V., Cock-Esteb A., Li J. and Fendorf S. (2017) Depth Stratification Leads to Distinct Zones of Manganese and Arsenic Contaminated Groundwater. *Environ. Sci. Technol.* **51**, 8926–8932.

Chapter 5. Conclusions

1. Overview

The work presented herein demonstrates the importance of multi-scale investigation on geogenic contaminant dynamics. At the soil aggregate scale, oxidation of Cr(III) from Cr(III)-bearing minerals by Mn oxides is attenuated by the presence of Fe(II) from reducing zones in a dose-dependent manner (Chapter 2). Further consideration of redox dynamics on the regional aquifer scale have been used to improve understanding of Mn exposure through groundwater resources. Manganese contamination higher than health-based threshold values occurs within California community water systems at point-of-entry and are attenuated by water treatment. However, due to the lack of available infrastructure, more exceedances of health-based levels were observed in very small and small water systems (Chapter 3). Private, shallow well users are also at risk of Mn overexposure via drinking water within California's Central Valley. Drilling of deeper wells was not observed to be protective of Mn exposure within this user group. In addition, financial barriers in communities with high rates of poverty may make point-of-use treatment cost-prohibitive (Chapter 4).

2. Multi-scale approach to understanding redox sensitive contaminants

Since water flows through many heterogeneous soil, treatment, and distribution systems, a holistic, multi-scale approach may better predict the release, attenuation, and migration of contaminants to points-of-use. For example, redox sensitive contaminants can interact with co-occurring constituents and mineral surfaces prior to distribution to

users, which may attenuate or exacerbate the severity of contamination. This work demonstrates that co-occurring groundwater constituents, such as Fe(II), can attenuate Cr(VI) contamination. However, this is dependent on the metal concentration and mineral composition within the system which is highly site-specific. In addition, geogenic Mn contamination of groundwater is lessened by water treatment prior to distribution but is also dependent on the treatment capacity of that system. Smaller systems that may lack infrastructure critical to water treatment, may therefore be unable to access this mitigation option.

Yet despite these attenuating factors, Cr and Mn contamination is still observed in many public and private water systems at concentrations harmful to human health. Through a multi-scale interrogation of the systems where geogenic contaminants may be mobilized or immobilized will help build tools that can be used to identify "hot-spots" at higher risk of contamination.

3. Use of this work to improve water quality

Currently, lack of reported data for domestic well communities and small water systems does not allow further assessment of contamination risk and available treatments. Therefore, specific attention in future work needs to be directed to these vulnerable communities including the collection and distribution of high-resolution water quality data.

In addition, increased identification of "hot-spot" zones within aquifer basins, although critical, does not always translate to reduced exposure. To do so, consistent monitoring and treatment of water is required. Small water systems and domestic well

communities unable to access the managerial, political, and financial resources needed may be unable to improve water quality for users. Therefore, when allocating attention and resources, these communities need to be prioritized.

Appendix 1. Appendix to Inhibition of chromium (III) oxidation through manganese (IV) oxide passivation and Fe(II) abiotic reduction

1. Reactor Schematic

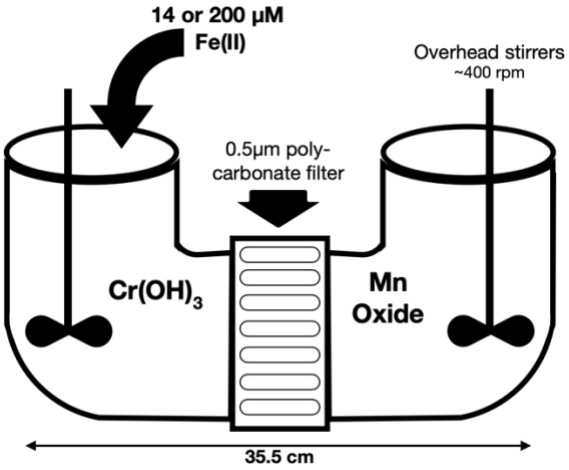

Figure S1. Schematic of diffusion limited reactor setup.

2. Additional Data

2.6. Controlled experiments

To determine the diffusion rate of Fe(II) through the diffusion reactor, low (25 µM) and high (200 µM) concentrations of Fe(II) were injected into one chamber of the reactor in the absence of solid $Cr(OH)_3$ and Mn oxides. Using calculations based on the Thiele modulus, the oxidation of Fe(II) and Cr(III) by Mn oxides was diffusion and not kinetically limited (Table S2).

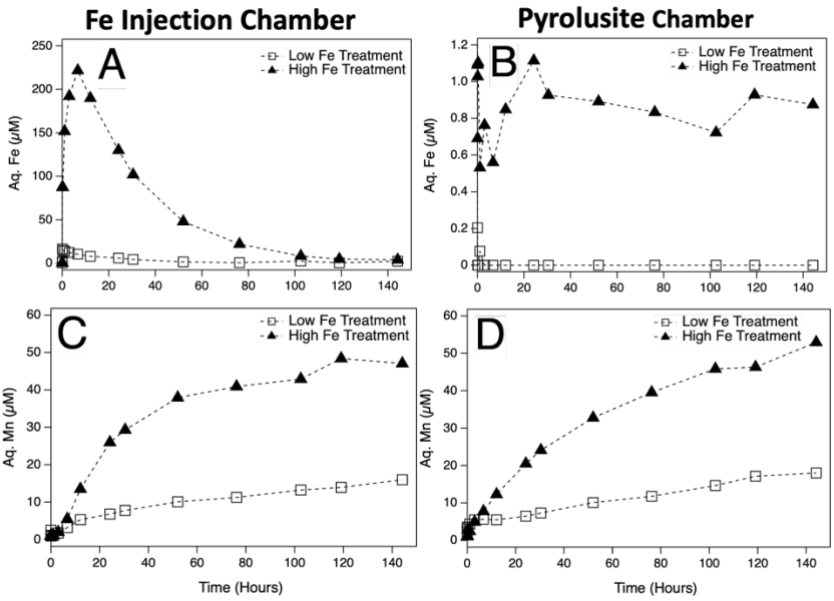

Figure S2. Iron and pyrolusite control reactors run without the addition of $Cr(OH)_3$. Aqueous concentration of iron (graph A and B) and manganese (C and D) in the iron injection chamber (left panel) and pyrolusite chambers after the addition of and low (16 µM, white boxes) and high (220 µM, black triangles) Fe(II).

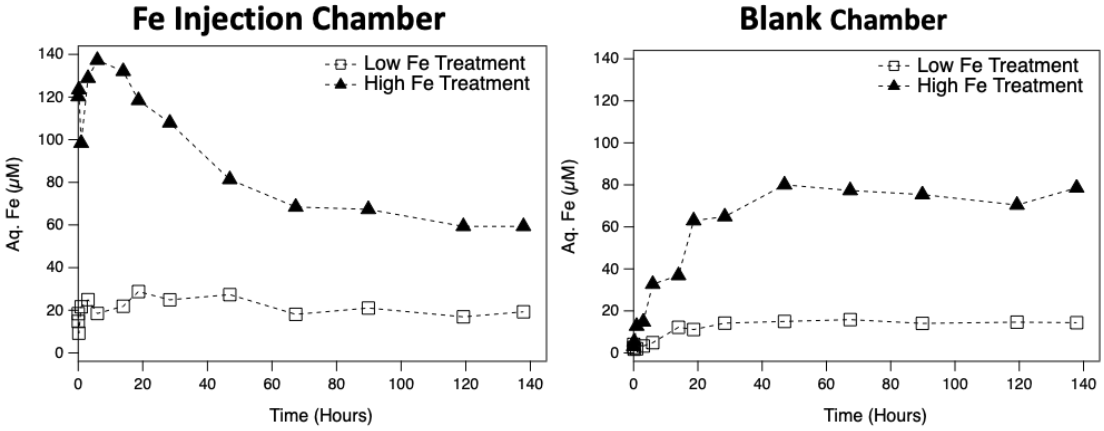

Figure S3. Iron diffusion control reactors run without the addition of $Cr(OH)_3$ or Mn oxides. Aqueous concentration of iron in the iron injection chamber (left) and blank chamber (right) after the addition of low (25 µM, white boxes) and high (140 µM, black triangles) Fe(II).

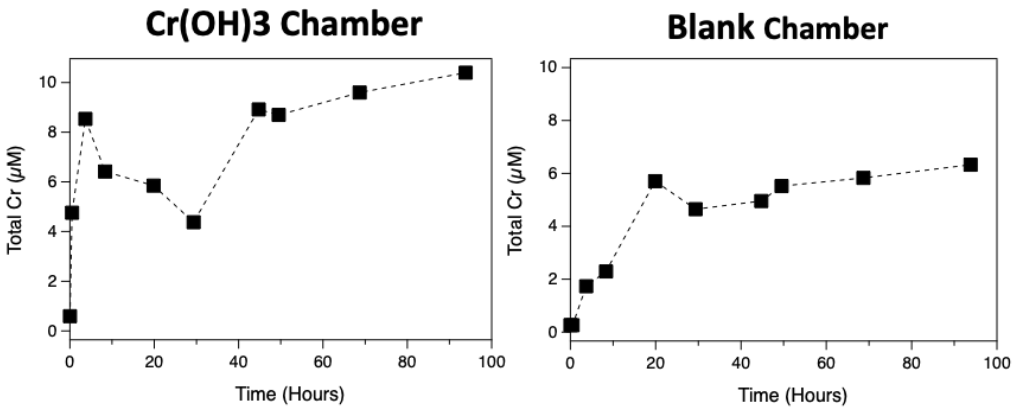

Figure S4. $Cr(OH)_3$ dissolution and diffusion control reactors run without the addition of aqueous Fe or Mn oxides. Aqueous concentration of total Cr in the $Cr(OH)_3$ chamber (left) and blank chamber (right).

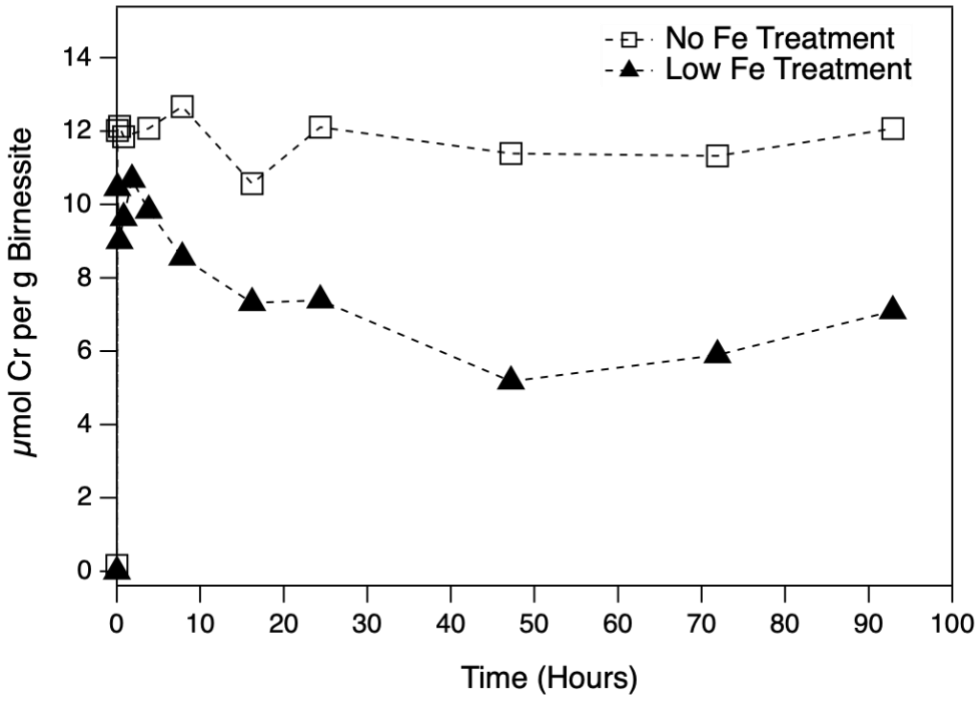

Figure S5. Solid concentration of chromium per gram of birnessite after the addition of no (white boxes) and low (14 μM, black triangles) concentrations of Fe(II) determined using acid digestion.

2.7. X-Ray Absorption Spectroscopy

Table S1. Linear combination analysis of Fe EXAFS of pyrolusite solids collected at the termination of the experiment

	Goethite Weight	Hematite Weight	Ferrihydrite Weight	R Factor	Chi Squared
High Fe	0.52	0.00	0.43	0.11	0.04
Low Fe	0.75	0.22	0.03	0.25	0.11

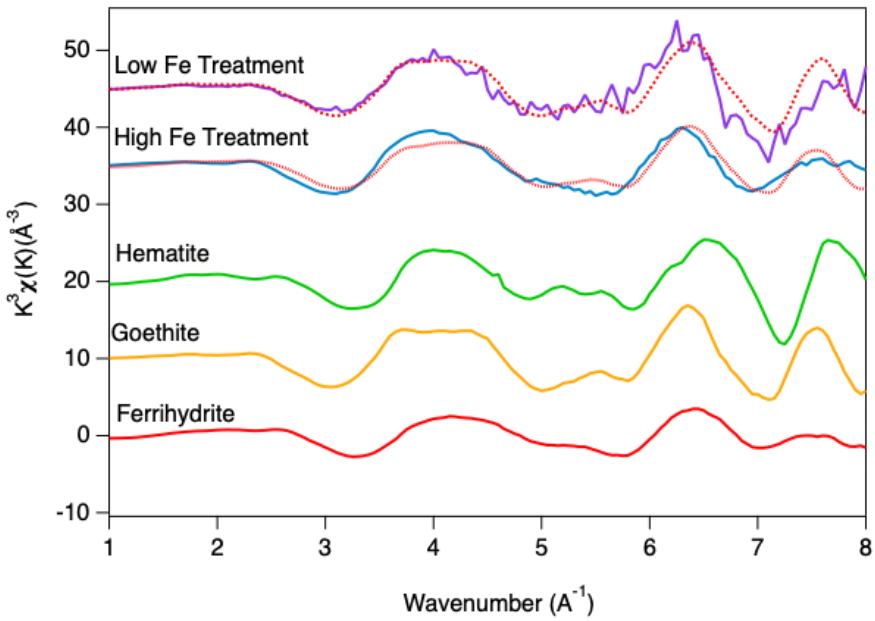

Figure S6. K^3-weighted EXAFS of pyrolusite solids collected at the termination of the experiment (solid line) and LCA fits (red dashed line). Ferrihydrite, goethite, and hematite were used as standards.

2.8. XPS Spectra

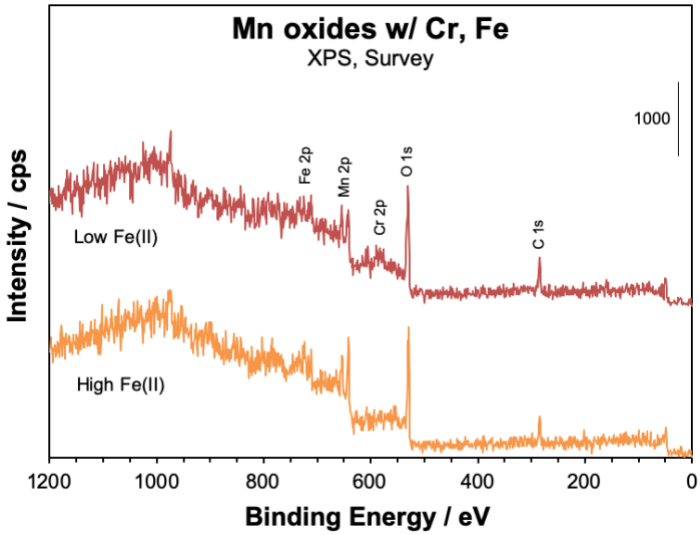

Figure S7. Survey spectra of pyrolusite at the termination of low Fe(II) and high Fe(II) treatment.

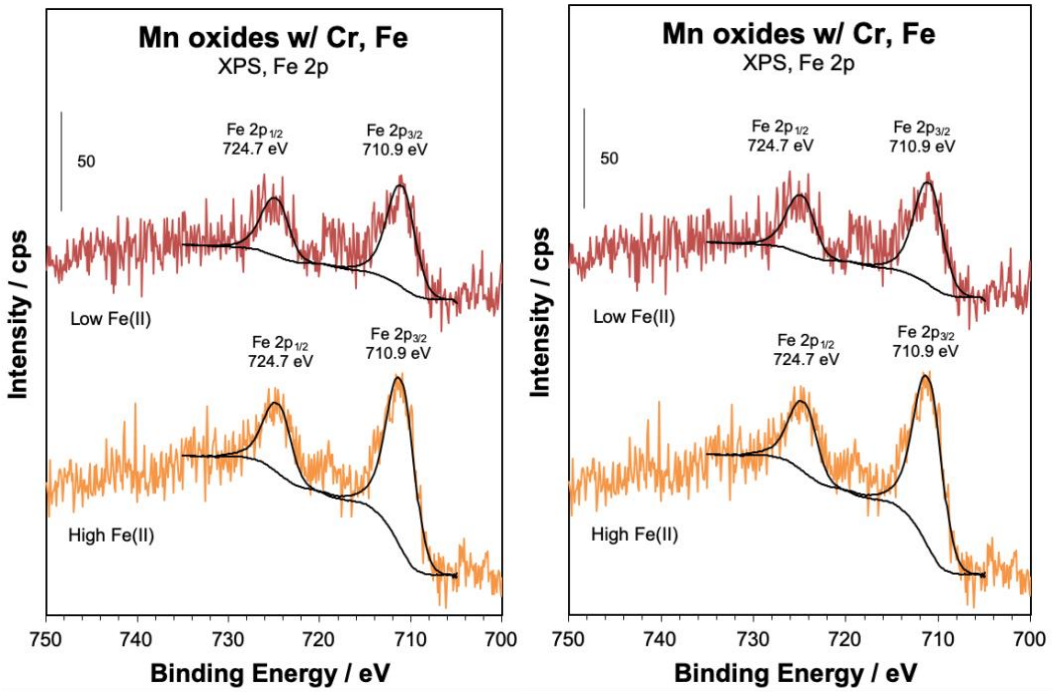

Figure S8. Fe 2p (left) and Mn 2p (right) spectra of pyrolusite at the termination of low Fe(II) and high Fe(II) treatment.

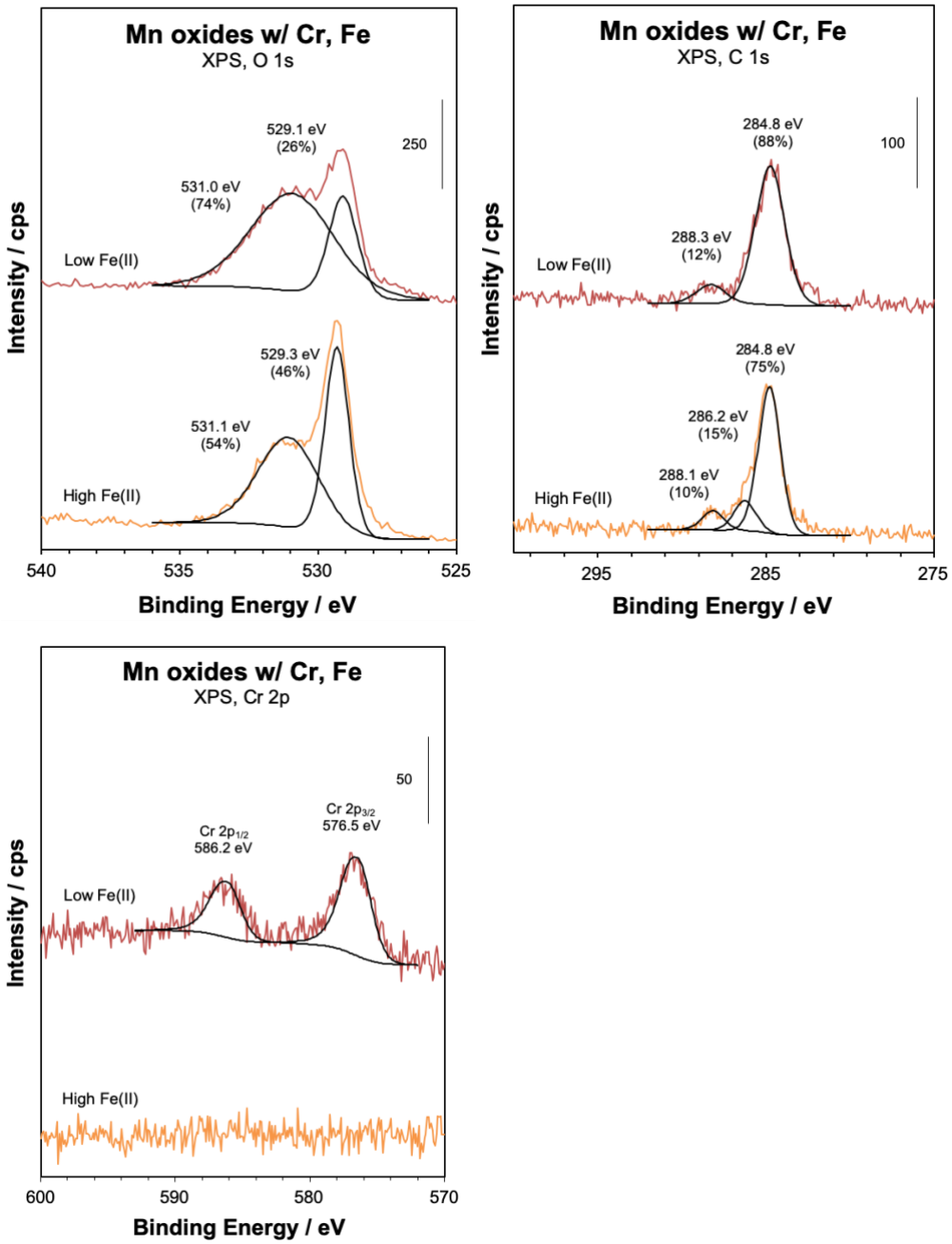

Figure S9. Spectra of O 1s (left), C 1s (middle), and Cr 2p (right) of pyrolusite at the termination of low Fe(II) and high Fe(II) treatment.

3. Rates and Coefficients

3.9. Diffusion Coefficient

Diffusion coefficients (D) were calculated following:

Equation 1. Diffusion coefficient

$$\gamma = -\frac{2SDH}{LV}$$

S (m^2) = membrane surface area (0.18 m^2)
D (m^2 s^{-1}) = diffusion coefficient for the solute
H (mol)= partition coefficient
V (m^3) = compartment volume (0.00075 m^3)
L (m) = length of reactor (0.14 m)
(mol L^{-1} s^{-1}) = slope of the line for a plot of versus time and is calculated following:

Equation 2. Slope of line

$$\gamma = ln\frac{(conc1 - conc2)}{100}$$

Conc1 (mol L^{-1}) = solute concentration in starting chamber
Conc1 (mol L^{-1}) = solute concentration in chamber solute is diffusing into

3.10. Thiele Modulus

Table S2. Thiele Modulus calculations at different aggregate radiuses.

R (mm)	No Fe	Low Fe
0.1	0.34	1.14
1	3.37	11.39
5	16.87	56.94
10	33.75	113.89
70	236.23	797.22

3.11. Reaction Rates

Table S3. Initial rates of Cr(III) oxidation and Mn(II) dissolution in diffusion limited environments.

	Pyrolusite		Birnessite
Initial Rates (μM/hr)	**No Fe(II)**	**Low Fe(II)**	**No Fe(II)**
Cr(III) oxidation by Mn oxides	0.05	0.03	0.4
Mn(II) release during oxidation	0.2	1.1	1.3

Appendix 2. Appendix to Assessment of manganese in California's community water systems and geochemical controls of release into groundwater

1. Summary of available data

Table S1. Publicly available data sources.

Data Type	Link to data
Water quality data in CWSs	https://www.waterboards.ca.gov/drinking_water/certlic/drinkingwater/EDTlibrary.html
CWS boundary	https://drinkingwatertool.communitywatercenter.org/data/
CWS information and population served	https://data.ca.gov/dataset/drinking-water-public-water-system-information

Table S2. Count of available Mn data from SDWIS from 2011 to 2021 used to estimate potentially exposed population.

Data processing step	Total	Extra Small	Small	Medium	Large	Extra Large
Count of reported Mn for active CA CWSs between 2011-2021	177723	25460	21584	19663	58207	52809
Count of reported Mn for active CA CWSs at point-of-entry	58735	10804	8581	7246	20188	11916
Total active CA CWSs with reported Mn	2654	1623	408	201	316	106
Total active CA CWSs with reported Mn at point-of-entry	1284	822	170	86	150	56

Table S3. Count of water quality data from SDWIS from 2011 to 2021 used to characterize geochemical parameters favorable to Mn release into groundwater.

	Mn	Cr	NO_3	As	Fe	$CaCO_3$	pH	Sulfate	DOC
Count reported to SDWIS between 2011-2021 (retained inactive and proposed systems)	203544	69314	553018	231241	188308	82511	85109	88941	48299
Count above detection limit	78138	45234	470429	150500	56909	82276	85109	84689	45234
Count reported as raw groundwater	50764	8661	268256	78867	34563	43988	45069	47701	5211
Count able to be joined with corresponding Mn by date and sample point	--	1338	5853	12546	25932	10115	9812	10381	1527

2. Statistical Results

Table S4. Results from Kruskall-Wallis test comparing median Mn concentration between different community water system sizes. All other pairs were not significantly different ($p>0.05$).

Size Pairs	p value
Small - Very Small	0.036
Very Small - Large	0.036
Very Small - Very Large	0.050

Table S5. Results from Mann-Whitney statistical tests for pre- and post-treatment mean Mn concentration between 2011-2021.

	Count	Median Pre-treatment	Median Post-treatment	p
Very Small	134	147.7	17.3	0.000
Small	69	76.3	14.3	0.000
Medium	48	79.1	14.3	0.000
Large	96	57.1	14.3	0.000
Very Large	50	27.7	14.3	0.000

Table S6. Results from Mann-Whitney statistical tests of Mn concentration in raw groundwater co-occurring with other groundwater constituents sampled at the same point and time. All samples below detection were removed from analysis. DOC=dissolved organic carbon. Cut-off values were captured from all listed MCL or SMCLs.

	Low	n	Median Mn	High	Median Mn	n	p-value
Mn-NO_3	NO_3 <10 mg L^{-1}	4433	56.1	NO_3 >10 mg L^{-1}	53	1421	0.45
Mn-Cr	Cr <10 µg L^{-1}	1063	26.7	Cr >10 µg L^{-1}	40	275	0
Mn-DOC	DOC <1.5 mg L^{-1}	701	84.3	DOC >1.5 mg L^{-1}	780	827	0
Mn-As	As <10 µg L^{-1}	6912	75	As >510 µg L^{-1}	115	5640	0
Mn-Fe	Fe <200 µg L^{-1}	11453	84	Fe >200 µg L^{-1}	210	14493	0
Mn-pH	pH <7.5	1090	140	pH>7.5	75	8733	0
Mn-Sulfate	Sulfate > 250 µg L^{-1}	6849	70.4	Sulfate > 250 µg L^{-1}	200	3534	0

Table S7. Results from Spearman correlations of Mn and other co-occurring groundwater constituents in raw, untreated groundwater samples.

Variables	n	p-values	Correlation Coefficient (r)
Mn-NO_3	5853	0.00	-0.06
Mn-Cr	1338	0.00	0.08
Mn-DOC	1527	0.00	0.49
Mn-As	12546	0.00	0.15
Mn-Fe	25932	0.00	0.43
Mn-pH	9812	0.00	-0.22
Mn-Sulfate	10381	0.00	0.28
Mn-$CaCO_3$	10115	0.00	0.29

Table S8. Results from Spearman correlations of Mn and other co-occurring groundwater constituents in treated groundwater samples.

Variables	n	p-values	Correlation Coefficient (r)
Mn-NO_3	222	0.00	-0.27
Mn-Cr	128	0.27	0.1
Mn-DOC	85	0.25	-0.13
Mn-As	1688	0.00	0.11
Mn-Fe	4319	0.00	0.74
Mn-pH	976	0.83	0.01
Mn-Sulfate	583	0.00	0.26
Mn-$CaCO_3$	705	0.49	-0.03

Table S9. Results from Mann-Whitney statistical tests of Mn concentration in raw groundwater co-occurring with high (>10 μg L^{-1} As) and low (<10 μg L^{-1} As) concentrations of arsenic sampled at the same point and time.

	Low Arsenic (<10 μg L^{-1})		High Arsenic (>10 μg L^{-1})		
CWS size	n	Median Mn (μg L^{-1})	n	Median Mn (μg L^{-1})	p
Very Small	1485	110	1534	170	0.00
Small	1040	68.5	1559	91.7	0.00
Medium	1000	569	805	250	0.00
Large	2569	58	1268	75.5	0.00
Very Large	753	40	394	81.4	0.00

Appendix 3: Appendix to Predicting manganese in drinking water accessed by domestic well communities and community water systems in Central Valley, California

1. Summary of data used

Table S1. Publicly available data sources.

Description	Data Source
Likely DWC Boundaries	https://drinkingwatertool.communitywatercenter.org/data/
CWS Boundary	https://drinkingwatertool.communitywatercenter.org/data/
Groundwater Mn Predictive Model (33 m, 67 m, 100 m)	https://www.sciencebase.gov/catalog/item/57f433c3e4b0bc0bec033fc9
Reported Mn Concentrations at Point of Entry	https://www.waterboards.ca.gov/drinking_water/certlic/drinkingwater/EDTlibrary.html
US Census population	https://drinkingwatertool.communitywatercenter.org/data/
CWS user population	https://data.ca.gov/dataset/drinking-water-public-water-system-information
Percentage below 2FPL (OEHHA)	https://oehha.ca.gov/calenviroscreen/indicator/poverty
Disadvantaged Community Designation	https://data.ca.gov/dataset/sb-535-disadvantaged-communities-2017

Table S2: Count of available Mn data from SDWIS between 2011-2019. CWS = community water system. Small CWS = 15-199 service connections; Medium CWS = 200-9,999 service connections; Large CWS > 10,000 service connections.

Data Processing Step	**Total**	**Small CWS**	**Medium CWS**	**Large CWS**
Count of reported Mn for active community water systems statewide	138,072	-	-	-
Count of reported Mn for active community water systems in Central Valley *	28,852	3,916	9,977	14,959
Count of reported Mn for active community water systems in Central Valley at point-of-entry *	13,113	2,323	4,736	6,054
Total active CWS in Central Valley with reported Mn	639	398	188	53
Total active CWS in Central Valley with reported Mn at point-of-entry	373	245	87	41

*All CWS with 0 reported population and <15 service connections were removed from analysis (n=400 reported Mn concentrations within the Central Valley)

Table S3. Summary of mean Mn concentrations between 2011-2019 for small, medium, and large CWS.

	Small CWS	Medium CWS	Large CWS
Median (IQR)[A]	14.2 (16.2)	14.3 (2.7)	14.3 (0.9)
Mean	52.5	26.7	18.7
95th Percentile	224.4	65.2	30.5

[A]Interquartile range

2. Distribution of predicted Mn exceedances in DWC and CWS

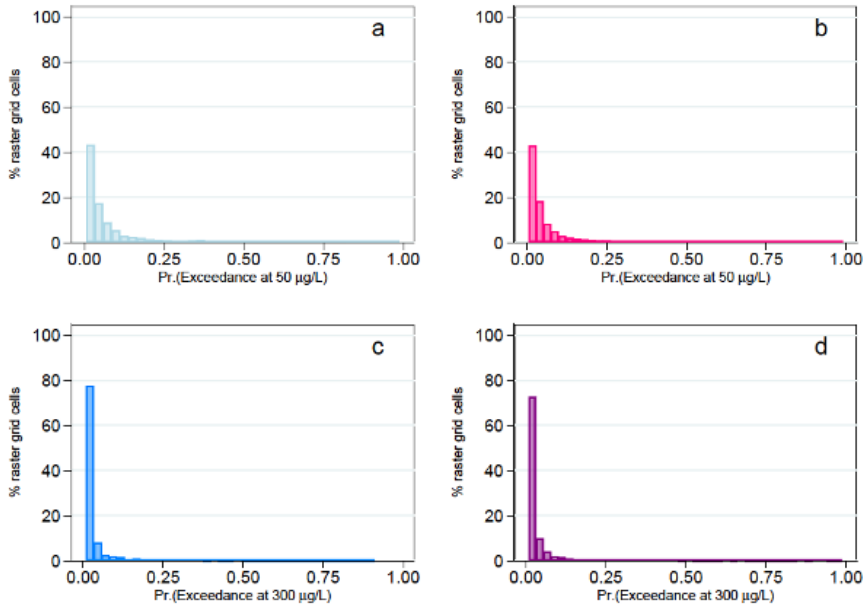

Figure S1. Distributions of the probability of groundwater Mn exceeding secondary contaminant level and health advisory limits in DWC. (A) Probability of exceeding the 50 µg L^{-1} threshold in rasters containing domestic well users. (B) Probability of exceeding the 300 µg L^{-1} threshold in rasters containing domestic well users.

3. Reported Mn Water Quality in Domestic Wells

We estimated Mn concentrations in groundwater serving domestic wells using water quality and depth data from the United States Geological Survey (USGS), National Water Information System (NWIS), and California State Water Board Groundwater Ambient Monitoring Assessment (GAMA) database (https://gamagroundwater.waterboards.ca.gov/gama/datadownload). All water quality estimates from wells between 15 - 61 m were included in estimates for ambient Mn water quality.

Table S4. Reported Mn concentrations in domestic wells between 2001-2019.

	Domestic Wells
Service connections	1 to 4
Total observations	125
Median (IQR)	0.58 (17.5)
Mean	61.2
Max	1130
95th percentile	365.8

4. Summary of Statistical Results

To determine if there was a difference in mean predicted Mn concentration in groundwater exceeding SMCL and HAL, a paired-t test was used. Although the data was non-normally distributed, non-parametric tests are less useful in studies with large sample sizes (Fagerland et al. 2012) and a parametric t-test was used. Since we were comparing reported values at two depths, a paired t-test was used to determine the difference in mean within the sample. A paired Cohen's d was also determined to describe the magnitude of the difference in means (Sullivan and Fein, 2012). All statistical analyses were performed using RStudio.

Table S5: Summary of paired t-test between the current average depth of domestic wells (33 m) and the predicted depth if wells were drilled deeper during times of drought (67 m).

		Mn conc. > 50 ug/L	**Mn Conc > 300 ug/L**
Well depth	**DWCs**	**Mean**	**Mean**
Normal (33 m)	n=6953	0.128	0.0599
Drought (67 m)	n=19528	0.139	0.0607
	Difference	-0.011	-0.0008
	t-statistic	44.92	5.69
	p value	0.000	0.000
	Effect size	0.03 (negligible)	0.01 (negligible)

Table S6: Summary of paired t-test between the current average depth of domestic wells (33 m) and depth if domestic wells were drilled to the depth of public wells (100 m) as a protective measure against contamination.

		Mn conc. > 50 ug/L	**Mn conc. > 300 ug/L**
Well depth	**DWC s**	**Mean**	**Mean**
Normal (33 m)	n=6953	0.128	0.0599
Deep (100 m)	n=19528	0.139	0.0608
	Difference	-0.011	-0.0009
	t-statistic	61.55	5.028
	p value	0.000	0.000
	effect size	0.04 (negligible)	0.01 (negligible)

To determine the difference in the percentage of the population in DWC below 2FPL within the Central Valley and outside of the Central Valley, we used a Welch t-test due to the variation within the sample size. The effect size was determined using Cohen's d.

Table S7: Summary of Welch t-test between percentage of DWC communities within and outside of the Central Valley that are below 2FPL.

		Percentage below 2FPL
Groups	**DWC Count**	**Mean**
DWC in the Central Valley	n= 6,953	42.3
DWC outside the Central Valley	n=19,528	32.4
	Difference	9.9
	t-statistic	-47.51
	p value	0.000
	effect size	0.72 (medium)

To determine the difference in the percentage of the population in DWC below 2FPL within the Central Valley and outside of the Central Valley, we used a Welch t-test due to the variation within the sample size. The effect size was determined using Cohen's d.

Table S8: Summary of Welch t-test between the probability of the Mn concentration exceeding threshold values within and outside of disadvantaged communities

		Mn conc. > 50 ug/L	**Mn conc. > 300 ug/L**
Well depth	**DWC s**	**Mean**	**Mean**
DWC in DAC	n=2998	0.131	0.072
DWC outside DAC	n=3421	0.125	0.050
	Difference	0.006	0.022
	t-statistic	1.016	6.253
	p value	0.310	0.000
	effect size	0.03 (negligible)	0.16 (negligible)

5. Probability of Mn Exceedance for DWC users within CWS boundary

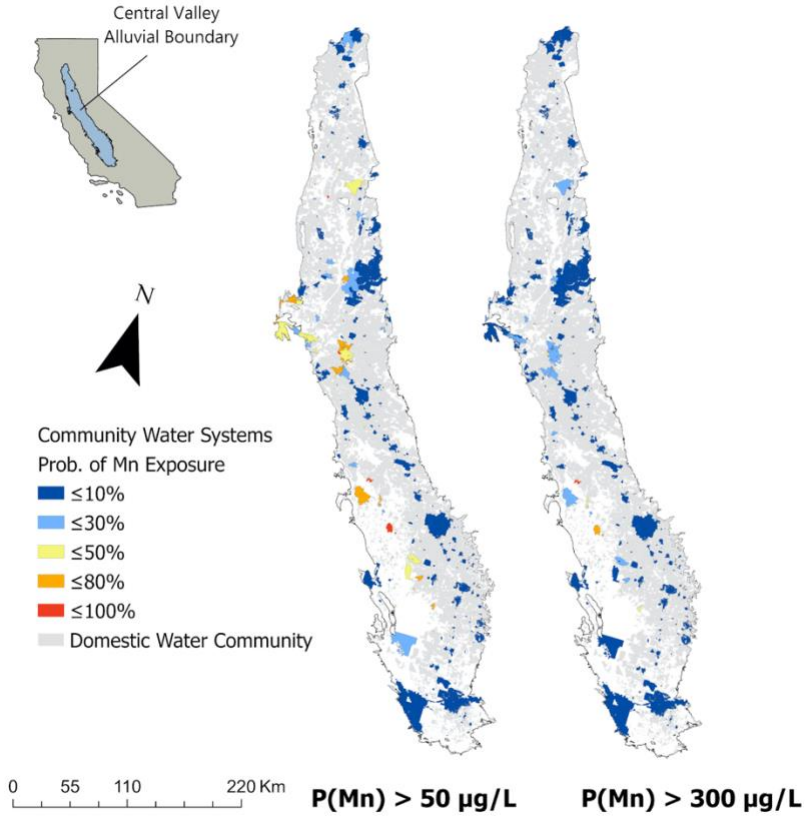

Figure S2. Probability of Mn in groundwater exceeding 50 µg L^{-1} or 300 µg L^{-1} for shallow (33 m) domestic well users residing within CWS boundaries.

6. Probability of Mn Exceedance at various depths

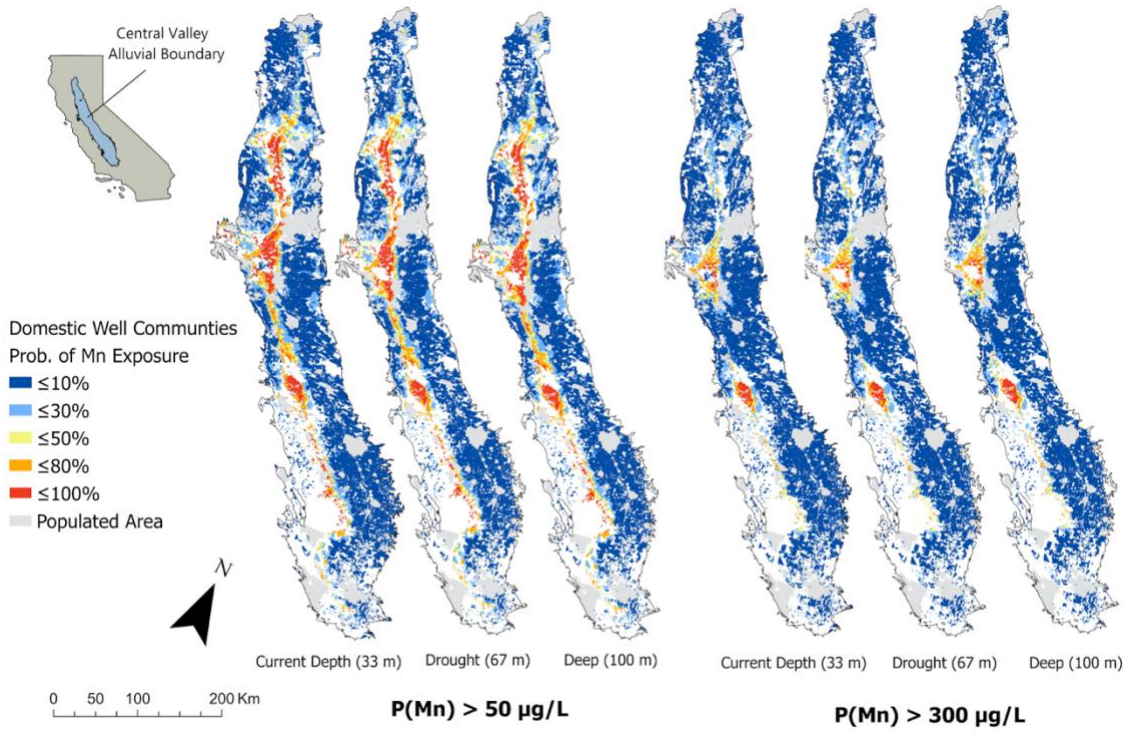

Figure S3. Probability of Mn in groundwater exceeding 50 µg L^{-1} or 300 µg L^{-1} in DWC at three depths (current depth = 33 m, drought = 67 m, deep =100 m).

7. Summary of DWCs within or outside disadvantaged communities

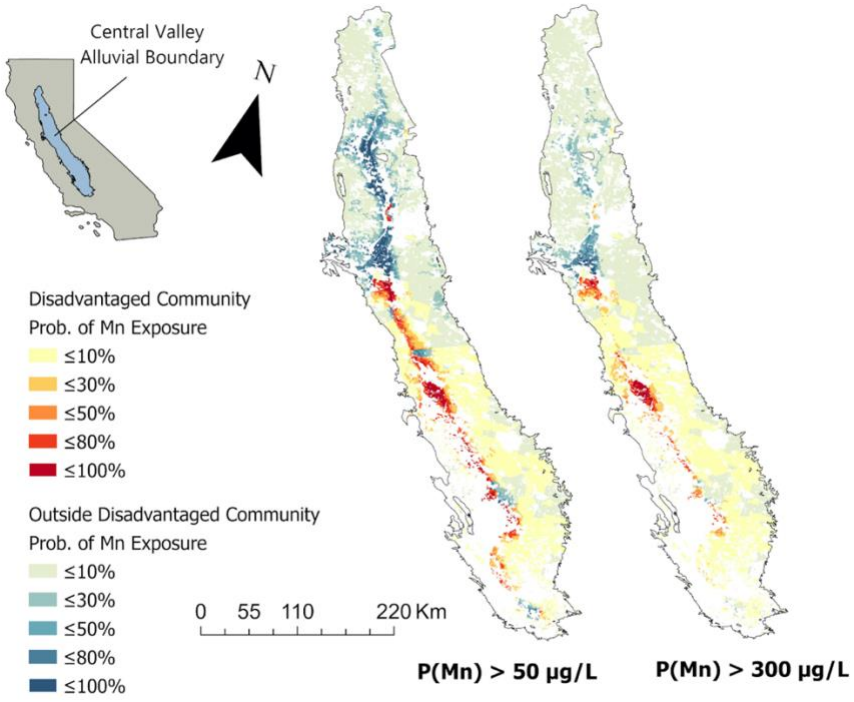

Figure S4. Probability groundwater Mn exceeding 50 µg L^{-1} or 300 µg L^{-1} within disadvantaged communities as designated by CalEPA and defined by the communities that are most likely to suffer from economic, health, and environmental burdens (SB 535). Data sourced from **https://data.ca.gov/dataset/sb-535-disadvantaged-communities-2017** and last updated in 2017.

Table S9. DWC population within DAC and outside of DAC.

	Within DAC	Outside DAC
Total population	268,706	285,730
Total wells	24,365	43,621
Population (%) >80% 50 µg/L Mn	4,066 (1.5)	18,603 (6.5)
Population (%) <80% 50 µg/L Mn	264,640 (98.5)	267,127 (93.5)
Population (%) >80% 300 µg/L Mn	2,079 (0.8)	263 (0.1)
Population (%) <80% 300 µg/L Mn	266,627 (99.2)	285,467 (99.9)

8. Possible point of use treatments for Mn in drinking water

Table S10. Summary of possible point-of-use treatments for Mn in drinking water and costs associated.

Method	Description	Disadvantages	References for Method	Normalized cost
Oxidation, precipitation, and removal	Chemical oxidation and precipitation of dissolved Mn (II) and filtration of Mn solids; common oxidants include oxygen, chlorine dioxide, ozone, or permanganate	Generates sludge which must be properly disposed of; strong oxidant or high pH required to ensure effective removal; competition with other oxidant demands (e.g. iron or organic carbon); water must be monitored to ensure effective oxidant dosing	Wong 1984; Knocke et al. 1987	Air injecting filter (0.3 ppm removal): $220-300 per year Chlorination and filtration (2 ppm removal): $100-120 per year
Sorption	Sorption of dissolved Mn on solid surface (often metal or Mn oxide, such as "greensand" filter); can be combined with catalytic oxidation by free chlorine to continuously regenerate Mn oxide surface	Once surface is saturated, breakthrough occurs and must be monitored; filter must be regenerated or replaced once breakthrough occurs	Wang et al. 2021; Knocke et al. 1988; Knocke et al 1991	Greensands Filter (5 ppm removal): $300-400 per year Iron or Mn filter media (0.3 ppm removal): $50-80 per year
Ion exchange	Cation exchange resins (strong-acid exchangers or weak-acid exchangers) bind divalent ions present in water (e.g. Ca^{2+}, Zn^{2+}, Fe^{2+}, Mg^{2+} , and Mn^{2+})	Other divalent cations present in the water may interfere with binding or leach sorbed Mn(II), often a problem in water with high hardness; exchange media must be replaced; pour over filter only effective for low flow volumes	Carriere et al. 2011	Water softener (0.5 ppm): $70-200 per year Pour over filter (0.5 ppm): $70 per year
Membrane filtration	Water is passed through a semipermeable membrane (e.g. microfiltration, nanofiltration, reverse osmosis, ultrafiltration)	Membrane must be maintained or replaced often; slow filtration depending on membrane permeability; potential membrane fouling	Choo et al. 2005; Teng et al. 2001	Reverse osmosis (ppm): $100-200 per year
Biological removal	Water passed through media with biofilm containing microbes able to directly oxidize Mn(II), adsorb it extracellularly, or catalyze Mn(II) oxidation through biopolymers	Proper nutrient solution must be maintained to sustain the biofilm; varying acclimation time required; continuous monitoring required	Ramsay et al 2018; Gouzinis et al. 1998; Breda et al. 2017; Hoyland et al. 2014	Not commonly used as point of use treatment
Infrastructure management	Modifications to wells to prevent high exposure to Mn such as blending water, installing deeper wells, or monitoring of private wells to take them offline when in exceedance	Requires monitoring of all private and public wells; may not be feasible for private wells where cost is carried by owner	Tobiason et al. 2016	Drilling deeper well (90.06 m): $30-65/ft, $9,000 to 17,500 total Joining municipal water system: $1,500 to 20,000 total depending on location Water monitoring cost: $100-400 per sample

9. Appendix References

Breda I. L., Ramsay L. and Roslev P. (2017) Manganese oxidation and bacterial diversity on different filter media coatings during the start-up of drinking water biofilters. *Journal of Water Supply: Research and Technology-Aqua* **66**, 641–650.

California Environmental Protection Agency (2017) Designation of Disadvantaged Communities Pursuant to Senate Bill 535. https://calepa.ca.gov/wp-content/uploads/sites/6/2017/04/SB-535-Designation-Final.pdf

California State Water Resource Control Board (2020) Groundwater Ambient Monitoring and Assessment (GAMA). , 37.

Carrière A., Brouillon M., Sauvé S., Bouchard M. F. and Barbeau B. (2011) Performance of point-of-use devices to remove manganese from drinking water. *Journal of Environmental Science and Health, Part A* **46**, 601–607.

Choo K.-H., Lee H. and Choi S.-J. (2005) Iron and manganese removal and membrane fouling during UF in conjunction with prechlorination for drinking water treatment. *Journal of Membrane Science* **267**, 18–26.

Fagerland M. W. (2012) t-tests, non-parametric tests, and large studies—a paradox of statistical practice? *BMC Medical Research Methodology* **12**, 78.

Gounot A. M. (1994) Microbial oxidation and reduction of manganese: consequences in groundwater and applications. *FEMS Microbiol Rev* **14**, 339–349.

Gouzinis A., Kosmidis N., Vayenas D. V. and Lyberatos G. (1998) Removal of Mn and simultaneous removal of NH3, Fe and Mn from potable water using a trickling filter. *Water Research* **32**, 2442–2450.

Knocke W., Benschoten J. V., Kearney M. J., Soborski A. W. and Reckhow D. (1991) Kinetics of Manganese and Iron Oxidation by Potassium Permanganate and Chlorine Dioxide.

Knocke W. R., Hoehn R. C. and Sinsabaugh R. L. (1987) Using Alternative Oxidants to Remove Dissolved Manganese From Waters Laden With Organics. *Journal AWWA* **79**, 75–79.

Knocke W. R., Ramon J. R. and Thompson C. P. (1988) Soluble Manganese Removal on Oxide-Coated Filter Media. *Journal (American Water Works Association)* **80**, 65–70.

Ramsay L., Breda I. L. and Søborg D. A. (2018) Comprehensive analysis of the start-up period of a full-scale drinking water biofilter provides guidance for optimization. *Drinking Water Engineering and Science* **11**, 87–100.

Sullivan G. M. and Feinn R. (2012) Using Effect Size—or Why the P Value Is Not Enough. *J Grad Med Educ* **4**, 279–282.

Teng Z., Yuan Huang J., Fujita K. and Takizawa S. (2001) Manganese removal by hollow fiber micro-filter. Membrane separation for drinking water. *Desalination* **139**, 411–418.

Tobiason J. E., Bazilio A., Goodwill J., Mai X. and Nguyen C. (2016) Manganese Removal from Drinking Water Sources. *Curr Pollution Rep* **2**, 168–177.

Wang P., Wang H., Zhang Y., Yi J., Chen M., Jiang H., Yan J., Liu H. and Ma J. (2021) Accelerated catalytic oxidation of dissolved manganese(II) by chlorine in the presence of in situ-growing 3D manganese(III)/(IV) oxide nanosheet assembly in zeolite filter. *Water Res* **201**, 117223.

Wong J. M. (1984) Chlorination-Filtration for Iron and Manganese Removal. *Journal AWWA* **76**, 76–79.